Dynamics of climate variability over the all-year rainfall region of South Africa

By

Christina J. Engelbrecht

A Thesis Submitted in Partial Fulfilment of the Requirements for the Degree of Doctor of Philosophy (Meteorology)

Department of Geography, Geoinformatics and Meteorology

Faculty of Natural and Agricultural Sciences

University of Pretoria, South Africa

September 2015

Declaration

This is to declare that this thesis, which I submit for the degree PhD in Meteorology at the University of Pretoria, is my own work, unless or otherwise explicitly acknowledged by citation of published and unpublished sources. Furthermore, I would like to state that, even if the work presented from chapter 2 to 4 has been co-authored with my promotor and other colleagues, the conceptualization and execution of the research were executed by me. This research has not previously been submitted for a degree at this or any other tertiary institution.

Christina J. Engelbrecht (94054292)

SIGNATURE: ..……………………………………

DATE: ………………………………………………….

Acknowledgements

Many thanks and appreciation to:

- Prof. W.A. Landman (CSIR, UP) for his positive energy towards this study and for guidance when I tended to diverge.
- The South African Weather Service for rainfall data.
- The UK Met Office for GloSea5 data.
- The Agricultural Research Council for supporting my studies. Thank you very much.
- The Water Research Commission (Project K5/2257/1) for funding that made it possible for me to perform parts of this study as part of my daily duties at the ARC.
- The Applied Centre for Climate and Earth System Studies (ACCESS) for funding that made it possible to attend conferences, locally as well as an international conference. These conferences were very valuable. All university fees were also covered by ACCESS and are appreciated.
- Liesl, Johan and Francois. Thanks very much for many study related talks over liters of coffee (Liesl).
- Ma, Stoffel (and now Heloise as well) and Annie. Thanks for accepting fewer holiday trips and welcoming my laptop.
- Francois. I'm back.

"Who covers the heavens with clouds, Who prepares rain for the earth, Who makes grass to grow on the mountains."

PSALM 147:8

Thesis promotor

Prof. Willem A. Landman

Council for Scientific and Industrial Research (CSIR), Natural Resources and the Environment (NRE), and Department of Geography, Geoinformatics and Meteorology, University of Pretoria, Lynnwood Road, Pretoria 0002, South Africa

List of acronyms

ACCESS	Applied Centre for Climate and Earth System Studies
AGCM	Atmospheric General Circulation Model
AOH	Atlantic Ocean High
ARC	Agricultural Research Council
COL	Cut-Off Low
CORDEX	COordinated Regional climate Downscaling EXperiment
CPC	Climate Prediction Center
CRU	Climatic Research Unit
DEM	Digital Elevation Model
DJF	December-January-February
ENSO	El Niño Southern Oscillation
FEWS	Famine Early Warning System
GloSea5	Global Seasonal forecast system version 5
JAS	July-August-September
JJA	June-July-August
MAM	March-April-May
NCEP	National Centers for Environmental Prediction
NWP	Numerical Weather Prediction
ONI	Oceanic Niño Index
OND	October-November-December
RE	Ridging high pressure system situated East/southeast of the subcontinent
ROC	Relative Operating Characteristic
RSW	Ridging high pressure system from the SouthWest of the subcontinent
SAM	Southern Annular Mode
SAWS	South African Weather Service
SLP	Sea-level pressure
SOM	Self-Organizing Map
SON	September-October-November
SRTM	Shuttle Radar Topography Mission
SST	Sea-Surface Temperature
TSE	Trough SouthEast of the subcontinent
TSW	Trough SouthWest of the subcontinent
TTT	Tropical-Temperate Trough
UKMO	United Kingdom Meteorological Office
WSF	Weak Synoptic Flow

Contents

Abstract

Climatologically, the Cape south coast is unique in the sense that it lacks the pronounced seasonality observed over the remainder of South Africa. Here, rainfall occurs all-year round, implying that rainfall-producing systems characteristic of both the winter and summer rainfall regions contribute to rainfall over the Cape south coast. However, the relative contributions of different rain-producing weather systems to annual rainfall have not been quantified to date. This region has also not received as much attention as the winter and summer rainfall regions of the country with regards to quantifying and understanding its interannual rainfall variability. Furthermore, seasonal forecast skill over the Cape south coast region is generally poorer and less well investigated than forecast skill over the summer rainfall region and to a lesser extent the winter rainfall region. This study addresses these issues through objective identification of the prevailing synoptic types of the Cape south coast region by application of the self-organizing map (SOM) technique, with a subsequent analysis of their interannual variability, intraseasonal variability, and predictability.

The relative contribution of different rain-producing systems to annual rainfall over the Cape south coast is quantified. Ridging high pressure systems contribute most to the mean annual rainfall (46%), followed by tropical-temperate troughs (28%) and cut-off lows (COLs). COLs, co-occurring with ridging high pressure systems and tropical-temperate troughs contribute to 16% of the mean annual rainfall. When extreme rainfall is considered, COLs contribute to 29% of all extreme rainfall events along the Cape south coast. Particular configurations of ridging high pressure systems and tropical-temperate troughs that are linked to interannual variability of seasonal rainfall are identified. These systems are primarily ridging high pressure systems, in particular those ridging from far south of the subcontinent, and tropical-temperate troughs occurring during seasons with weaker zonal mid- and upper air winds. COLs are also linked to interannual variability of seasonal rainfall, despite their infrequent occurrence - highlighting the importance of COLs as high impact weather systems. The COL link with rainfall variability is particularly strong during March-April-May (MAM) and even more so for June-July-August (JJA). It is also shown that the interannual variability in the frequency distribution of the occurrence of synoptic types within a season is linked to the El Niño Southern Oscillation (ENSO) and the Southern Annular Mode (SAM), suggesting potential predictability of intraseasonal variability at the seasonal time scale. The predictability of intraseasonal characteristics over the Cape south coast at the seasonal time

scale is subsequently assessed by utilizing an ensemble of simulations performed by an atmosphere-ocean coupled global circulation model administered by the UK Met Office. Hindcasts of 14 austral spring and summer seasons initialized at a 1-month lead time are used to assess the model's ability to predict the intraseasonal characteristics of weather systems. This assessment revealed that some skill exists in the predictability of the intraseasonal characteristics of synoptic types over the Cape south coast region of South Africa at the seasonal time scale. The result implies that there is potential to predict whether specific high impact weather systems (e.g. COLs) or systems associated with good rainfall (e.g. ridging highs ridging from anomalously far south of the subcontinent) will occur at anomalously high or low frequencies during the next season, with associated benefits to the agricultural and water sectors.

Chapter 1: Introduction

1.1 Background

South Africa is located in the subtropics and is on the average situated underneath the descending component of the Hadley cell circulation. Except for at the surface, anticyclonic circulation prevails over the country throughout the year (Taljaard, 1959). However, the position and intensity of the anticyclonic circulation exhibits seasonal characteristics (Taljaard, 1986). In response to seasonal changes in the atmospheric circulation, three precipitation regimes can be discerned over South Africa. Most of the country predominantly receives rainfall during the austral summer (Harrison, 1984; Weldon and Reason, 2014) when the core of the anticyclonic circulation is located further poleward compared to winter (Taljaard, 1959), while its equatorward flank interacts with the various convergence zones over tropical Africa. It is also during summer that the surface anticyclonic circulation over South Arica is replaced by a heat driven synoptic trough system that aids in facilitating the southward flow of moist tropical air (Taljaard, 1986). The extreme southwestern area of the country is characterized by austral winter rainfall (Harrison, 1984; Weldon and Reason, 2014), when cold fronts follow a more equatorward track. A small strip along the southern coastal region of the country, referred to as the Cape south coast, receives rainfall throughout the year (Harrison, 1984; Weldon and Reason, 2014) with smallish peaks during the transitional seasons (Taljaard, 1996; Pohl et al., 2014). These peaks have been qualitatively attributed to cut-off lows (COLs) and ridging high pressure systems occurring during autumn and spring, respectively (Jury and Levey, 1993). Rainfall-producing weather systems characteristic of both the winter and summer rainfall regions of South Africa occur over the Cape south coast, contributing to the region's unique climate. These weather systems are cold fronts, west-wind troughs, COLs, ridging high pressure systems (Taljaard, 1996; Favre et al., 2013; Weldon and Reason, 2014) and tropical-temperate troughs (Taljaard, 1996; Hart et al., 2013). Apart from tropical-temperate troughs that are considered unique to the summer months, the other rainfall producing weather systems occur throughout the year, although they do exhibit preferential seasons of occurrence. Cold fronts are mainly winter weather systems, although weak cold fronts occur during summer as well (Taljaard, 1996). COL frequencies occurrences peak during the transitional seasons (Jury and Levey, 1993; Singleton and Reason, 2007) and ridging highs during summer (Taljaard, 1996). The contribution of tropical-temperate troughs (Crimp et al., 1997; Hart et al., 2013), COLs

(Favre et al., 2013) and landfalling tropical systems invading the far northern part of the country from the southwest Indian Ocean (Malherbe et al., 2012) have all been quantified. Although it is generally accepted that a variety of weather systems contribute to rainfall over the Cape south coast, their relative contributions have not been quantified to date. For example, the relative contributions of ridging high pressure systems and cold fronts to rainfall over the region are not known. Knowledge of the relative contribution by the various configurations of cold fronts, ridging high pressure systems and tropical-temperate troughs can provide insight into the relevant circulation dynamics, which in turn can potentially be applied to improve rainfall forecasts over the region. The Cape south coast is a region with complex topography that can interact with the atmospheric circulation and modify the regional rainfall distribution (e.g. Singleton and Reason, 2006), as is evident from the presence of indigenous forests on the seaward side of the mountain ranges over the central parts of the region. Over these mountainous areas over the Cape south coast region, daily rainfall totals in excess of 0.25 mm and 10 mm occur on average about 80 and 30 days per year, respectively (Taljaard, 1996). Consideration of the various configurations within a particular rain-producing synoptic type can implicitly account for the topographical effect on rainfall, in particular when ridging high pressure systems are considered.

Interannual rainfall variability is an integral characteristic of climate over South Africa (Mason and Jury, 1997; Reason et al., 2002; Washington and Preston, 2006; Weldon and Reason, 2014). In comparison to the number of interannual rainfall variability studies performed over the summer and winter rainfall regions of South Africa, the Cape south coast has been neglected (Weldon and Reason, 2014), notwithstanding the Cape south coast region being an important agricultural region (Weldon and Reason, 2014). Large areas of this rainfall region are dependent on rainfed agriculture, whereas the areas that employ irrigation practices are dependent on rainfall maintaining dam levels at desirable levels. Sufficient dam levels are also crucial for household purposes as an increasing demand for water is experienced in the region due to rapid urban growth (Holloway et al., 2012). Given the importance of the agricultural sector for the economy of the region and this sector being vulnerable to the impacts of climate variability, this study explores interannual rainfall variability from a synoptic type frequency perspective since rainfall variability is the result of changes in the frequency, duration, intensity (Mason and Jury, 1997) and location (Hart et al., 2013) of rain producing weather systems. The anomalous behaviour of tropical-temperate interactions and frontal systems is generally linked to interannual rainfall variability over the summer and winter rainfall regions, respectively (e.g. Todd et al. 2004; Reason and Rouault, 2005). The frequency and location of rain-producing weather systems can in turn be affected by large-scale climate modes such as the Southern Annular Mode (SAM) (Reason and Rouault, 2005; Malherbe et al., 2014) and the El Niño Southern Oscillation (ENSO) (Mason and Jury 1997; Reason et al., 2000; Washington and Preston, 2006; Philippon et al., 2012). Changes in the location of rain-producing weather systems over the winter and summer rainfall regions of South Africa associated with SAM and ENSO are evident during wet and dry seasons. For example, wet winters over the southwestern part of the country are associated with the negative phase of SAM (Reason and Rouault, 2005) as well as with El Niño (Philippon et al., 2012). The variability in the location and frequency of tropical-temperate troughs (Todd et al., 2004; Fauchereau et al., 2009), an important contributor to summer rainfall (Hart et al., 2013), can be influenced by ENSO (Lindesay, 1988). El Niño events are usually associated with below-normal rainfall totals and the less frequent occurrence of tropical-temperate troughs over the central and eastern interior regions of South Africa. It may be noted that wet summers are not necessarily associated with increased tropical-temperate trough frequencies (Hart, 2012). Our current understanding of rainfall variability over the Cape south coast region is not as fully explored as that compared to the winter and summer rainfall regions of the country and is based on a few studies only (Jury and Levey, 1993; Weldon and Reason, 2014). It has been suggested that COLs and ridging high pressure systems play a part in interannual rainfall variability, in the sense that the occurrence of these systems are disrupted during dry years (Jury and Levey, 1993). There are also indications that an association exists between anomalous rainfall years over the Cape south coast, ENSO and COLs via increased COL frequencies observed during the mature phase of La Niña events (usually associated with wet conditions over South Africa) (Weldon and Reason, 2014). Dry years over the Cape south coast are usually associated with a lower frequency of COLs, but without an ENSO association. It has also been shown that during La Niña events, a link is observed with wet-day frequencies over the Cape south coast for the months of December and January (Weldon and Reason, 2014).

With the Cape south coast being largely an agricultural region, it can benefit from reliable rainfall forecasts, in particular forecasts on the seasonal time scale as most decision making in the agricultural sector is needed on a season to season basis. The predictability of rainfall over the Cape south coast region (at both short and long-range time scales) has remained relatively unexplored. Seasonal forecasting over South Africa has focused mostly on the summer rainfall region for the December to February period (e.g. Landman and Goddard, 2005) when the association between rainfall totals and the ENSO is known to exist. The most skillful seasonal forecasts are indeed found over the northeastern interior of South Africa during ENSO seasons (Landman and Beraki, 2012). For these forecasts, the seasonal mean of circulation (e.g. 850 hPa geopotential height) is used as predictor. This seasonal forecasting approach do not yield skill over the Cape south coast comparable to skill found over the remainder of the country and in particular over the northeastern interior.

In this study the synoptic types contributing to rainfall over the Cape south coast are objectively determined, and their respective roles in determining the seasonal cycle in rainfall over the region are investigated. Associations between the large-scale modes of variability (e.g. ENSO and SAM) with the intraseasonal distribution of synoptic types are subsequently explored, and the interannual variability of the intraseasonal frequencies of the synoptic types is described. Finally, the predictability of the intraseasonal frequency of different synoptic types at seasonal time scales is explored for the Cape south coast. If it can be shown that the intraseasonal variation in circulation over the Cape south coast can be predicted skilfully at interannual time scales, it will imply that skilful rainfall forecasts can be generated through the use of daily circulation statistics.

1.2 Research problem

From a climatological perspective, the relative contribution to rainfall over the Cape south coast by the different rain-producing systems and the various configurations of these systems have not been collectively quantified to date. The contributions from tropical-temperate troughs and COLs to rainfall over the country at station level have been determined (Favre et al., 2013; Hart et al., 2013) as these systems have long being recognized as important rainfall producing weather systems (e.g. Harrison, 1984; Taljaard, 1996) and from time to time are associated with high impact rainfall events (e.g. Hart et al., 2010; Singleton and Reason, 2006). With regards to the Cape south coast it is known that other synoptic weather systems, such as cold fronts and ridging high pressure systems also contribute to rainfall (Jury and Levey, 1993; Taljaard, 1996). As a first step to better understand the circulation dynamics responsible for the all-year nature of rainfall along the Cape south coast, quantification of the contribution by the different rain-producing weather systems is needed.

The Cape south coast is also known to be vulnerable to the impacts of interannual rainfall variability, even though variability here is not as pronounced as over the remainder of the country (Taljaard, 1996). Floods and droughts occur over the Cape south coast from time to time, with the impact of droughts being particularly severe due to urban growth in the region and an associated increase in water demand. New insight into the variability of synoptic types on interannual time scales and potential relationships with large-scale climate modes may lead to improved understanding and forecasts of climate variability over this region. However, rainfall variability studies concerning the Cape south coast is scarce and those that exist have not explicitly considered synoptic type characteristics and the frequency distribution of synoptic types in an attempt to better understand the variability. A synoptic type frequency distribution approach in studying rainfall variability can complement and potentially improve our current understanding of the underlying dynamics associated with rainfall variability. Furthermore, an improved understanding of the synoptic type frequency distribution can contribute to verification of climate model simulations of circulation over the region. If climate models are not able to simulate circulation systems realistically over the region, it may be challenging to reliably predict rainfall there with these models.

1.3 Aim and objectives of the study

Given the problem statement above, the aim of the research is to describe the contribution of different synoptic types to rainfall over the Cape south coast region, explore the potential association between synoptic type distributions within a season with interannual rainfall variability over the Cape south coast and then finally to investigate within-season predictability of synoptic type frequencies.

Hence the specific objectives are:

- To objectively identify the main synoptic types prevailing over the Cape south coast and to quantify the relative contribution of the different synoptic types in causing rainfall over the region.
- To gain more insight into the synoptic climatology responsible for the region's all-year rainfall uniqueness and the existence of the autumn and spring rainfall maximums. Even though the existence of these rainfall peaks is attributed to cut-off lows and ridging anticyclones as stated in the literature (e.g. Jury and Levey, 1993), there is no evidence that daily circulation patterns have already been explicitly and objectively analysed to support this notion.
- To determine the association between the frequency of synoptic types and interannual variability of seasonal rainfall.
- To investigate the influence of large-scale climate modes such as ENSO and SAM on rainfall variability over the all-year rainfall region, in particular in the context of the frequency of occurrence of circulation regimes that favour the occurrence of rainfall events.
- To investigate predictability of the intraseasonal synoptic type frequency distribution at the seasonal time scale

1.4 Thesis outline

Chapter 2 provides, in the form of an already published peer-reviewed journal paper, a synoptic decomposition of rainfall over the Cape south coast of South Africa. The contribution by the different rain-producing weather systems over the Cape south coast is quantified and the nature of the annual rainfall cycle is subsequently explored. In particular, the existence of the autumn and spring rainfall peaks is investigated. Particular attention is given to the role of COLs in explaining the nature of the annual rainfall cycle. Chapter 3, also presented in journal paper format, has been published online in a peer-reviewed journal. In this chapter, the links between interannual variability of seasonal rainfall over the Cape south coast of South Africa and different synoptic types as well as ENSO and SAM are explored. Chapter 4 is in the form of a journal paper under review, and investigates the predictability of within-season synoptic type frequencies at the seasonal scale by making use of a coupled global circulation model. Chapter 5 provides a summary of the main findings of the thesis, states the conclusions that can be drawn and makes some recommendations for future research related to this thesis.

Given that all figures and tables are specific to two published and an under-review paper, a list is not provided in the contents section. Furthermore, each paper (Chapter 2 – 4) is followed by the reference list specific to that paper and journal requirements. The reference list for this chapter (Chapter 1) is provided below.

1.5 References

Crimp SJ, van den Heever SC, D'Abreton PC, Tyson PD and Mason SJ. 1997. Mesoscale modelling of tropical-temperate troughs and associated systems over southern Africa. WRC Report 595/1/97, 395 pp.

Fauchereau N Pohl B, Reason CJC, Rouault M and Richard Y. 2009. Recurrent daily OLR patterns in the southern Africa/southwest Indian Ocean region, implications for South African rainfall and teleconnections. *Climate Dynamics* **32**:575-591.

Favre A, Hewitson B, Lennard C, Cerezo-Mota R and Tadross M. 2013. Cut-off lows in the South Africa region and their contribution to precipitation. *Climate Dynamics* **41**: 2331-2351. doi: 10.1007/s00382-011-1030-4.

Harrison MSJ. 1984. A generalized classification of South African summer rain-bearing synoptic systems. *International Journal of Climatology* **4**: 547-560.

Hart NCG, Reason CJC and Fauchereau N. 2010. Tropical-Extratropical Interactions over Southern Africa: Three Cases of Heavy Summer Season Rainfall. *Monthly Weather Review* **138**: 2608-2623.

Hart NCG. 2012. Synoptic-scale rainfall patterns over southern Africa: Scale-interactions with large-scale modes of variability. Unpublished PhD thesis. 99 pp.

Hart NCG, Reason CJC and Fauchereau N. 2013. Cloud bands over southern Africa: seasonality, contribution to rainfall variability and modulation by the MJO. *Climate Dynamics* **42**: 1199-1212. doi: 10.1007/s00382-012-1589-4.

Holloway A, Fortune G, Zweig P, Barrett L, Benjamin A, Chasi V and de Waal J. 2012. Eden and Central Karoo Drought Disaster 2009 – 2011; "The Scramble for Water." For the Provincial Disaster Management Centre, Western Cape by the Disaster Mitigation for Sustainable Livelihoods Programme, Department of Geography and Environmental Studies, Stellenbosch Unversity. 158 pp.

Jury MR, Levey K. 1993. The climatology and characteristics of drought in the eastern Cape of South Africa. *International Journal of Climatology* **13**: 629-641.

Landman WA and Goddard L. 2005. Predicting southern African summer rainfall using a combination of MOS and perfect prognosis. *Geophysical Research Letters* **32**: L15809, doi: 10.1029/2005GL022910.

Landman WA and Beraki A. 2012. Multi-model forecast skill for mid-summer rainfall over southern Africa. *International Journal of Climatology* **32**: 303-314. doi: 10.1002/joc.2273.

Lindesay JA. 1988. South African rainfall, the Southern Oscillation and a Southern Hemisphere semi-annual cycle. *Journal of Climatology* **8**: 17-30.

Malherbe J, Engelbrecht FA, Landman WA and Engelbrecht CJ. 2012. Tropical systems from the southwest Indian Ocean making landfall over the Limpopo River Basin, southern Africa: a historical perspective. *International Journal of Climatology* **32**: 1018-1032. doi: 10.1002/joc.2320.

Malherbe J, Landman WA and Engelbrecht FA. 2014. The bi-decadal rainfall cycle, Southern Annular Mode and tropical cyclones over the Limpopo River Basin, southern Africa. *Climate Dynamics* **42**: 3121-3138. doi: 10.1007/s00382-013-2027-y.

Mason SJ and Jury MR. 1997. Climatic variability and change over southern Africa: a reflection on underlying processes. *Progress in Physical Geography* **21**: 23-50.

Philippon N, Rouault M, Richard Y and Favre A. 2012. The influence of ENSO on winter rainfall in South Africa. *International Journal of Climatology* **32**: 2333-2347. doi: 10.1002/joc.3403.

Pohl B, Rouault M and Sen Roy S. 2014. Simulation of the annual and diurnal cycles of rainfall over South Africa by a regional climate model. *Climate Dynamics* **43**: 2207-2226. doi: 10.1007/s00382-013-2046-8.

Reason CJC, Allan RJ, Lindesay JA and Ansell TJ. 2000. ENSO and climatic signals across the Indian Ocean basin in the global context: Part 1, interannual composite patterns. *International Journal of Climatology* **20**: 1285-1327.

Reason CJC, Rouault M, Melice JL and Jagadheesha D. 2002. Interannual winter rainfall variability in SW South Africa and large scale ocean-atmosphere interactions. *Meteorology and Atmospheric Physics* **80**: 19-29.

Reason CJC and Rouault M. 2005. Links between the Antarctic Oscillation and winter rainfall over western South Africa. *Geophysical Research Letter* **32**: L07705. 10.1029/2005GL022419.

Singleton AT and Reason CJ. 2006. Numerical simulations of a severe rainfall event over the Eastern Cape coast of South Africa: sensitivity to sea surface temperature and topography. *Tellus* **58**: 355-367.

Singleton AT and Reason CJ. 2007. Variability in the characteristics of cut-off low pressure systems over subtropical southern Africa. *International Journal of Climatology* **27**: 295-310.

Taljaard JJ. 1959. South African airmasses: their properties, movement and associated weather. Ph.D. Thesis, University of the Witwatersrand, 221 pp.

Taljaard JJ. 1986. Change of rainfall distribution and circulation patterns over southern African summer. *International Journal of Climatology* **6**: 579-592.

Taljaard JJ. 1996. Atmospheric circulation systems, synoptic climatology and weather phenomena of South Africa. Part 6: Rainfall in South Africa. South African Weather Bureau, Technical paper 32

Todd M, Washington R and Palmer PI. 2004. Water vapour transport associated with tropical-temperate trough systems over southern Africa and the southwest Indian Ocean. *International Journal of Climatology* **24**: 555-568.

Washington R and Preston A. 2006. Extreme wet years over southern Africa: Role of Indian Ocean sea surface temperatures. *Journal of Geophysical Research* **111**: D15104, doi: 10.1029/2005JD006724.

Weldon D and Reason CJC. 2014. Variability of rainfall characteristics over the South Coast region of South Africa. *Theoretical and Applied Climatology* **115**: 177-185. doi: 10.1007/s00704-013-0882-4.

Chapter 2: A synoptic decomposition of rainfall over the Cape south coast of South Africa

Preface

This chapter consists of one published peer-reviewed paper as follows:

Engelbrecht CJ, Landman WA, Engelbrecht FA, Malherbe J (2015) A synoptic decomposition of rainfall over the Cape south coast of South Africa. *Climate Dynamics* **44**: 2589-2607. doi: 10.1007/s00382-014-2230-5

Towards reaching the first objective of the study, the contribution of various synoptic types to rainfall over the Cape south coast of South Africa is quantified in this paper. To determine the contribution of synoptic types to rainfall a synoptic climatology is derived by application of the self-organizing map (SOM) technique before rainfall is associated with each of the identified synoptic types. The seasonal cycle of rainfall over the Cape south coast is reassessed, and the synoptic types responsible for the autumn and spring rainfall peaks are identified. Additional to the synoptic type classification by application of a SOM, COLs were objectively identified and tracked in order to determine the contribution of COL- induced rain and the role they play in the observed autumn and spring rainfall peaks. To provide context of the limited extent of the all-year rainfall region and its unique seasonal cycle, comparisons are made to two adjacent regions in the interior to the north. The synoptic climatology derived in this paper is used in an investigation of interannual variability of seasonal rainfall and synoptic type association, presented in the next chapter.

The paper was co-authored with WA Landman, FA Engelbrecht and J Malherbe. The conceptualization of the paper, collection of all the data as well as the analysis performed in this paper were done by me.

A synoptic decomposition of rainfall over the Cape south coast of South Africa

C.J. Engelbrecht[1,2], W.A. Landman[2,3], F.A. Engelbrecht[3,4] and J. Malherbe[1]

1. Institute for Soil, Climate and Water, Agricultural Research Council, Pretoria, South Africa

2. Department of Geography, Geoinformatics and Meteorology, University of Pretoria, Pretoria, South Africa

3. Climate Studies, Modelling and Environmental Health, CSIR Natural Resources and Environment, Pretoria, South Africa

4. GAES, University of the Witwatersrand, Pretoria, South Africa

Abstract

A synoptic climatology is derived for the Cape south coast region of South Africa by application of the self-organizing map (SOM) technique. The SOM is applied to average daily low-level circulation fields, as represented by sea-level pressure (SLP) anomalies for the period 1979-2011. This coastal region receives rainfall all-year round with slight peaks during March-April and with more pronounced peaks during August and October-November. The synoptic forcing responsible for this annual multi-modal rainfall distribution is identified, and the relative contribution of different synoptic types to the annual rainfall is quantified. Ridging high pressure systems contribute to 46% of the annual rainfall, while tropical-temperate troughs contribute 28%. Cut-off lows (COLs) co-occurring with ridging highs and tropical-temperate troughs are associated with 16% of the annual rainfall total. The contribution of ridging high pressure systems decreases from south to north, whilst the opposite is true for tropical-temperate troughs. COLs, ridging high pressure systems and tropical-temperate troughs are associated with the March-April rainfall peak, while COLs are largely associated with the August rainfall peak. Ridging high pressure systems and to a lesser extent tropical-temperate troughs, are responsible for the October peak observed along the coast, while the November peak over the adjacent interior regions is associated with COLs that occur in combination with the tropical-temperate troughs during this month.

Key words: All-year rainfall region, Cape south coast of South Africa, Synoptic types, Cut-off lows, Ridging high pressure systems.

2.1 Introduction

The Cape south coast of South Africa (Fig. 1) receives rainfall all-year round, with peaks during autumn and spring (e.g. Taljaard 1996; Weldon and Reason 2014). The all-year nature of rainfall of this region is in strong contrast to the pronounced seasonality that characterizes rainfall over most of South Africa: the country is largely a summer rainfall region (e.g. Fauchereau et al. 2009), with winter rainfall occurring over the southwestern Cape area (Fig. 1) (e.g. Philippon et al. 2011). The southern areas of South Africa largely receive rainfall from organized synoptic-scale weather systems (Tennant and Hewitson 2002), whilst rainfall over the northern and eastern interior regions are mostly of a convective and sometimes tropical nature (e.g. Malherbe et al. 2012). The all-year rainfall region of the Cape south coast, which to some extent may be thought of as forming a boundary region between the winter and summer rainfall regions, is meteorologically one of the more complex regions of South Africa. Rainfall over the region results from well-defined mid-latitude systems, tropical systems and convection from the north, and complex interactions and linkages between these very different systems. Superimposed on the synoptic circulation there are also meso-scale circulation systems, which result from interactions of the larger scale flow with mountainous topography inland of the coastal area and the moisture laden air above the Agulhas current flowing along the Cape south coast of South Africa. (e.g. Rouault et al. 2002; Singleton and Reason 2006).

Mid-latitude weather systems bringing rainfall to the Cape south coast include cold fronts, west-wind troughs, cut-off lows and ridging high pressure systems (e.g. Taljaard 1996; Favre et al. 2013; Weldon and Reason 2014). When rainfall over the region is of a tropical nature, it is usually from tropical-temperate trough cloud bands (e.g. Taljaard 1996; Hart et al. 2013). Of the different rain bearing systems, it is mostly COLs that are associated with high-impact events over the region. In fact, across South Africa, COLs are known to on occasion produce 24-hour rainfall totals exceeding the relevant climatological monthly rainfall total at particular locations (e.g. Singleton and Reason 2006; Singleton and Reason 2007a; Muller et al. 2008). These systems can be extremely hazardous, producing floods with consequent damage to infrastructure and sometimes loss of life (Weldon and Reason 2014). An important example is the Laingsburg floods of January 1981, in which 104 people drowned in a flood of the Buffels river (Roberts and Alexander 1982; Singleton and Reason 2007b). To date, the most rainfall that has been recorded from a single COL event occurred during September 1987 when the 3-day rainfall total along the KwaZulu-Natal coast exceeded 900 mm (Singleton and Reason 2007b). COLs have also been associated with numerous extreme rainfall events along the Cape south coast (e.g. Hayward and van den Berg 1968; Hayward and van den Berg 1970; Rouault et al. 2002; Singleton and Reason 2006; Singleton and Reason 2007a), with the COL event during September 1968 causing floods in the Port Elizabeth area as 500 mm rain fell within 24-hours. These high-impact rainfall events may have led to a perception that COLs are the main rain-producing weather systems over the region.

However, the relative contributions of different weather systems in causing rainfall over the Cape south coast have not been formally quantified. Recently, the contribution of COLs to rainfall over the southern African region has been analysed by Favre et al. (2013). COLs have been shown to explain a higher proportion (more than 20%) of rainfall totals over the Cape south coast compared to the winter and summer rainfall regions (Favre et al. 2013). For this region, the largest contribution of COLs to rainfall is experienced during the period July to September (JAS), compared to the periods October to December (OND), April to June (AMJ) and January to March (JFM) when the lowest contribution of COLs to rainfall is experienced (Favre et al. 2013). Apart from COLs, ridging high pressure systems have also been recognised as important in contributing to rainfall over the mountainous regions bordering the Cape south coast (e.g. Weldon and Reason 2014). In fact, it has been suggested that COLs are responsible for the autumn rainfall peak, with ridging high pressure systems driving the spring rainfall peak over the all-year rainfall region (Jury and Levey 1993). However, the contribution of ridging high pressure systems to rainfall over the Cape south coast has not been quantified to date. The weather system responsible for the bulk of summer rainfall over the southern African region is the tropical-temperate trough, characterized by a north-west to south-east aligned cloud band that develops as a result of the interaction between a tropical low and a temperate westerly wave by means of a subtropical trough (Washington and Todd 1999). Tropical-temperate troughs cause on the average about 39% of rainfall over the summer rainfall region (Crimp et al., 1997). The maximum frequency of occurrence of tropical-temperate troughs is during November (Hart et al. 2013), when they are also responsible for 30-60% of rainfall occurring along the Cape south coast (Hart et al. 2013). Their relative contribution for December remains high (30-50%) (Hart et al. 2013).

The main aims of this paper are to objectively determine the relative importance of different synoptic types in causing rainfall over the Cape south coast, and to gain more insight into the synoptic climatology that results in the region's all-year rainfall uniqueness. Of particular interest is the relative importance of ridging highs in causing rainfall over the Cape south coast (i.e. compared to COLs). Interactions between ridging highs and COLs, and tropical-temperate troughs and COLs in causing rainfall over the region are also considered.

2.2 Data and methodology

2.2.1 Weather station data

Rainfall station data for the Cape south coast and adjacent interior extending to the southern escarpment were selected based on completeness (more than 66% of the days in a particular month need to be present and pass data quality tests) of daily rainfall records for the period 1979-2011. Twenty-two weather stations from the South African Weather Service (SAWS) complied with the desired criteria (see Fig. 1 for the locations of the selected stations). The selected station data were subjected to extreme and missing value tests to ascertain data quality. Entries failing these tests were replaced by estimated values derived from neighbouring stations. The beginning of the study period was selected to be 1979, as reanalysis data from the National Centers for Environmental Prediction (NCEP) (Kalnay et al. 1996) prior to 1979 do not have the advantage of satellite data being incorporated into the reanalysis procedure (Tennant 2004). The station data are used in the research to quantify the contribution of different synoptic types to rainfall over the Cape south coast and adjacent interior regions.

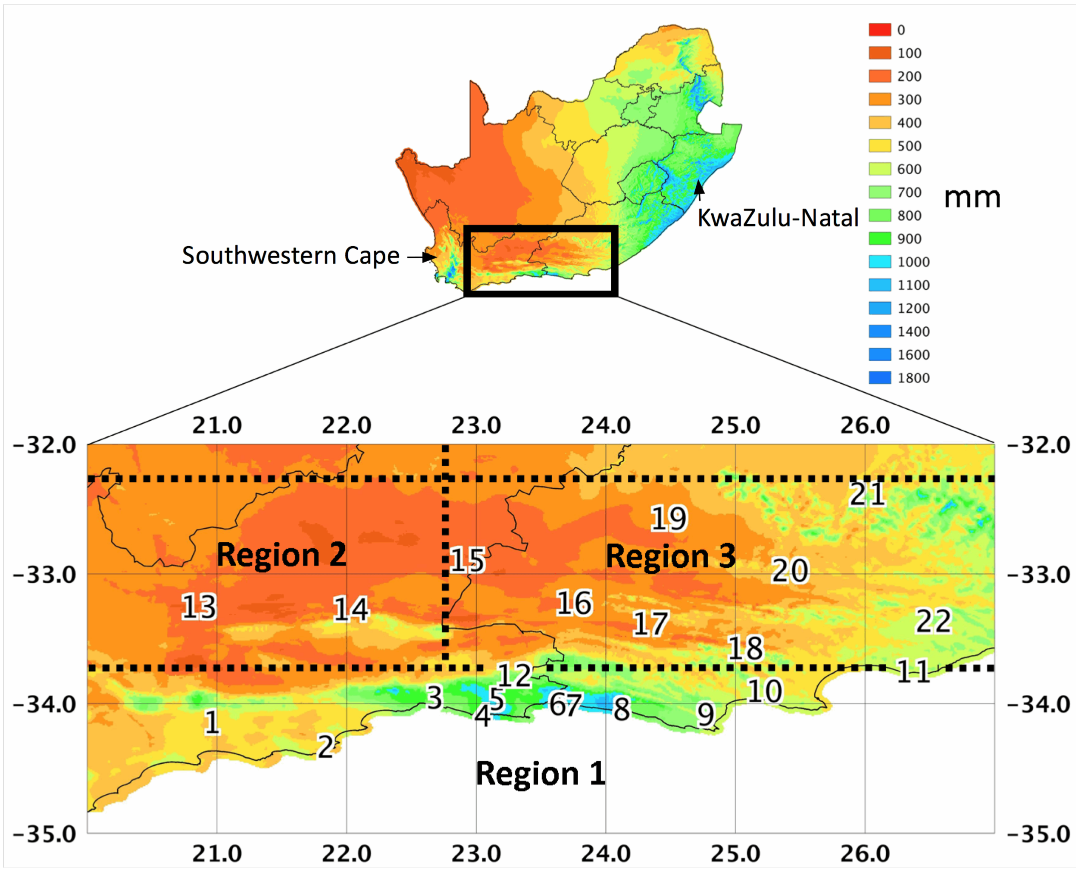

Fig. 1 The geographic location of the study region within South Africa (indicated by the rectangle - solid black lines). The 3 sub-regions of interest, labeled as Region 1, Region 2 and Region 3, are delineated by the black dotted lines on the zoomed-in view of the study region. Numbers 1 to 22 indicate the selected rainfall stations used in the analysis of rainfall attributes. The background shaded color contours of the mean annual rainfall are based on the ARC in-house developed gridded rainfall dataset

2.2.2 Gridded data

Two independently constructed gridded rainfall datasets, the Famine Early Warning System (FEWS) and the Climatic Research Unit (CRU) version TS3.1, were utilized for the delineation of the all-year rainfall region. Gridded data were used for this purpose rather than the station data described above, due to the uneven distribution in space of stations with records of sufficient length and quality. The FEWS data are a merged satellite-gauge gridded daily rainfall dataset with a resolution of 0.1˚ longitude by 0.1˚ latitude, with records commencing in January 1983 (Sylla et al. 2013). The CRU TS3.1 monthly gridded rainfall dataset has a resolution of 0.5˚ longitude by 0.5˚ latitude, is based solely on station data and is available for the period 1901 to 2009 (Harris et al. 2014). The all-year rainfall region may be defined using the following criteria as guidelines:

- The ratio of the rainfall amount for the month of minimum rainfall to rainfall of the month of maximum rainfall is relatively high compared to regions of strong seasonality.
- Each month of the year needs to be associated with at least 5% of the annual rainfall. This 5% threshold is based on graphs produced by Taljaard (1996), where the monthly contribution to the annual rainfall for various rainfall regions as identified by van Rooy (1972) is presented.
- The average monthly fluctuation of rainfall relative to the average monthly rainfall over the all-year rainfall region should be small compared to that of the winter and summer rainfall regions (see Section 3 for details).

It may be noted that prior to using the gridded datasets for the purpose of identifying the spatial extent of the all-year rainfall region, it was first established that these rainfall sets sufficiently describe the annual rainfall cycle over South Africa. This was achieved through a comparison of the monthly rainfall climatologies of the gridded datasets against those of the selected weather stations, as well as those of a third gridded rainfall climatology. The latter was developed at the Agricultural Research Council (ARC), using station data from both the ARC and SAWS. Despite the general underestimation of rainfall totals over Africa in FEWS data, in particular over regions of orography (Sylla et al. 2013), both datasets have been found to give representations of the area of all-year rainfall consistent with the raw weather station data and the mentioned ARC dataset. The mean annual distribution of rainfall over South Africa, as described by the ARC dataset, is shown in Figure 1. Note that mean annual rainfall totals exceeding 1000 mm occur in places along the Cape south coast.

2.2.3 Atmospheric circulation data

Daily averaged sea-level pressure (SLP) and geopotential height data of the 850, 700, 500 and 200 hPa pressure levels from NCEP reanalysis data, NCEP 1 (Kalnay et al. 1996), for the period January 1979 to December 2011 are utilized. The NCEP data has a horizontal resolution of 2.5° by 2.5° and a vertical resolution of 17 pressure levels. The daily weather over the Cape south coast region is strongly dependent on the low-level circulation, and the main source of moisture is the ocean. In particular, major rainfall events over the region are associated with the low-level moisture flux originating from the Agulhas current to the southeast (e.g. Rouault et al. 2002; Singleton and Reason 2006; Singleton and Reason 2007a). Therefore, daily SLP is employed for the identification of low-level circulation patterns.

2.2.4 Weather pattern identification

Weather patterns that influence the Cape south coast region of South Africa were objectively identified by application of the self-organizing map (SOM) technique (Kohonen 2001). The technique is based on an unsupervised nonlinear clustering algorithm that organizes the input data into a user-specified number of nodes that span the continuum of types in the input data. The technique is well suited for weather pattern identification where the daily transitions between weather patterns are important (Hewitson and Crane 2002). SOMs are increasingly being employed in climate studies focusing on the southern African region (e.g. Hewitson and Crane 2002; Tennant and Hewitson 2002; Tozuka et al. 2014; Van Schalkwyk and Dyson 2013). NCEP reanalysis daily averaged SLP data for the period 1979-2011 was used to develop a SOM relevant to the Cape south coast region. Atmospheric circulation, here the SLP circulation, is driven by the SLP gradients and do not depend on the actual magnitudes of the SLP (Schuenemann et al. 2009). To obtain the required daily gradient fields, the daily domain average of SLP was subtracted from the SLP at each grid point. The SOM was constructed for the region 45º S to 32.5º S and 10º E to 40º E. The selected region allows for capturing the progression of high pressure systems and troughs, advancing from west to east, to the south of the Cape south coast. The northern boundary of the SOM region was purposefully selected to extend to only 32.5º S. If this boundary is chosen further to the north, to include most of the interior of South Africa, the synoptic types identified by the SOM are dominated by the prevailing wintertime high pressure systems over the interior. Furthermore, SLP is used as a variable to develop the SOM, as the circulation over the oceans bordering the subcontinent is crucial in inducing rainfall over the Cape south coast (see Section 2.3). It may be noted that tropical-temperate trough linkages are captured with the SOM configuration as described, even though the northern boundary of the SOM region is limited to the extreme southern parts of the interior (see Section 3). The typical SLP patterns associated with COLs (e.g. Taljaard 1985; Tennant and van Heerden 1994) are also captured. For the purpose of this study, it is appropriate to apply a relatively large SOM to avoid over generalizing the richness of weather patterns that occur over the region into a too small number of nodes (synoptic types). SOMs that classify daily SLP circulation into 12, 20 and 35 synoptic types, respectively, have been considered. It was found that the 12 and 20 node SOMs do not capture the various stages of sea-level anticyclones, ridges and troughs adequately. Of particular importance, is that the known variations in the position and amplitude of SLP ridges and troughs that are representative of weather patterns ranging from weak synoptic flow to tropical-temperate troughs and COLs, are well represented in the SOM. Capturing the variations in ridging anticyclones is important as the rainfall produced by these systems is influenced by the nature of the onshore flow onto the coastal mountains (e.g. Taljaard 1985; Weldon and Reason 2014). Topographically induced rainfall occurs on the seaward side of the west-east orientated Cape Folded mountain range along the Cape south coast (Philippon et al. 2011), where strong topographic gradients are found (Singleton and Reason 2006). Figure 2 shows a map of the topography as represented by the Shuttle Radar Topography Mission (SRTM) Digital Elevation Model (DEM) data (Weepener et al. 2012). Some peaks of the Cape Folded mountain range are of comparable elevation to the mountains found over the interior plateau located further northwards (Fig. 2).

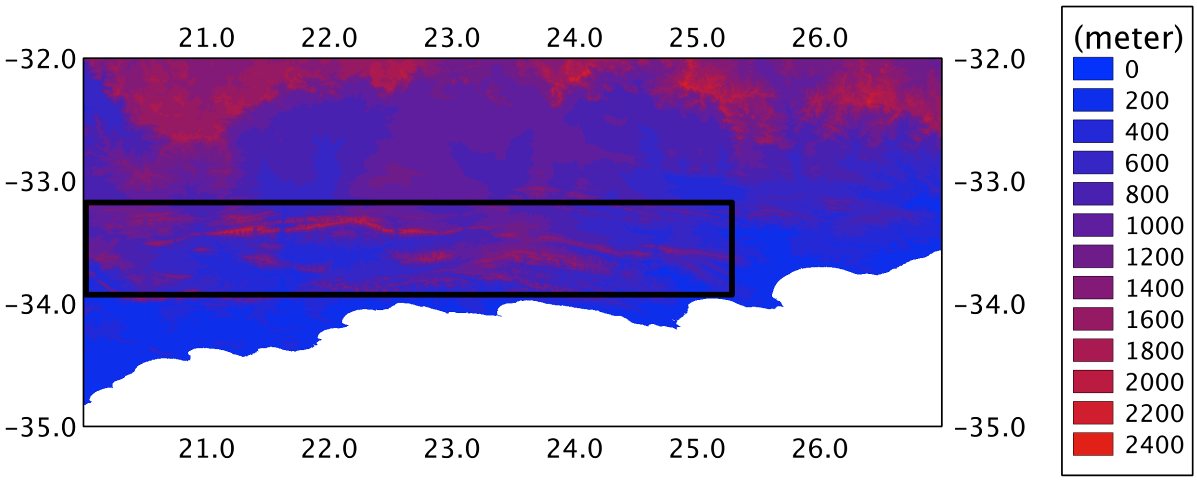

Fig. 2 Topography of the Cape south coast as represented by SRTM DEM data. The Cape Folded mountain range is indicated by the black rectangle.

Following Schuenemann et al. (2009), the statistical significance of the frequency for which the daily SLP anomalies map to each node is determined by calculating a 95% confidence interval around the probability that any daily SLP anomaly would map to any node (2.86% for the 7x5 SOM used in this study). By assuming that the process is binomial, the 95% confidence limits are calculated by

$$p \pm 1.96 \left[\frac{p(1-p)}{n}\right]^{1/2},$$

where p is 2.86% (the probability that any daily SLP anomaly field would map to any node) and n is 12053 (number of daily SLP anomaly fields). The calculated confidence interval around 2.86% is 2.56 to 3.15%. The observed frequency of a node is considered significantly different from 2.86% at the 95% confidence level if it falls outside this calculated interval.

2.2.5 Identification of cut-off lows

On the average, only about 11 COLs occur annually over the southern African region (Singleton and Reason 2007b), implying that these systems would not feature as a stand-alone synoptic type in the 7x5 SOM based on daily circulation fields presented in this paper. Indeed, COLs may occur in conjunction with a number of different low-level circulation patterns - most commonly in association with a strong ridge of high pressure in the low-levels polewards of the upper COL (e.g. Taljaard 1985; Tennant and van Heerden 1994; Katzfey and McInnes 1996; Favre et al. 2012), in combination with tropical-temperate troughs (Hart et al. 2013), and further, as a COL system evolves, in association with the evolving high pressure system (ridging progressively from the southwest to southeast of South Africa). The typical low-level circulation associated with tropical-temperate troughs - a meridional trough that links the Angola low and a mid-latitude wave/cyclone, is illustrated in Tennant (2003) and Hart et al. (2010, 2012). An objective tracking methodology is therefore used in order to study the effects of these important rainfall producing systems on rainfall attributes over the Cape south coast region.

NCEP reanalysis data (Kalnay et al. 1996) was utilized for the purpose of identifying and tracking COLs over the period 1979-2011. Over South Africa, COLs exhibit a typical length scale of 1000 km (e.g. Singleton and Reason 2007b) and are therefore well resolved on the 2.5˚ resolution grid of the NCEP data. In this paper, a COL is defined as a closed-low (a local minimum in the geopotential height at the 500 hPa level) that possesses a cold core, following the criteria used by Favre et al. (2012). The daily-average geopotential height and temperature fields at 500 hPa are utilized for identifying and tracking COLs. All COLs that occurred for at least 24-hours within the domain bounded by 40˚ S – 20˚ S and 10˚ E – 40˚ E are considered in this study. The closed-lows are identified and tracked by applying an objective, automated tracking algorithm. Geopotential minima are identified by comparing the geopotential of each grid point in the domain bounded by 40˚ S – 20˚ S and 10˚ E – 40˚ E, to the geopotential values of the square of eight surrounding grid points on the latitude longitude grid. Closed-low tracks are constructed by identifying the geopotential minima of time step $t+1$ nearest to the geopotential minima at time step t, provided that this distance is less than 1000 km. This distance implies that closed-lows are assumed to have a mean daily speed that do not exceed 42 km/h (Favre et al. 2012). The tracking procedure is developed in such a manner that any geopotential minima can only be part of a single track (see Engelbrecht et al. 2013 for details). To identify the COL tracks from the database of closed-low tracks, the approach utilized by Favre et al. (2012) is applied in this study. All the closed-low tracks identified through the procedure outlined above are subsequently subjected to tests described in Favre et al. (2012) to ensure that it is of extra-tropical origin, detached from the westerlies and has a cold-core. Figure 3 and 4 show the geographical distribution (expressed as the number of COL days per grid point) and the annual cycle in the number of COLs for the domain 40˚ S – 20˚ S and 10˚ E – 40˚ E respectively. There are two geographical regions of preferred COL day occurrence, namely in the Mozambique Channel as well as over the Atlantic Ocean extending in over the southwestern part of South Africa (Fig. 3). The spatial pattern of the geographical distribution of COL days identified in this study is in good agreement with that of Favre et al. (2013), while the two regions of preferred COL occurrence correspond with the two quadrants representative of the highest frequency distribution of the number of COLs as found by Singleton and Reason (2007b). COL events peak during autumn (Fig. 4, March-May) with the least occurrence in November-January (Fig. 4), consistent with the findings of Taljaard (1985), Singleton and Reason (2007b) and Favre et al. (2013).

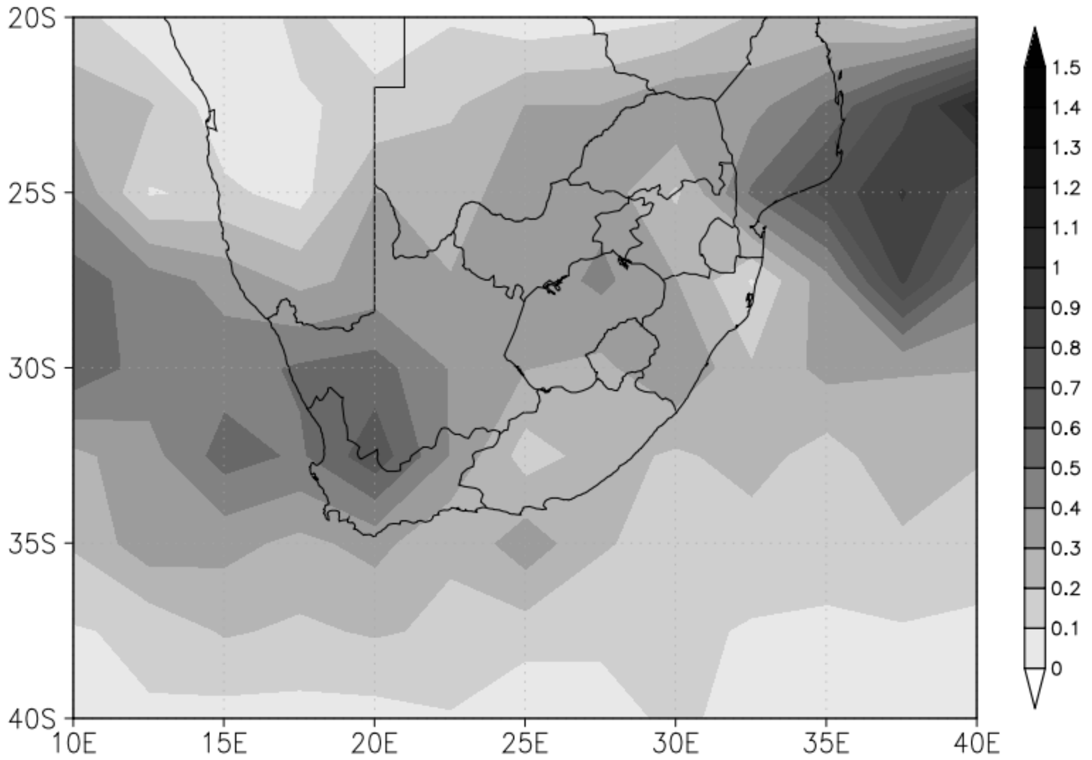

Fig. 3 Mean annual COL frequency over the domain 40˚ S – 20˚ S and 10˚ E – 40˚ E expressed as the number of COL days per grid point

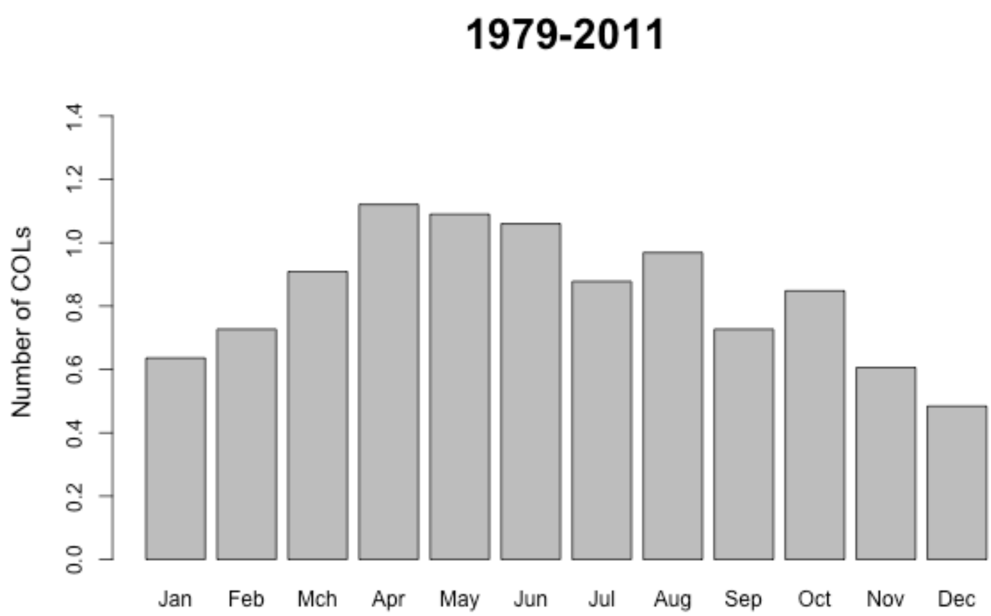

Fig. 4 Annual cycle of COLs over the domain 40˚ S – 20˚ S and 10˚ E – 40˚ E expressed as the monthly mean number of COL events

Rainfall associated with cold-cored systems occurs mainly some hundreds of kilometers to the northeast, east and southeast of the centers of these systems (Taljaard 1995). From the constructed COL dataset for the period 1979-2011, all the COLs that occurred west of 32.5 °E were considered to be potentially responsible for rainfall over the region (e.g Favre et al. 2013). Such COLs associated with rainfall over the study region, at least at a single station, are defined as rainfall producing COLs. Finally, for each day that a COL was identified as a rain-producing weather system over the study area, the circulation of that day was mapped onto the synoptic types identified by the SOM. This enables the identification of the synoptic types that are most frequently associated with COLs that influence the study area.

2.2.6 Relating rainfall to the identified synoptic types

To relate rainfall to the main synoptic types identified by the SOM, daily rainfall data (1979-2011) for weather stations in the Cape south coast region and adjacent interior were mapped to the SOM. That is, for each day in the time series the relevant circulation pattern may be associated with one of the SOM's synoptic types (e.g. Tennant 2003). The corresponding daily rainfall totals are subsequently associated with the relevant synoptic type, on a station-by-station basis. This enables calculating the percentage of annual rainfall associated with a specific synoptic type for each station in the region. Note that the study region allows for the contributions of different synoptic types to rainfall over the all-year rainfall region to be compared to contributions to rainfall over the summer rainfall region to the north (Fig. 1). The spatial distribution of rainfall over the study region exhibits a marked north-south gradient, with annual rainfall totals exceeding 1000 mm along the Cape Folded mountain range in the south whilst less than 200 mm of rain is observed over the Karoo just north of the Cape Folded mountain range. Further to the east, over the interior of the study region, the annual rainfall totals vary between 300 and 700 mm. These different rainfall distributions were used to identify 3 separate regions for which rainfall was categorized according to the different synoptic types (see Section 3 for details). The percentage contribution by each node to the annual rainfall for a particular region was calculated by averaging the percentage contributions to rainfall recorded at each of the weather stations in the particular region.

2.3 Results

2.3.1 Attributes of rainfall over the Cape south coast and adjacent regions

2.3.1.1 Spatial extent of the all-year rainfall region

Application of the criteria describing all-year rainfall attributes (see Section 2.2) on CRU TS3.1 and FEWS mean monthly rainfall data, yields remarkably similar spatial patterns (Fig. 5) – across the 3 different metrics, and across the 2 data sets. Qualitatively, the metrics indicate that the spatial extent of the area receiving rainfall all-year round along the Cape south coast is found within the collective boundaries described in other studies (e.g. Taljaard 1996; Landman et al. 2001; Rouault and Richard 2003; Weldon and Reason 2014). Along the coast, the all-year rainfall region is found approximately between 21° E and 27° E, while its northern extent is mostly restricted by the Cape Folded mountain range (Fig. 2). The extent of the all-year rainfall region is well illustrated by the metric of the number of months of the year that receive 5% or more of the annual rainfall. In both CRU (Fig. 5c) and FEWS (Fig. 5d), 11-12 months of the year satisfies the criteria over the mentioned area. Weather stations number 1 to 12 in Figure 1 are located in this region – and all receive 5% or more of the annual rainfall total during each month of the year. This region will be referred to as Region 1 in the study and from here onwards is regarded to define the Cape south coast (or all-year rainfall) region. The data from weather stations number 1 to 12 as seen on Figure 1 are used for the analysis concerning rainfall attributes of Region 1. From the western part of the all-year rainfall region along the Cape south coast, a relatively narrow region that exhibits pseudo all-year rainfall characteristics extends northwards, to the east of the western escarpment (see the arrows in Figs. 5c and 5d). As the main focus of this study is on the Cape south coast, this secondary all-year rainfall region is analysed separately as Region 2. It is defined to have 32.3 °S as northern boundary and 22.8 °E as eastern boundary, and includes weather stations number 13 and 14 (Fig. 1). For these two stations all months, with the exception of September, receive 5% or more of the annual rainfall. Region 3 comprises of weather stations number 15 to 22. Region 3 exhibits summer rainfall characteristics, as seen in the ratio of the month of minimum rainfall to the month of maximum rainfall (Fig. 5a, b). For the stations located in this region, at least 3 months receive on the average monthly rainfall totals that are less than 5% of the annual rainfall. It may finally be noted that there is a small area along the north coast of KwaZulu-Natal that also exhibits all-year rainfall attributes, according to the metrics presented in Figure 5. The circulation dynamics of this region are likely to be very different to that of the Cape south coast, and its investigation falls beyond the scope of the current paper.

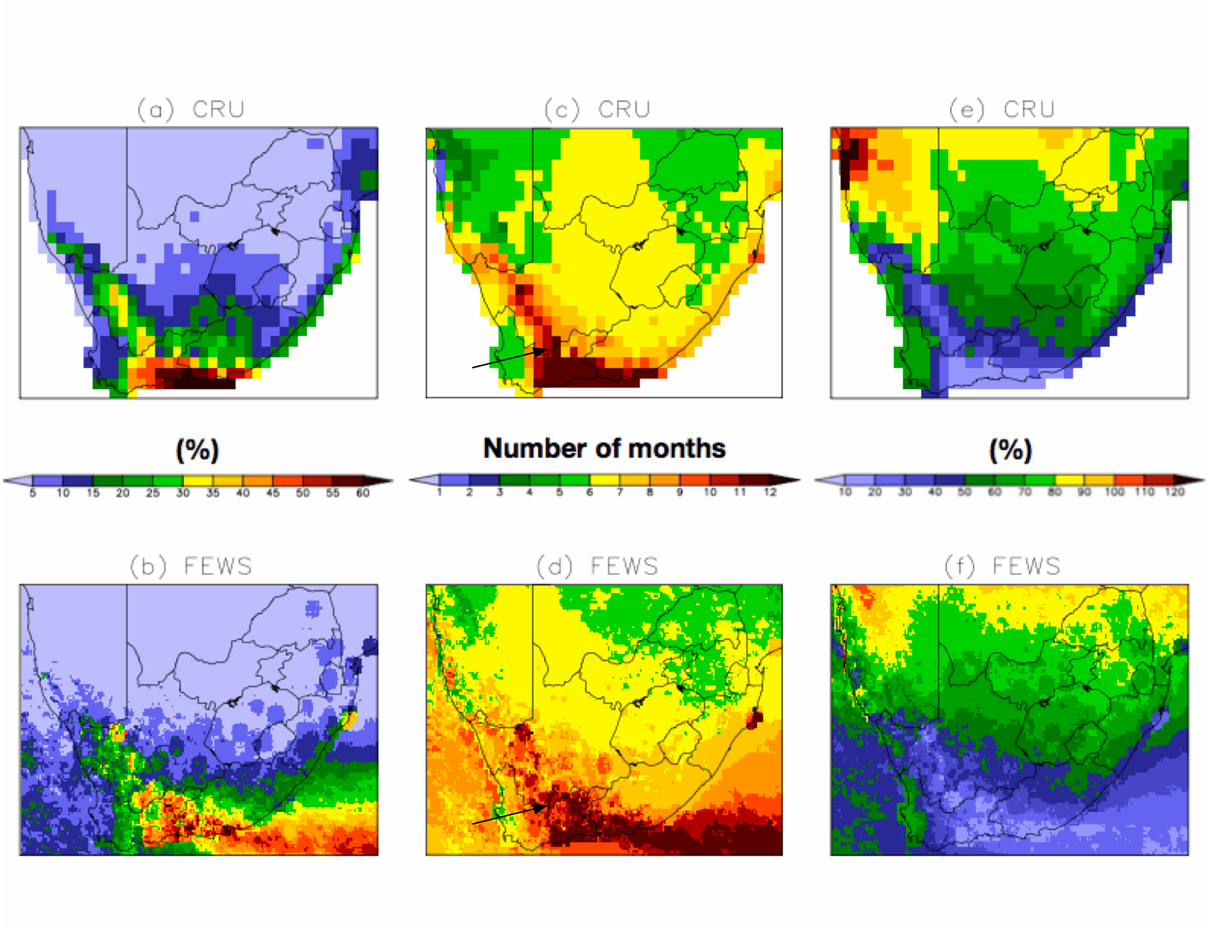

Fig. 5 Delineation of rainfall regions in South Africa according to the ratio of the month of minimum rainfall to the month of maximum rainfall (a, b), the number of months for which the mean monthly rainfall total contributes 5% or more to the mean annual rainfall total (c, d), and the average fluctuation of monthly rainfall from the monthly mean rainfall expressed as a percentage (e, f), calculated from CRU (a, c, e) and FEWS (b, d, f) data for the period 1983-2009

2.3.1.2 Annual rainfall cycle

The annual rainfall cycle over Region 1 (based on the monthly rainfall totals averaged over weather stations number 1 to 12) exhibits 3 peaks (Fig. 6). These peaks occur during March-April, August and October, with the October peak of 80 mm being the highest (monthly totals averaged over the period 1979-2011 are shown). A rainfall hiatus occurs in September. Region 2 has rainfall peaks during April and November (based on weather stations number

13 and 14), with April the month with the highest rainfall total. Over Region 3, a summer rainfall region, rainfall peaks over the period November to March. The November peak is slightly higher than the February-March peak. The September rainfall hiatus is present over Regions 2 (Fig. 6b) and 3 (Fig. 6c) as well, although less prominent in amplitude compared to the Region 1 hiatus. (Fig. 6a). A key objective of the paper is to explain the existence of the three rainfall peaks of Region 1, from a synoptic type perspective.

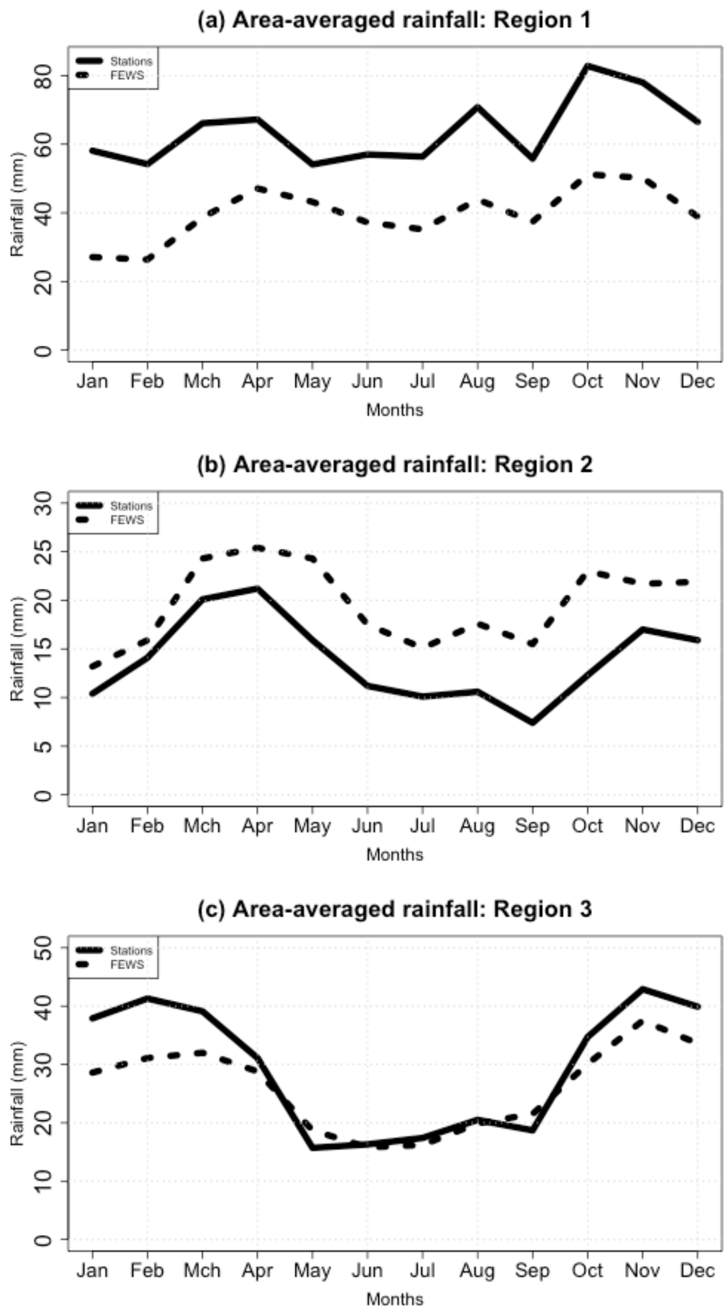

Fig. 6 Area-averaged annual rainfall cycle for the period 1979-2011 over (a) Region 1, (b) Region 2 and (c) Region 3 as described by weather station data (solid line) and FEWS rainfall (dotted line)

Regarding the delineation of the all-year rainfall region, the application of the all-year rainfall criteria on CRU and FEWS rainfall data produced in general similar results and is useful to describe the spatial extent of the region (Fig. 5). Application of the criteria to the weather station data produced consistent results. Similarly, the annual rainfall cycle described by the weather station data for Regions 1 to 3 is qualitatively captured by the FEWS rainfall estimates (Fig. 6) and CRU data (not shown). That is, despite the monthly rainfall totals being underestimated by FEWS, the annual rainfall cycle with respect to the peaks and September hiatus is captured. All subsequent rainfall analyses presented in this study are based on the weather station data.

2.3.2 Synoptic type classification

Figure 7 shows the synoptic type classification produced by the SOM algorithm. Each node in the SOM represents a single SLP anomaly pattern representative of a portion of the 12053 daily patterns used to train the SOM. The frequency of occurrence for each of the nodes is indicated at the top right of the relevant node, with the node number shown at the top left (Fig. 7).

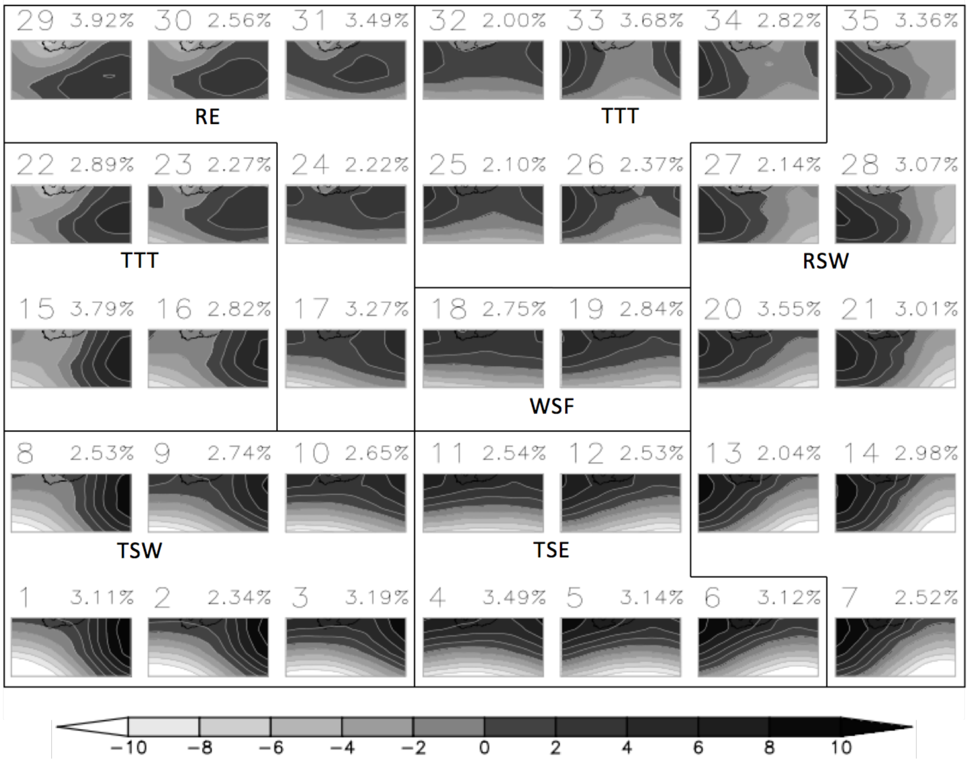

Fig. 7 SOM of SLP anomalies (hPa) based on daily NCEP reanalysis data from 1979 to 2011. Anomaly SLP contour interval is 2 hPa. Light and dark shades represent negative and positive SLP anomalies, respectively. The node numbers as well as the node frequency of occurrence are indicated on the figure. Nodes occurring outside the range of 2.56-3.15%, have lower or higher than average occurrences statistical significant at the 95% confidence level. Clustering of the main synoptic types is indicated and represent ridging high pressure systems southeast of the subcontinent (RE), tropical-temperate troughs (TTT), troughs southwest of the subcontinent (TSW), troughs southeast of the subcontinent (TSE), ridging high pressure systems from the southwest (RSW) and weak synoptic flow (WSF)

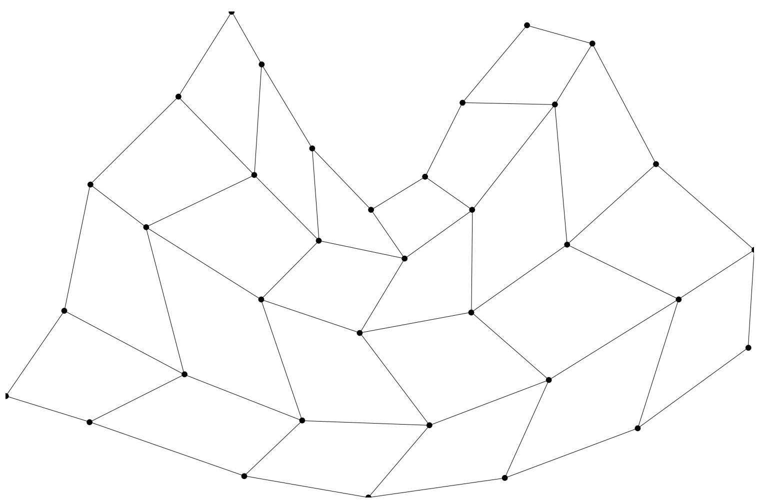

Fig. 8 Sammon map for the SOM shown in Fig. 7

On a SOM, similar synoptic patterns are grouped together with nodes characterized by very different patterns being further apart. From the Sammon map shown in Figure 8 it can be seen that the nodes in the top half of the SOM, in particular the top-middle region, are more similar to adjacent nodes compared to the nodes found in the lower half of the SOM. Generally, the lower part of the SOM is occupied by circulation patterns typical of winter, the upper part by circulation patterns typical of summer and the central part by circulation patterns occurring throughout the year. The spatial rainfall distribution associated with the SOM nodes, represented by composites derived from FEWS data and expressed as mm/day, is shown in Figure 9. The synoptic patterns differentiate between distinct rainfall patterns, including rainfall maxima over the Southwestern Cape (e.g. nodes 1-5) tropical-temperate rainband events (e.g. nodes 22, 23, 26, 33), rainfall maxima over the east coast (e.g. nodes 27, 28, 35) and typical summer convection over central and eastern South Africa (e.g. nodes 17-19). The nodes that occur most frequently during each month of the year may be discerned from analysis presented in Figure 10. The circulation patterns represented in the lower left corner of the SOM (Fig. 7) are strong frontal troughs that occur most frequently during June to August (Fig. 10g, h, i). For September (Fig. 10j), the nodes occurring most frequently are placed in the lower right corner of the SOM. Here, the paths of the frontal troughs are displaced slightly polewards compared to the winter tracks, allowing for the Atlantic Ocean High (AOH) to extend a ridge along the southern coastal belt of the subcontinent, mainly overland. At the start of the summer season (Fig. 10k, l) and during December (Fig. 10a), ridging high pressure systems from the southwest ridge from further south (nodes middle and upper right part of the SOM) as the frontal troughs continue to be displaced polewards, with a cell of high pressure moving eastwards to be situated southeast of the subcontinent (upper left corner of the SOM). For January, February and March (Fig. 10b, c, d), the nodes in the upper part of the SOM represent the dominant synoptic types. These nodes are representative of the various configurations of tropical-temperate troughs, transforming to tropical-temperate linkages over the western interior during April (Fig. 7 node 15, Fig. 10e). By May (Fig. 10f), the nodes representative of frontal troughs that have migrated equatorward after the summer months, are becoming more frequent again.

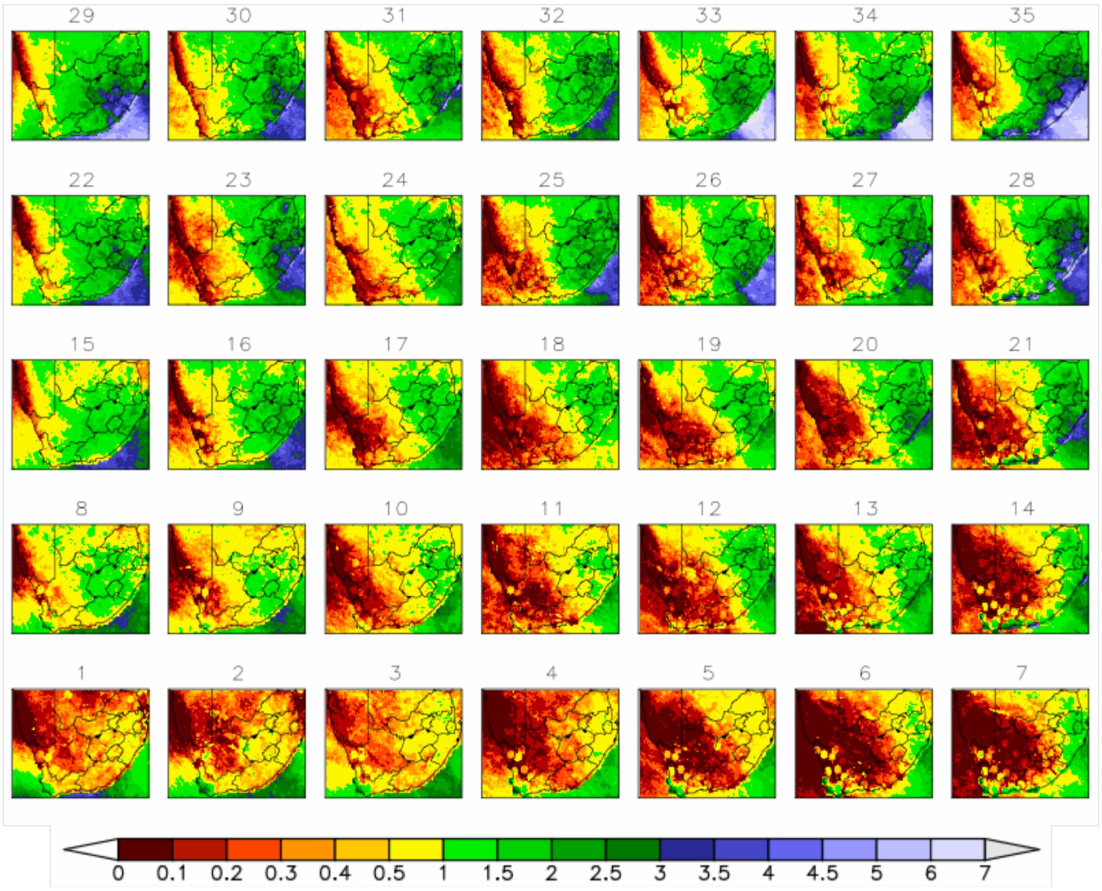

Fig. 9 Rainfall composites expressed as mm/day derived from FEWS data for the period 1983-2011 for each of the SOM nodes as seen in Fig. 7

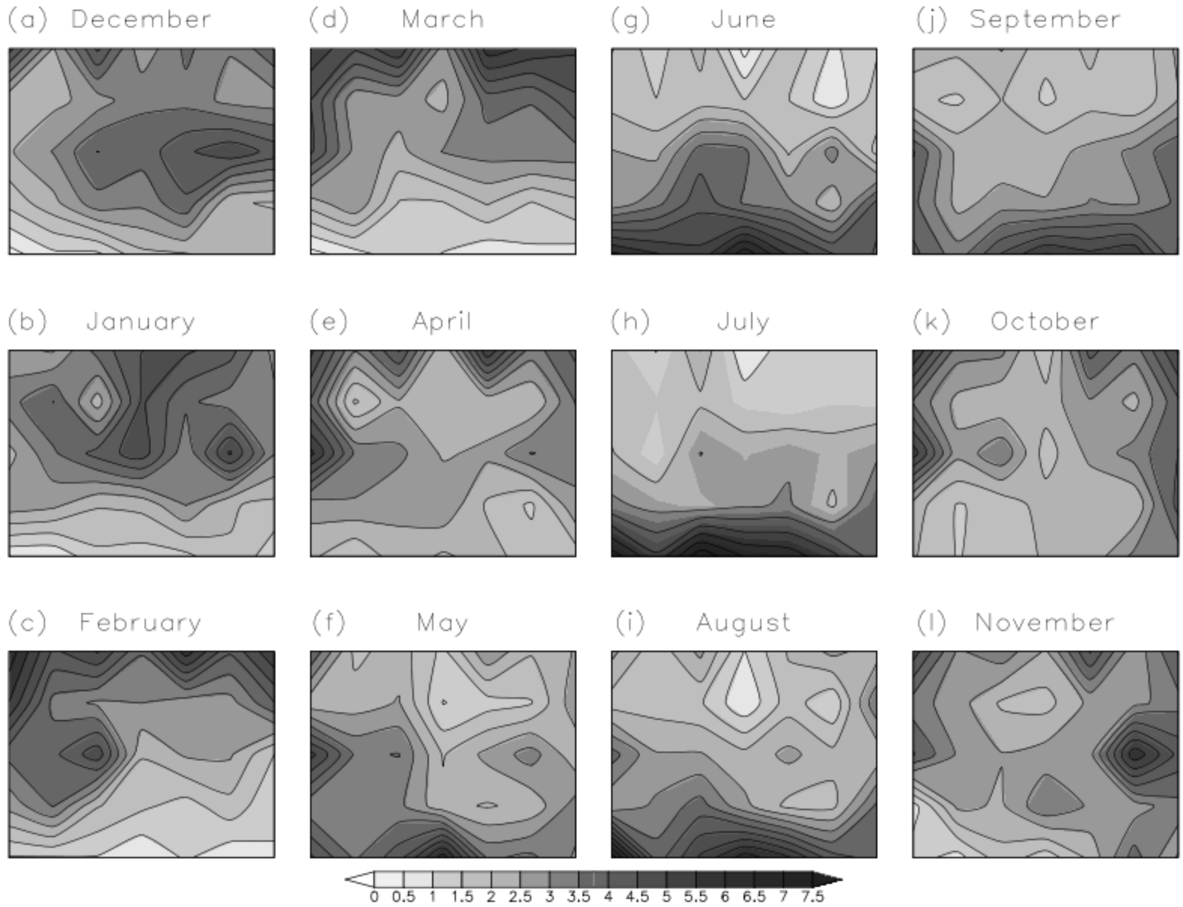

Fig. 10 Node frequencies (%) for (a) December (1023 days), (b) January (1023 days), (c) February (932 days), (d) March (1023 days), (e) April (990 days), (f) May (1023 days), (g) June (990 days), (h) July (1023 days), (i) August (1023 days), (j) September (990 days), (k) October (1023 days) and (l) November (990 days) that map to each node based on the total days of the particular month from 1979-2011

2.3.3 Relative contribution of synoptic types to rainfall over sub-regions

The regionally averaged daily rainfall associated with each node as well as the percentage contribution of each node to the annual rainfall over each of the regions are shown in Fig. 11. The COLs identified by the tracking algorithm were mapped to the relevant node of the SOM for inclusion in the analysis with regards to the relative contribution of the synoptic types to the annual rainfall over the sub-regions (Fig. 12). During 1979-2011, 222 COL events (511 COL days) were associated with rainfall over the study region. COL-induced rainfall over the study region is mostly associated with COLs located over the southwestern interior and over the ocean to the west of the country (Fig. 12).

Over all the regions, nodes in the upper right part of the SOM are responsible for a relatively large contribution to the annual rainfall (Fig. 11d, e and f). These nodes are typical of the late summer months, February and March (Fig. 10). Over the Cape south coast (Region 1), the six nodes in the upper right corner are responsible for 43% of the annual rainfall (Fig. 11d), while the frequency of occurrence of these nodes is only 17% (Fig. 7). These nodes represent the AOH that extends a ridge eastwards at about 40˚ S (nodes 27, 28, 35), as well as tropical-temperate troughs (nodes 26, 33, 34). Node 35 is associated with the largest average daily rainfall over Region 1 (Fig. 11a) and Region 3 (Fig. 11c). It also has a significantly higher than average occurrence, which in combination with the high average daily rainfall totals lead to this node being associated with 13% and 11% of the annual rainfall over Regions 1 (Fig. 11d) and 3 (Fig. 11f), respectively. It may further be noted that this node is associated with the second highest frequency of COL days associated with rainfall over the region (Fig. 12). Node 14 (Fig. 7) is also associated with high average daily rainfall totals over Region 1 (Fig. 11a). This node has a maximum frequency of occurrence during winter (Fig. 10), and represents a high pressure system ridging behind a frontal system that is situated southeast of the subcontinent.

Nodes 15, 22 and 29 (Fig. 7) are prominent in contributing to the annual rainfall over Regions 2 (Fig. 11e) and 3 (Fig. 11f). Nodes 15 and 22 represent tropical-temperate linkages. Node 29 is characterized by a high pressure system southeast and south of the subcontinent, and of all the nodes is associated with the highest frequency of COL days (Fig. 12). The association of node 29 with COLs as well as the location of the surface trough in the extreme west are probably the reasons for this node being responsible for the highest average daily rainfall over Region 2 (Fig. 11b). The higher than average occurrence of node 29 is statistically significant at the 95% confidence level. It contributes 16% of the annual rainfall occurring over Region 2 (Fig. 11e). The nodes representative of frontal troughs located in the lower and middle central part of the SOM, are generally associated with small average daily rainfall totals over all the regions, and consequently with the smallest contribution to the annual rainfall.

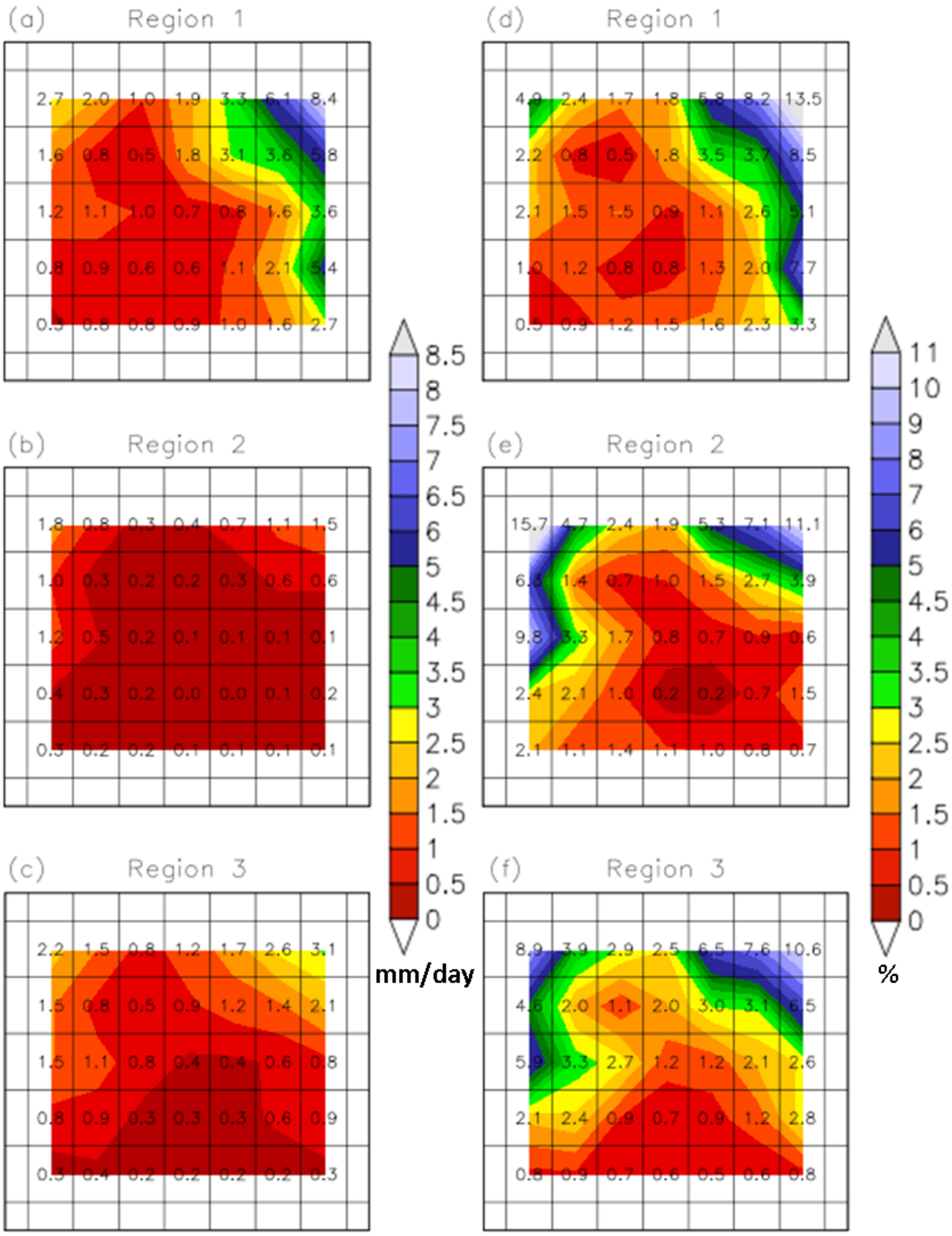

Fig. 11 The regionally averaged daily precipitation (mm/day) for each SOM node for (a) Region 1, (b) Region 2 and (c) Region 3, and the average annual contribution (%) by node to rainfall over (d) Region 1, (e) Region 2 and (f) Region 3

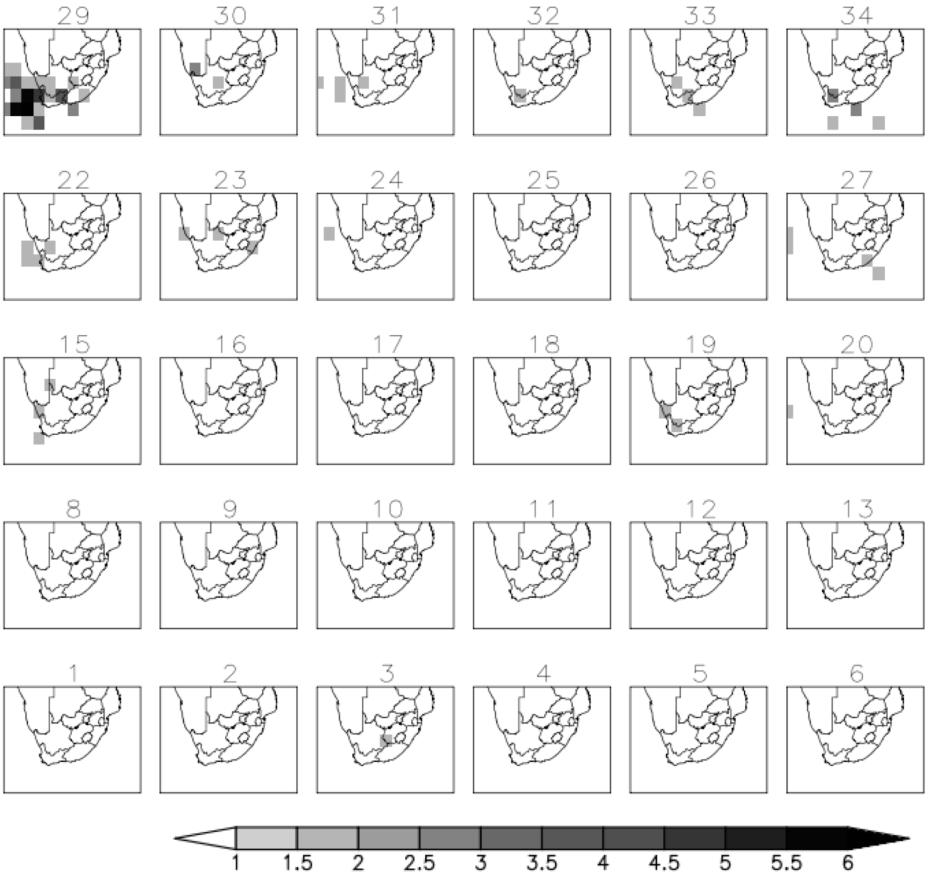

Fig. 12 Accumulated frequency of rainfall-producing COLs (units: COL days/grid point) for each SOM node for the period 1979-2011. Only grid points with a frequency of at least 1 day are indicated

The 35 synoptic types may be grouped into main synoptic classes that are relevant to the Cape south coast region. These are troughs southwest and southeast of the subcontinent, ridging high pressure systems from the southwest, high pressure systems located east of the subcontinent, tropical-temperate troughs and weak synoptic flow (Fig. 7). The clustering of the 35 nodes into the 6 main synoptic classes is based on additional evaluation of composite maps of the 850, 700, 500, 200 hPa geopotential heights as well as the spatial distribution of rainfall over southern Africa associated with each node. The spatial rainfall distribution over southern Africa is employed to aid in the identification of nodes representative of tropical-temperate troughs – characterized by the presence of a cloud band originating from tropical Africa extending south or southeastwards over South Africa (e.g. Hart et al. 2013). As the station data used is limited to the study region, the FEWS rainfall estimate was employed to represent the spatial rainfall distribution associated with each node over southern Africa (Fig. 9).

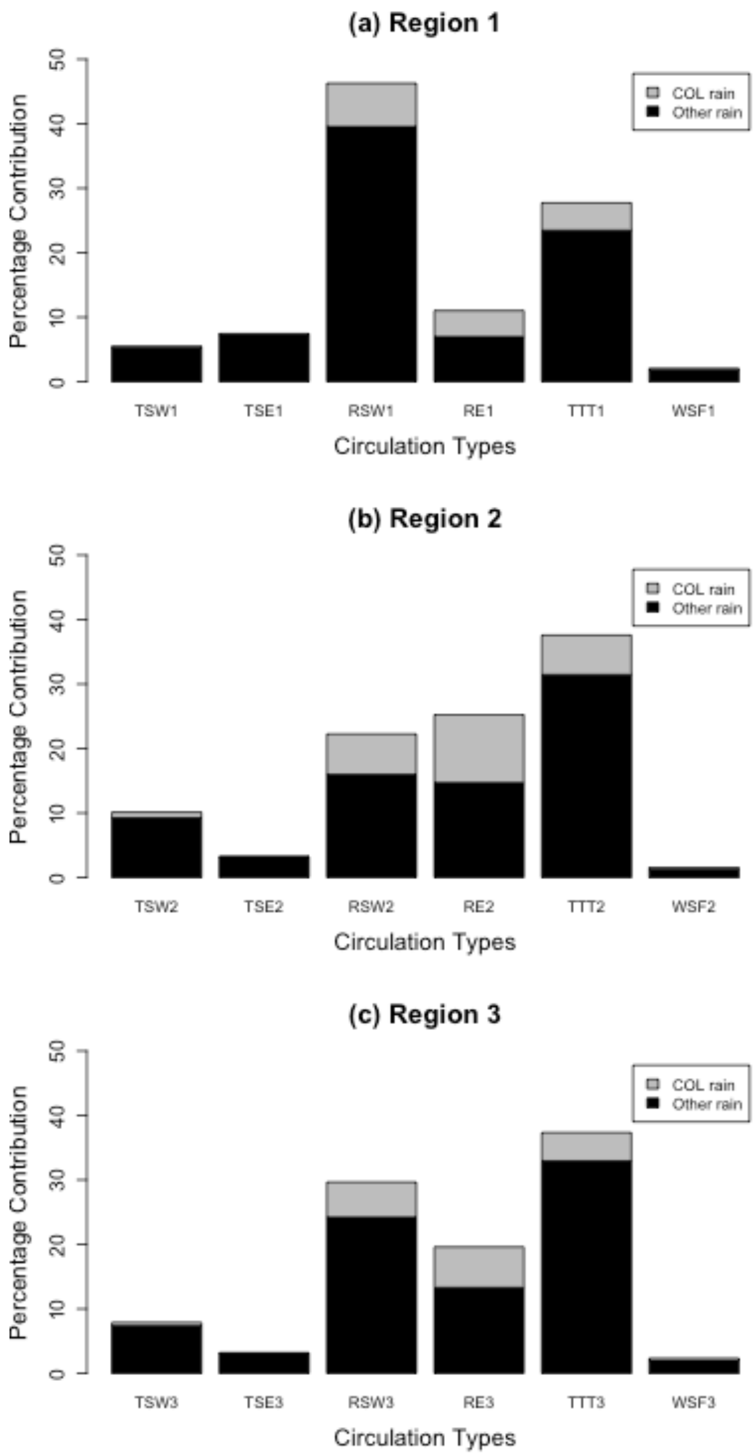

Fig. 13 The percentage contribution to the average annual rainfall of the 6 main synoptic classes identified in this study for (a) Region 1, (b) Region 2 and (c) Region 3. The percentage of rainfall contributed by COLs to the average rainfall, in association with the 6 main synoptic classes, is shown in grey

Of the 6 synoptic classes identified, high pressure systems ridging from the southwest contribute most to rainfall over Region 1 (Fig. 13a, bar 3). In fact, the various configurations of these systems are associated with a staggering 46% of the region's rainfall. The subset of ridging highs from the southwest occurring in conjunction with COLs contributes 7% to total annual rainfall. It is likely though, that the remaining cases are often associated with other forms of upper-air support (e.g. upper air troughs). Still, this result is indicative that the low-level flow around favorably positioned near-surface highs, and possible interactions with the mountainous topography adjacent to the coastal area, are factors of key importance in causing rainfall over the Cape south coast region. Over Regions 2 and 3 (Fig. 13b, c, bar 3), the contribution of ridging high pressure systems from the southwest to the annual rainfall is much less – 22 and 30% respectively (6% and 5% in conjunction with COLs respectively). This result confirms that it is the low-level flow and interaction with topography that causes this synoptic class to be of key importance to the Cape south coast region itself. Tropical-temperate troughs contribute to 28, 38 and 37% of the annual rainfall over Regions 1, 2 and 3 respectively (Fig. 13a, b, c, bar 5). The overall contribution of COLs to annual rainfall over the Cape south coast is 16%, much less than the contribution of 39% of ridging highs that occur in the absence of COLs. Regional variation occurs in the contribution of COLs to annual rainfall, as shown in Figure 14. At the stations in Region 1, the contribution of COLs to annual rainfall ranges between 13% and 22%. Favre et al. (2013) have found the contribution of COLs to annual rainfall over the Cape south coast to be somewhat higher – in the order of 20 to 30%. COLs are estimated to contribute about 24% and 17% of the annual rainfall over Region 2 and 3 respectively, with the percentage contribution ranging between 13% and 25% at the various weather stations. Taking into account that only a small number (7 on the average) of COLs contribute to rainfall over the Cape south coast per year, the relatively large portion of rain these systems contribute to the annual rainfall is quite noteworthy. Not surprisingly, when extreme daily rainfall for each station are considered, defined here as the 95th percentile of all recorded rain days, the contribution of COLs to extreme rainfall exceeds that of the contribution of COLs to annual rainfall at all the weather stations (Fig. 14). The largest differrence in the contribution of COLs to annual and extreme rainfall occurs along the coast and adjacent interior, with the COL contribution to extreme rainfall reaching double that of it's annual rainfall contribution at some stations.

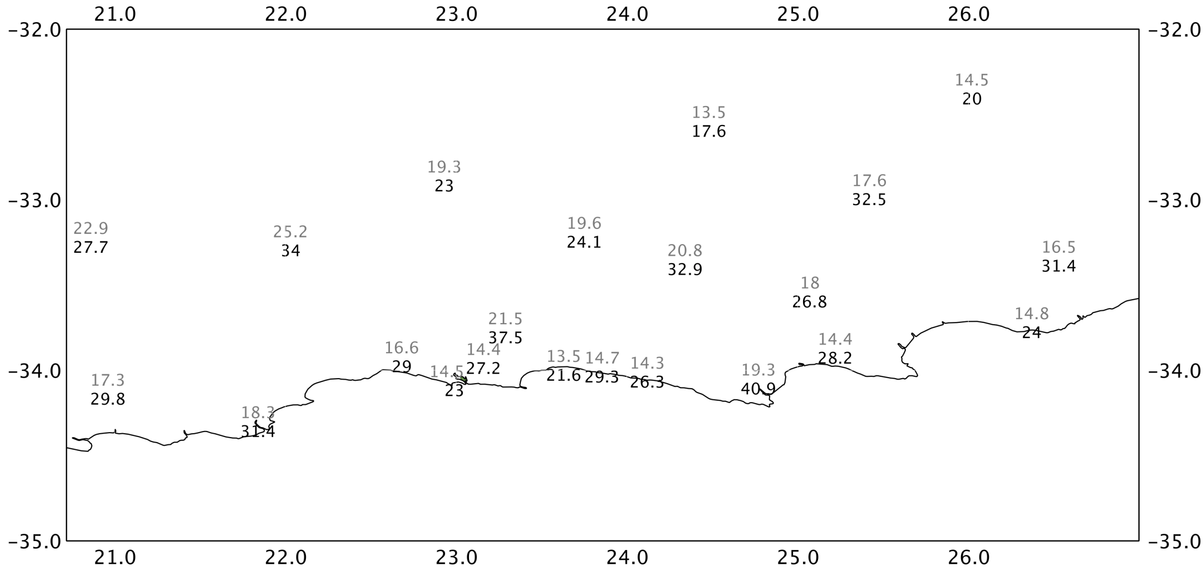

Fig. 14 Percentage contribution of COLs to annual rainfall (grey) and extreme rainfall (black) at the weather stations

The statistics for the nodes associated with the highest average daily rainfall, the highest average contribution to annual rainfall as well as the nodes contributing > 5% each to average annual rainfall are summarized in Table 1.

Table 1 Synoptic types most important to rainfall over the Cape south coast and adjacent interior

Synoptic type rainfall attributes	Region 1	Region 2	Region 3
Highest average daily rainfall	35 (8.4 mm/day)	29 (1.8 mm/day)	35 (3.1 mm/day)
Highest average contribution to annual rainfall	35 (13%)	29 (16%)	35 (11%)
Nodes contributing > 5% each to average annual rainfall (ranked according to contribution)	35, 28, 34, 14, 33, 21	29, 35, 15, 34, 22, 33	35, 29, 34, 33, 28, 15

2.3.4 Synoptic types driving the annual rainfall cycle over the Cape south coast

The decomposition of the synoptic types responsible for rainfall over the Cape south coast performed in the previous section shows the relative importance of ridging high pressure systems, tropical-temperate troughs and COLs over this region. The role that each of these systems play in the annual rainfall cycle over the region will subsequently be discussed. Of particular interest is the role of COLs and their association with the observed rainfall peaks (Fig. 6), since COL occurrences over South Africa reach maximum numbers during March-May and October (Singleton and Reason 2007b; Favre et al. 2013), corresponding with two of the three rainfall peaks observed over the Cape south coast region. Moreover, COLs are associated with significant rainfall events along the Cape south coast region (e.g. Taljaard 1985; Singleton and Reason 2006; Singleton and Reason 2007a, also see Section 3.3). In order to investigate the relative contribution of COLs to the rainfall cycle over the Cape south coast, the percentage contribution of COLs to monthly rainfall totals was calculated.

Over the 33-year period analysed, 222 rain-producing COLs occurred that were associated with rainfall over the study region. The preferred geographical location of these COLs is the southwestern interior of South Africa and adjacent oceanic area off the west coast (Fig. 12). This region has been identified by Favre et al. (2013) as being one of the areas of southern Africa with the highest frequency of COLs. Autumn (March-May) and winter (June-August) have the highest frequency of occurrence of COLs over the study region, with the highest frequencies in April, May and June (Fig. 15).

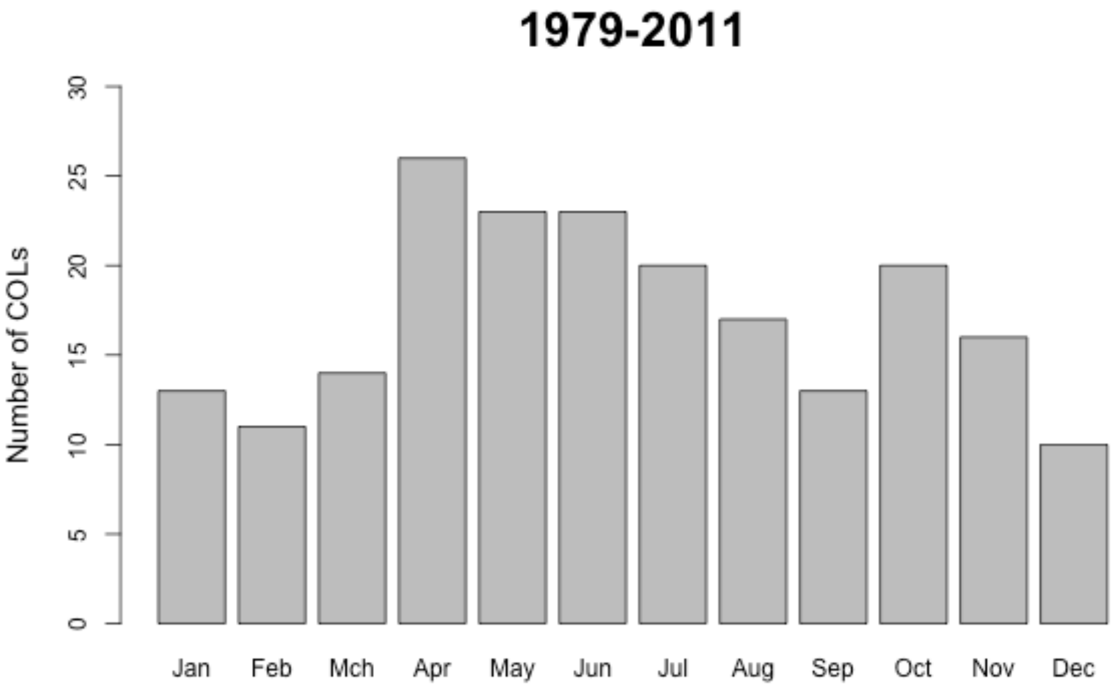

Fig. 15 Accumulated monthly number of COLs associated with rainfall at 1 station or more, over the period 1979-2011

Synoptic types associated with the March-April rainfall peak over Region 1 (Fig. 16a) include troughs, ridging high pressure systems and tropical-temperate troughs, with nodes 21, 28, 33, 34, 35 being the most prominent in contributing rainfall during March, and nodes 7, 14, 21, 26, 28, 33, 34, 35 the most prominent during April (Fig. 17a). Ridging high pressure systems and tropical-temperate troughs accompanied by COLs contribute to the March rainfall peak while the April rainfall peak is dependent on the contribution by COLs (Fig. 16a). During March, COLs occur in combination with ridging high pressure systems from the southwest and tropical temperate troughs (represented by nodes 26, 27, 34 and 35) (Fig. 17a). The COL-induced rainfall peak during April is characterized by low-level circulation representative of ridging high pressure systems from the southwest and- southeast as well as tropical temperate troughs – nodes 21, 22, 29, 34 and 35 are representative of the aforementioned synoptic types (Fig. 17d). Over Region 2, the March-April peak (Fig. 16b) in rainfall is associated with troughs from the southwest, ridging high pressure systems and tropical-temperate troughs. Nodes 9, 15, 22, 29, 34 and 35 are representative of the synoptic types contributing the most to the rainfall peak during March while nodes 15, 16, 17, 28, 29, 33, 34 and 35 are prominent during April (Fig. 17b). The synoptic types associated with COL-induced rainfall that contribute most prominently to the rainfall peak during March are representative of nodes 22, 29, 31 and 35 (Fig. 17e). During April, the rainfall peak receives the largest contribution by COL-induced rain. Nodes 22, 29 and 35 are representative of the synoptic types that accompany COLs during April, with node 29 in particular prominent to contribute to the rainfall peak (Fig. 17e). Over Region 3, January to March experience the same rainfall-producing synoptic types (node 8, 9, 15, 16, 22, 29, 33 and 34), with the rainfall peak occurring in February, driven by tropical-temperate troughs as represented by nodes 15, 22 and 33 (Fig. 17c).

During August, COLs associated with nodes 29 and 35 (Fig. 17d) as well as ridging high pressure systems (nodes 7, 14, 21, 28) and tropical-temperate troughs (nodes 26, 34) contribute to the rainfall peak over Region 1 (Fig. 16a and 17a). Over Regions 2 and 3, the August rainfall peak is significantly less prominent than the autumn and spring peaks. For Region 2, nodes 29 and 35 (Fig. 17e) in combination with COLs as well as nodes 17, 22 and 34 (Fig. 17b) contributes to the small-amplitude August peak in the annual rainfall cycle (Fig. 16b). A small amplitude August rainfall peak is also present over Region 3 (Fig. 16c) and seems to occur in association with synoptic types 13, 14, 28, 34 and 35 (Fig. 17c) as well as with COLs in combination with nodes 29, 30, 31 and 35 (Fig. 17f).

The month of October is characterized by a prominent rainfall peak over the Cape south coast, and strong rises in the monthly rainfall totals compared to the September totals over all three regions (Fig. 16). However, Figure 16 also reveals that COL-induced rainfall doesn't peak or rise significantly relative to September totals during October. Ridging high pressure systems from the southwest (nodes 14, 20, 28, 35), tropical-temperate troughs (nodes 33, 34) and high pressure systems southeast of the subcontinent (node 29) are associated with the October rainfall peak over Region 1 (Fig. 17a). Of these weather systems, ridging high pressure systems from the southwest are responsible for the largest contribution to the rainfall peak. Over Regions 2 and 3 ridging high pressure systems from the southwest, a ridge southeast of the subcontinent and tropical-temperate troughs (nodes 15, 28, 29, 34, 35 and nodes 15, 28, 29, 33, 34, 35 respectively) are the main synoptic types contributing to the October rainfall (Fig. 17b, c). The largest contribution to the October rainfall over Region 2 is from a ridge southeast of the subcontinent, represented by node 29 (Fig. 17b) while node 35 (ridge from the southwest) is associated with the largest contribution to October rainfall over Region 3 (Fig. 17c). The November rainfall peaks over Region 2 (Fig. 16b) and Region 3

(Fig. 16c) can be ascribed to COLs and their interaction with ridging high pressure systems southeast of the subcontinent, tropical-temperate troughs as well as high pressure systems ridging from the southwest. The nodes representative of these circulation patterns are nodes 19, 22, 29, 33, 35 (Fig. 17e) and nodes 22, 29, 34, 35 (Fig. 17f) for Region 2 and 3 respectively. COLs also contribute to the relatively high rainfall totals over Region 1 in November (Fig. 16a). November is the month with the highest frequency of tropical-temperate troughs (Hart et al. 2013), consistent with the accumulated contribution of nodes 22 and 29 (representative of tropical-temperate troughs) that occur in combination with COLs, to outscore the contribution of high pressure systems southeast and southwest of the subcontinent that are associated with COL-induced rain.

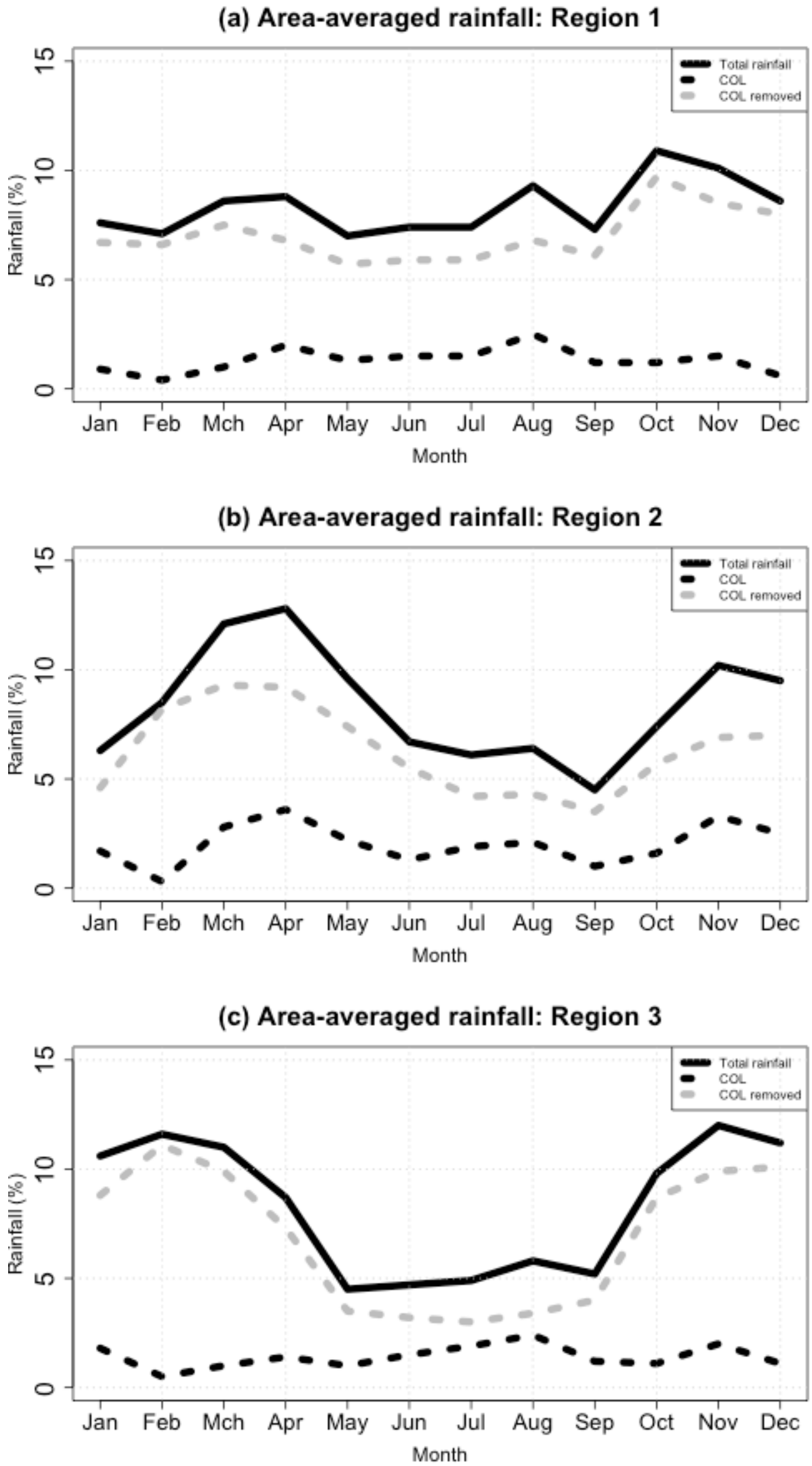

Fig. 16 Area-averaged annual rainfall distribution for the period 1979-2011 over (a) Region 1, (b) Region 2 and (c) Region 3. The black solid line represents the monthly rainfall (%), the black dotted line the monthly rainfall associated with COLs (%) and the grey dotted line the monthly rainfall without the COL-induced rainfall (%)

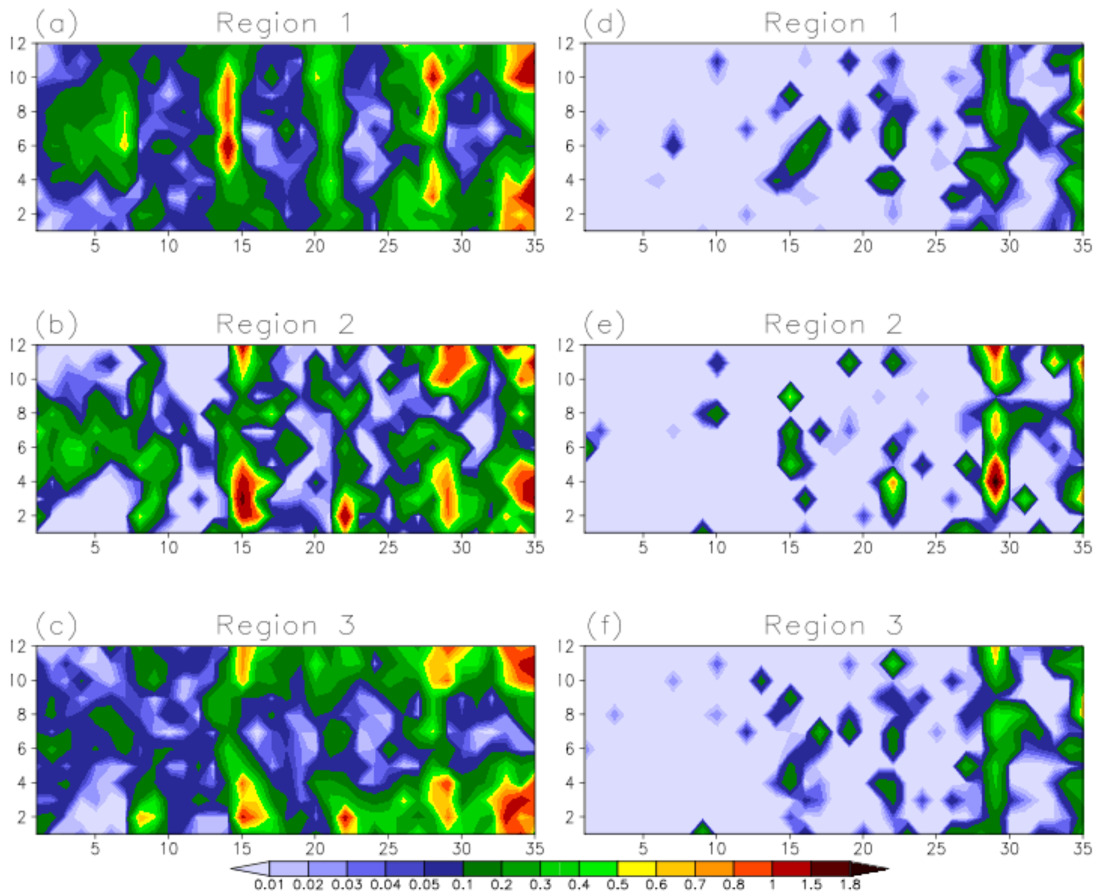

Fig. 17 Percentage contributions of monthly rainfall totals to the average annual rainfall (y-axis) not associated with COLs for (a) Region 1, (b) Region 2, (c) Region 3 and associated with COLs for (d) Region 1, (e) Region 2 and (f) Region 3. The 35 SOM nodes are indicated on the x-axis

2.4 Conclusions

The Cape south coast of South Africa, here defined as the region between 21 and 27 °E and south of the Cape Folded mountains (that is, south of about 33.7 °S), is an all-year rainfall region. Over this region, at least 11 but mostly all 12 months of the year contribute 5% or more to the long-term average annual rainfall total, in both gridded (CRU TS3.1 and FEWS) and weather station data analysed over the region. Other features that distinguish the region from the winter and summer rainfall regions of South Africa is the relatively high ratio of the rainfall total for the month of minimum rainfall to the total for the month of maximum rainfall, and the relatively small average fluctuation of monthly rainfall totals around the monthly mean rainfall total.

The SOM technique was used to develop a synoptic climatology for the Cape south coast of South Africa, and the synoptic forcing of rainfall over the region was subsequently analysed. The synoptic types identified depend to some extent on the specific reanalysis data set used. Here NCEP reanalysis daily SLP anomaly data were used to train a 7x5 SOM. SLP was selected as the metric for synoptic typing due to the Cape south coast region being close to sea-level (different metrics such as 850 hPa heights would lead to the identification of somewhat different types). A number of well-known synoptic classes, such as ridging highs, tropical-temperate troughs and weak synoptic flow have been identified by the SOM, as well as subtle but systematic differences within different synoptic types that make up the main classes. The importance of the SOM to capture these subtle differences is illustrated by the nodes' very different contributions to annual rainfall over the region. This is applicable in particular to the rain-producing synoptic types, such as ridging high pressure systems from the southwest and tropical-temperate troughs. For example, the results presented in this paper indicate that ridging high pressure systems where the ridge is located further southwards are more conducive to rainfall along the Cape south coast region than ridges located more equatorwards, even if the pressure distribution is otherwise similar. A similar observation was made regarding the intensity of the ridging high pressure systems. It has long been known that the geographical location and the intensity of ridging high pressure systems is a determining factor for the occurrence of rainfall and the nature of the rainfall over the Cape south coast region (e.g. Taljaard 1996). However, by application of a SOM, it is possible to quantify the rainfall associated with the different types within a main synoptic class. For example, over the 33-year period node 27 (ridging high pressure system from the southwest) yielded 3.6 mm/day, whereas node 28 (also a ridging high- pressure system from the southwest) yielded 5.8 mm/day. Similarly, ridging high pressure systems from the southwest represented by nodes 20 and 21 yielded approximately 1.6 and 3.6 mm/day. Taking the frequency of occurrence of the synoptic types into account, the contribution by a single type within a main synoptic class (e.g. ridging highs) becomes important with regard to seasonal or annual rainfall totals.

Ridging high pressure systems are the synoptic types that contribute most to rainfall totals over the Cape south coast region. These systems have a frequency of occurrence of 23% (of the total number of daily occurrences of synoptic types) but contribute 46% of the total rainfall over the Cape south coast. Over Regions 2 and 3, the contribution of ridging high pressure systems to rainfall totals is notably less, which suggests that topography plays some part in enhancing the rainfall along the coast (Region 1). Tropical-temperate troughs are responsible for 28% of the rainfall over Region 1, increasing northwards to contribute 38% and 37% to annual rainfall over Regions 2 and 3. The frequency of occurrence of the various configurations of tropical-temperate troughs accumulates to 25%. COLs occur in combination with ridging high pressure systems (ridging from the southwest and southeast) and tropical-temperate troughs. However, the contribution to rainfall by COLs has been isolated from these systems for comparison purposes using an objective tracking algorithm. COLs contribute 16% (7% in co-occurrence with ridging highs), 24% and 17% to the annual rainfall over Regions 1, 2 and 3 respectively. The contribution to rainfall by COLs is remarkable, considering that the COL-induced rainfall days over the Cape south coast region amount only to 4.2%. Transient frontal troughs were found to bring the least rain to Region 1 of the rain-bearing systems, consistent with the observations of the winter months being associated with a season characterized by lower rainfall totals compared to transitional seasons. The estimated relative contribution of synoptic types to annual rainfall depends to some extent on the spatial coverage and distribution of the weather stations recording rainfall.

The autumn and August rainfall peaks observed in the annual rainfall cycle over the Cape south coast (Region 1) cannot be attributed to a single rain-producing synoptic type. Both ridging highs, tropical-temperate troughs and COLs have been shown to contribute to these rainfall peaks, but with COLs driving the rainfall peak during April. COLs are the single synoptic type driving the subtle August rainfall peak over Region 3. The September hiatus in rainfall that occurs across the three regions, after the August peak, seems to be related to a poleward displacement of frontal systems and positioning of high pressure systems (ridging mainly over land) that are both unfavorable for rainfall. Along the Cape south coast, the October rainfall peak is the highest rainfall peak observed during the year. This rainfall peak is the result of ridging high pressure systems and to a lesser extent tropical-temperate troughs, with an insignificant contribution by COLs. The increase in rainfall during October is also observed over the interior regions. However, the rainfall peak over Regions 2 and 3 occurs in November when an increase in COL-induced rainfall is observed over all the regions, although very slight over Region 1. This November peak over Region 2 and 3 can largely be attributed to COLs. Noteworthy is the importance of ridging high pressure systems relative to COLs for the existence of the October rainfall peak along the coast (Region 1).

2.5 Acknowledgements

This research was funded by the Water Research Commission (Project K5/2257/1) and the Applied Centre for Climate and Earth System Studies (ACCESS) in South Africa. Rainfall data were supplied by the South African Weather Service – the assistance of Elsa de Jager is greatly acknowledged. The editing contributions of Dr Fyfield from the Agricultural Research Council are highly valued and acknowledged. Two anonymous reviewers are thanked for their constructive comments.

2.6 References

Crimp SJ, van den Heever SC, D'Abreton PC, Tyson PD, Mason SJ (1997) Mesoscale modelling of tropical-temperate troughs and associated systems over southern Africa. WRC Report 595/1/97, 395 pp

Engelbrecht CJ, Engelbrecht FA, Dyson LL (2013) High-resolution model-projected changes in mid-tropospheric closed-lows and extreme rainfall events over southern Africa. International Journal of Climatology 33:173-187. DOI: 10.1002/joc.3420

Fauchereau N, Pohl B, Reason CJC, Rouault M, Richard Y (2009) Recurrent daily OLR patterns in the Southern Africa/Southwest Indian Ocean region, implications for South African rainfall and teleconnections. Climate Dynamics 32: 575-591. DOI: 10.1007/s00382-008-0426-2

Favre A, Hewitson B, Tadross M, Lennard C, Cerezo-Mota R (2012) Relationships between Cut-off Lows and the Semiannual and Southern Oscillations. Climate Dynamics 38: 1473-1487. DOI: 10.1007/s00382-011-1030-4

Favre A, Hewitson B, Lennard C, Cerezo-Mota R, Tadross M (2013) Cut-off lows in the South Africa region and their contribution to precipitation. Climate Dynamics 41: 2331-2351. DOI: 10.1007/s00382-012-1579-6

Harris I, Jones, PD, Osborn TJ, Lister DH (2014) Updated high-resolution grids of monthly climatic observations – the CRU TS3.10 dataset. International Journal of Climatology 34: 623-642. DOI: 10.1002/joc.3711

Hart NCG, Reason CJC, Fauchereau N (2010) Tropical-Extratropical Interactions over Southern Africa: Three Cases of Heavy Summer Season Rainfall. Monthly Weather Review 138: 2608-2623

Hart NCG, Reason CJC, Fauchereau N (2012) Building a Tropical-Extratropical Cloud Band Metbot. Monthly Weather Review 140: 4005-4016

Hart NCG, Reason CJC, Fauchereau N (2013) Cloud bands over southern Africa: seasonality, contribution to rainfall variability and modulation by the MJO. Climate Dynamics 42: 1199-1212. DOI: 10.1007/s00382-012-1589-4

Hayward LQ, van den Berg H (1968) Die Port Elizabeth-stortreens van 1 September 1968. SA Weather Bureau News Letter No. 234, 157-169

Hayward LQ, van den Berg H (1970) The Eastern Cape Floods of 24 to 28 August, 1970. SA Weather Bureau News Letter No. 257, 129-141

Hewitson BC, Crane RG (2002) Self-organizing maps: Applications to synoptic climatology. Climate Research 22: 13-26

Jury MR, Levey K (1993) The climatology and characteristics of drought in the eastern Cape of South Africa. International Journal of Climatology 13: 629-641. DOI: 10.1002/joc.3370130604

Kalnay E, Kanamitsu M, Kistler R, Collins W, Deaven D, Gandin L, Iredell M, Saha S, White G, Woollen J, Zhu Y, Leetmaa A, Reynolds B, Chelliah M, Ebisuzaki W, Higgins W, Janowiak J, Mo KC, Ropelewski C, Wang J, Jenne R, Joseph D (1996) The NCEP/NCAR 40-year reanalysis project. Bulletin of the American Meteorological Society 77: 437-471

Katzfey JJ, McInnes KL (1996) GCM simulations of Eastern Australia cutoff lows. Journal of Climate 9: 2337-2355

Kohonen T (2001) Self-Organizing Maps. 3rd ed. Springer, 501 pp

Landman WA, Mason SJ, Tyson PD, Tennant WJ (2001) Retro-active skill of multi-tiered forecasts of summer rainfall over southern Africa. International Journal of Climatology 21: 1-19

Malherbe J, Engelbrecht FA, Landman WA, Engelbrecht CJ (2012) Tropical systems from the southwest Indian Ocean making landfall over the Limpopo River Basin, southern Africa: a historical perspective. International Journal of Climatology 32: 1018-1032. DOI: 10.1002/joc.2320

Muller A, Reason CJC, Fauchereau N (2008) Extreme rainfall in the Namib Desert during late summer 2006 and influences of regional ocean variability. International Journal of Climatology 28: 1061-1070. DOI: 10.1002/joc.1603

Philippon N, Rouault M, Richard Y, Favre A (2011) The influence of ENSO on winter rainfall in South Africa. International Journal of Climatology 32: 2333-2347. DOI: 10.1002/joc.3403

Roberts CPR, Alexander WJR (1982) Lessons learnt from the 1981 Laingsburg flood. Civil Engineer in South Africa 24: 17-21, 24-25, 27

Rouault M, White SA, Reason CJC, Lutjehams JRE, Jobard I (2002) Ocean-Atmosphere interaction in the Agulhas current region and a South African extreme Weather event. Weather and Forecasting 17: 655-669

Rouault M, Richard Y (2003) Intensity and spatial extension of drought in South Africa at different time scales. Water SA 29: 489-500

Schuenemann KC, Cassano JJ, Finnis J (2009) Synoptic Forcing of Precipitation over Greenland: Climatoloy for 1961-99. Journal of Hydrometeorology 10: 60-78

Singleton AT, Reason CJ (2006) Numerical simulations of a severe rainfall event over the Eastern Cape coast of South Africa: sensitivity to sea surface temperature and topography. Tellus 58: 355-367

Singleton AT, Reason CJ (2007a) A numerical model study of an intense cutoff low pressure system over South Africa. Monthly Weather Review 135: 1128-1150

Singleton AT, Reason CJ (2007b) Variability in the characteristics of cut-off low pressure systems over subtropical southern Africa. International Journal of Climatology 27: 295-310

Sylla MB, Giorgi F, Coppola E, Mariotti L (2013) Uncertainties in daily rainfall over Africa: assessment of gridded observation products and evaluation of a regional climate model simulation. International Journal of Climatology 33: 1805-1817. DOI: 10.1002/joc.3551

Taljaard JJ (1985) Cut-off lows in the South African region. South African Weather Bureau, Technical paper 14

Taljaard JJ (1995) Atmospheric circulation systems, synoptic climatology and weather phenomena of South Africa. Part 2: Atmospheric circulation systems in the South African region. South African Weather Bureau, Technical paper 28

Taljaard JJ (1996) Atmospheric circulation systems, synoptic climatology and weather phenomena of South Africa. Part 6: Rainfall in South Africa. South African Weather Bureau, Technical paper 32

Tennant WJ (2003) An assessment of intraseasonal variability from 13-yr GCM Simulations. Monthly Weather Review 131: 1975-1991

Tennant WJ (2004) Considerations when using pre-1979 NCEP/NCAR reanalysis in the southern hemisphere. Geophysical Research Letters 31: L11112. DOI: 10/1029/2004GLO197501

Tennant WJ, van Heerden J (1994) The influence of orography and local sea-surface temperature anomalies on the development of the 1987 Natal floods: a general circulation model study. Suid-Afrikaanse Tydskrif vir Wetenskap 90: 45-49

Tennant WJ, Hewitson BC (2002) Intra-seasonal rainfall characteristics and their importance to the seasonal prediction problem. International Journal of Climatology 22: 1033-1048. DOI: 10.1002/joc.778

Tozuka T, Abiodun BJ, Engelbrecht FA (2014) Impacts of convection schemes on simulating tropical-temperate troughs over southern Africa. Climate Dynamics 42: 433-451. DOI: 10.1007/s00382-013-1738-4

Van Rooy MP (1972) Climate of South Africa: District rainfall for South Africa and the annual march of rainfall over southern Africa, part 10. South African Weather Bureau Tech. Note WB 35, Dept. of Transport, Pretoria, South Africa, 116 pp.

Van Schalkwyk L, Dyson LL (2013) Climatological characteristics of fog at Cape Town International airport. Weather and Forecasting 28: 631-646. DOI: 10.1175/WAF-D-12-00028.1

Washington R, Todd M (1999) Tropcial-temperate links in the Southern African and southwest Indian Ocean satellite-derived daily rainfall. International Journal of Climatology 19: 1601-1616

Weepener HL, van den Berg HM, Metz M, Hamandawana H (2012) The development of a hydrologically improved Digital Elevation Model and derived products for South Africa based on the SRTM DEM. Water Research Commission, Pretoria. Report No. 1908/1/11. Press ISBN 978-1-4312-0217-1

Weldon D, Reason CJC (2014) Variability of rainfall characteristics over the South Coast region of South Africa. Theoretical and Applied Climatology 115: 177-185. DOI: 10.1007/s00704-013-0882-4

Synopsis

The spatial extent of the all-year rainfall region has been reassessed by making use of two independently constructed gridded rainfall datasets. The delineation of the all-year rainfall region performed in this study identified the region to be found within the collective boundaries described in previous studies. Along the coast, the all-year rainfall region is found approximately between 21°E and 27°E, while its northern extent is mostly restricted by the Cape Folded mountain range. The interaction of circulation and topography and the resulting rainfall response is demonstrated by the difference in contribution to rainfall totals by ridging high pressure systems over the all-year rainfall region compared to the two northwards neighbouring regions. The seasonal cycle of rainfall along the Cape south coast has also been reassessed, and revealed a rainfall maximum during August in addition to the already known rainfall peaks during autumn and spring. This paper's identification of the August rainfall peak has also been recently referred to in a paper on CORDEX model simulations, illustrating the value of the contribution of this study to model verification studies. The relative contribution of different synoptic types and their sub-types to annual rainfall is quantified, and the synoptic forcing responsible for the multi-modal rainfall distribution is identified, addressing objectives 1 and 2 respectively. The relative importance of ridging high pressure systems, tropical-temperate troughs and COLs have been demonstrated. It has also been shown that subtle differences within a rain-producing synoptic type can have very different contributions to annual rainfall totals, illustrating the need to consider sufficient variation within a specific main synoptic type in the synoptic decomposition of rainfall. The relative importance of the various rain-producing synoptic types and the variation that can occur within a rain-producing synoptic type (e.g. ridging highs, tropical-temperate troughs) underlines the need to understand the variability of these systems over the region and the associated rainfall variability. This notion as well as its potential link with larger-scale climate modes will be dealt with in the following chapter which addresses the third and fourth objectives of the study.

Chapter 3: Interannual variability of seasonal rainfall over the Cape south coast of South Africa and synoptic type association

Preface

This chapter consists of one peer-reviewed paper as follows:

Engelbrecht CJ, Landman WA (2015) Interannual variability of seasonal rainfall over the Cape south coast of South Africa and synoptic type association. Clim Dyn. DOI: 10.1007/s00382-015-2836-2

In this chapter, the link between interannual variability of seasonal rainfall over the Cape south coast of South Africa and different synoptic types is explored, therefore addressing the third objective of the study. The main rain-producing synoptic types have been identified in the previous chapter. In this chapter, the synoptic type frequency distribution associated with wet and dry seasons are investigated. This paper aims to potentially improve our understanding of rainfall variability within the context of the frequency distribution of synoptic types within a season that can allow us to identify distinguishable intraseasonal characteristics of wet and dry seasons. Furthermore, the potential link between the distribution of synoptic types within a season with SAM and ENSO is explored, in order to investigate predictability of intraseasonal synoptic type variability. This part of the work addresses the fourth objective of the study.

My co-author is WA Landman. I conceptualized the paper, was responsible for data acquisition, all analysis and also the synthesis of the results.

Interannual variability of seasonal rainfall over the Cape south coast of South Africa and synoptic type association

C.J. Engelbrecht[1,2] and W.A. Landman[2,3]

1. Institute for Soil, Climate and Water, Agricultural Research Council, Pretoria, South Africa

2. Department of Geography, Geoinformatics and Meteorology, University of Pretoria, Pretoria, South Africa

3. Climate Studies, Modelling and Environmental Health, CSIR Natural Resources and Environment, Pretoria, South Africa

Abstract

The link between interannual variability of seasonal rainfall over the Cape south coast of South Africa and different synoptic types as well as selected teleconnections is explored. Synoptic circulation over the region is classified into different synoptic types by employing a clustering technique, the self-organizing map (SOM), on daily circulation data for the 33-year period from 1979 to 2011. Daily rainfall data are used to investigate interannual variability of seasonal rainfall within the context of the identified synoptic types. The anomalous frequency of occurrence of the different synoptic types for wet and for dry seasons differs significantly within the SOM space, except for austral spring. The main rainfall-producing synoptic types are to a large extent consistent for wet and dry seasons. The main rainfall-producing synoptic types have a notable larger contribution to seasonal rainfall totals during wet seasons than during dry seasons, consistent with a higher frequency of occurrence of the main rainfall-producing synoptic types during wet seasons compared to dry seasons. Dry seasons are characterized by a smaller contribution to seasonal rainfall totals by all the different synoptic types, but with the largest negative anomalies associated with low frequencies of the main rainfall-producing synoptic types. The frequencies of occurrence of specific configurations of ridging high pressure systems, cut-off lows (COLs) and tropical-temperate troughs associated with rainfall are positively linked to interannual variability of seasonal rainfall. It is also shown that the distribution of synoptic types within the SOM space is linked to the

Southern Annular Mode (SAM) and El Niño Southern Oscillation (ENSO), implying some predictability of intraseasonal variability on the seasonal time scale.

Key words: Cape south coast of South Africa, Synoptic types, Interannual rainfall variability, El Niño Southern Oscillation, Southern Annular Mode, Intraseasonal predictability

3.1 Introduction

Three precipitation regimes are notable over South Africa. Most of the country receives rainfall in austral summer (Barclay et al. 1993; Fauchereau et al. 2009; Crétat et al. 2012; Pohl et al. 2014), with the extreme southwestern area characterized by austral winter rainfall (Reason et al. 2002; Philippon et al. 2012; Pohl et al. 2014). The third precipitation regime is found along the coast in the far south of the country, referred to as the Cape south coast. Here, pronounced seasonality in rainfall is absent and rainfall occurs throughout the year, with small peaks during the transitional seasons (Taljaard 1996; Pohl et al. 2014; Weldon and Reason 2014). Rainfall-producing weather systems characteristic of both the winter and summer rainfall regions of South Africa occur over the Cape south coast, contributing to the region's unique climate. Its unique climate is also linked to local topography and the Agulhas Current and their interaction with regional circulation (Rouault et al. 2002; Singleton and Reason 2006). The interaction between regional circulation, topography and the Agulhas Current is in particularly illustrated during events of southerly meridional flow when topographically enhanced uplift of moisture that has been advected over the Agulhas Current occurs. Weather systems responsible for rainfall over this region are cold fronts, west-wind troughs, cut-off lows (COLs), ridging high pressure systems (Taljaard 1996; Favre et al. 2013; Weldon and Reason 2014) and tropical-temperate troughs (Taljaard 1996; Hart et al. 2013). Of these weather systems, ridging high pressure systems, tropical-temperate troughs and COLs are the main rainfall-producing weather systems of the Cape south coast. The mean contribution of ridging high pressure systems, tropical-temperate troughs and COLs to annual rainfall totals was quantified to be 46%, 28% and 16% respectively by application of a self-organizing map (SOM) (Engelbrecht et al. 2015). It may be noted that COLs occur in combination with ridging high pressure systems and tropical-temperate troughs. COLs are known to be the main cause of extreme rainfall events along the Cape south coast (Taljaard 1985; Singleton and Reason 2006, 2007a, 2007b).

Seasonal-to-interannual variability is an integral characteristic of the climate over southern Africa (Mason and Jury 1997; Reason et al. 2002; Reason and Rouault 2005; Washington and Preston 2006), a region that is also characterized by substantial agricultural practices in the commercial and subsistence sectors. In comparison with rainfall variability studies concerning the summer rainfall region (van Heerden et al. 1988; Jury et al. 1992; Mason and Jury 1997; Cook 2004) where most crops are produced (Malherbe et al. 2014b), and to a lesser extent the winter rainfall region (Reason et al. 2002; Reason and Rouault 2005; Philippon et al. 2012), the Cape south coast has been neglected (Weldon and Reason 2014) with regard to rainfall variability studies. This notion is despite the region being an important agricultural area (e.g. dairy production, livestock farming and forestry). Noteworthy though is the smaller variability in rainfall over the Cape south coast compared to rainfall variability experienced over the winter and summer rainfall regions (Taljaard 1996). However, floods and droughts occur from time to time over the Cape south coast - usually impacting significantly on the region, in particular on agriculture. The flood events that occurred in August 2006 and in November 2007 led to agricultural losses exceeding ZAR 100,000,000 for each of the disasters (Holloway et al. 2012). The same kind of weather system that caused the 2006 and 2007 floods, namely a COL, brought an end to the severe meteorological drought of 2008-2009 that occurred over the region and impacted significantly on both rain-fed and irrigation dependent agriculture (Holloway et al. 2012).

Rainfall variability is the result of changes in the frequency, duration, intensity (Mason and Jury 1997) and location (Hart et al. 2013) of rain-producing weather systems and these attributes can in turn be affected by larger-scale climate modes such as the Southern Annular Mode (SAM) (Reason and Rouault 2005; Malherbe et al. 2014a) and El Niño Southern Oscillation (ENSO) (Mason and Jury 1997; Reason et al. 2000; Washington and Preston 2006; Philippon et al. 2012). Over the winter rainfall region of South Africa, interannual rainfall variability is linked to the geographical location of storm tracks, i.e. cold fronts, which are in turn linked to the SAM and more recently ascribed in the literature to ENSO as well. Wet winters are associated with the negative phase of the SAM (Reason and Rouault 2005) as well as with El Niño (Philippon et al. 2012) that cause storm tracks to be located further towards the equator, resulting in wet conditions (Reason and Rouault 2005; Philippon et al. 2012). ENSO is also linked to rainfall variability over the summer rainfall region, in particular mid-summer (Landman and Beraki 2012). Here, El Niño events are usually associated with below-normal rainfall and the less frequent occurrence of tropical-temperate troughs (e.g. Tozuka et al. 2014). However, the association between ENSO and the occurrence of tropical-temperate troughs is non-linear, as wet seasons do not necessarily experience more tropical-temperate troughs (Hart 2012). Our current understanding of rainfall variability over the Cape south coast region is based on very few studies (Jury and Levey 1993; Weldon and Reason 2014). A study that included part of the eastern half of the Cape south coast and that considered only the months of March and October, suggested qualitatively that COLs and ridging high pressure systems play a part in interannual rainfall variability by implication that the occurrence of these systems are disrupted during dry years (Jury and Levey 1993). In a more recent study, the association between anomalous rainfall years, ENSO and COLs was investigated (Weldon and Reason 2014). ENSO also seems to play a part in interannual rainfall variability over the Cape south coast via its association with the occurrence of COLs. Mature phase La Niña years are usually wet and accompanied by a higher frequency of COLs (Weldon and Reason 2014) from late spring to early autumn (Favre et al. 2013). Here, as with the association between tropical-temperate trough occurrence and ENSO, the association between COL frequency and ENSO is non-linear. Dry years are associated with a lower frequency of COLs, but without an ENSO association. The link between ENSO and rainfall variability over the Cape south coast seems mostly to be restricted to the association between increased COL frequency during the spring to autumn months of La Niña years, as other rainfall attributes such as monthly rainfall totals and monthly heavy rain event frequencies show unstable and weak correlations with the Niño 3.4 index (Weldon and Reason 2014). A stronger link is observed between wet-day frequency and the Niño 3.4 index (negative correlation) for December and January (Weldon and Reason 2014), the time of year when the impact of ENSO on rainfall over the summer rainfall region of South Africa is the strongest (Landman and Beraki 2012).

In this study, interannual variability in seasonal rainfall over the Cape south coast is investigated within the context of the high frequency variability of synoptic types, i.e. intraseasonal variability. The frequency of occurrence of the different synoptic types is therefore derived from daily circulation data and subsequently associated with anomalous rainfall on the seasonal time scales. Of specific interest are the regional features of rain-producing weather systems associated with rainfall variability. The aim of this study is to identify the specific configurations of the different synoptic types that are potentially linked to the interannual variability of seasonal rainfall, with the potential to apply the gained knowledge to application forecasts of intraseasonal variability. This aim requires the investigation of the potential link between the occurrence of COLs and rainfall variability as well, given the high impact rainfall events that can occur in association with COLs. Also, with the known ENSO association over the region (Weldon and Reason 2014) as well as the ENSO and SAM relationships over the winter (Reason and Rouault 2005; Philippon et al. 2012) and summer (van Heerden et al. 1988; Pohl et al. 2010; Malherbe et al. 2014a) rainfall regions, the potential association of these climate modes with the intraseasonal occurrence of synoptic regimes is explored.

3.2 Data and methodology

3.2.1 Rainfall data

Daily rainfall data for the 33-year period from 1979 to 2011 from 12 weather stations of the South African Weather Service (SAWS) over the Cape south coast were considered in this study (Fig. 1). These 12 stations were chosen based on their availability (defined here as the presence of data on more than 90% of the days in a specific month) and quality. Extreme and missing value tests were employed as data quality measures. Values that did not comply with these tests were replaced by estimated values derived from neighbouring stations. Seasonal rainfall totals for each station were calculated from this complete daily rainfall dataset. The seasons considered here are austral summer, autumn, winter and spring, comprising December to February (DJF), March to May (MAM), June to August (JJA) and September to November (SON) respectively. The seasonal rainfall totals were spatially averaged and then ranked in order to identify years of above-normal, near-normal and below-normal seasonal rainfall. Thirty-two years of seasonal rainfall totals were considered for each of the four seasons. For each of the seasons the upper-most 10 totals were used to define above-normal rainfall, the 10 lower-most totals define below-normal rainfall and near-normal rainfall is defined by the remaining 12 rainfall totals. The rainfall station data were used to quantify the contribution of COLs to seasonal rainfall totals in order to investigate the role of COLs in interannual variability of seasonal rainfall.

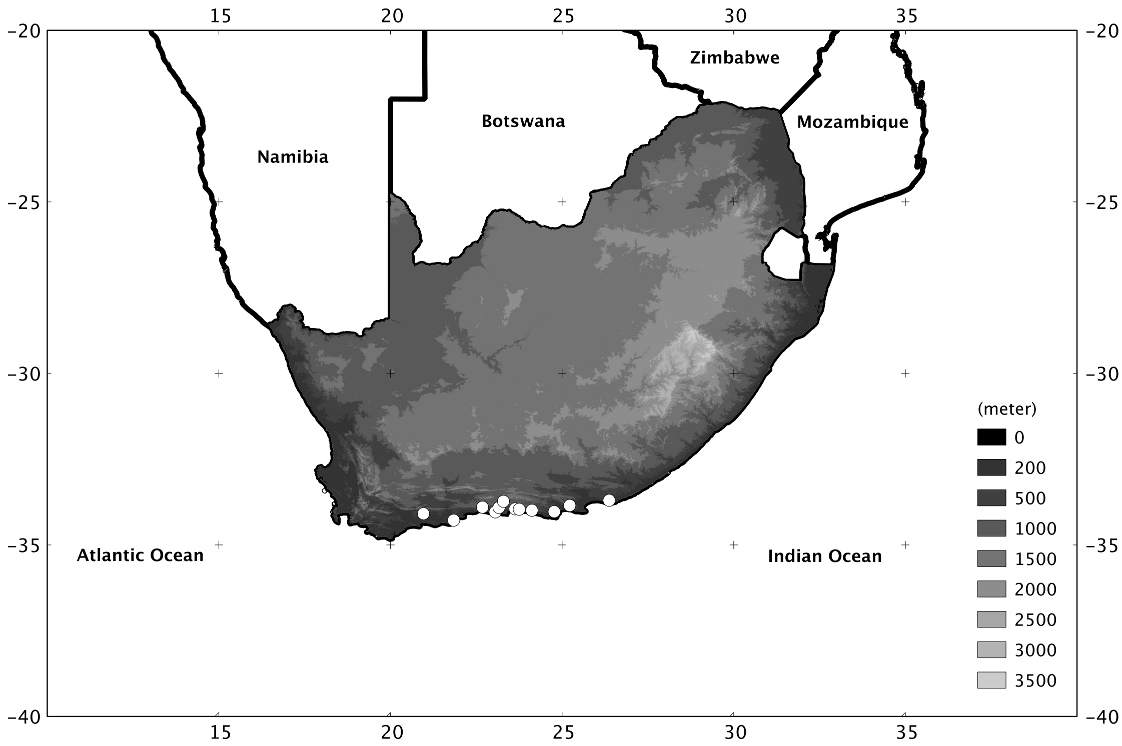

Fig. 1 Geographical location of rainfall stations. The circles represent the location of each of the 12 rainfall stations and the grey shading the topography

3.2.2 Classification of synoptic types and identification of COLs

The focus of this paper is to relate interannual variability in seasonal rainfall to synoptic types. Synoptic types that represent archetypical atmospheric states were classified by application of the SOM technique (Kohonen 2001). A 35-node SOM was developed from daily sea-level pressure (SLP) anomaly fields derived from the daily average SLP fields from the National Centers for Environmental Prediction (NCEP) reanalysis data (Kalnay et al. 1996) for the region bounded by 45°S-32.5°S and 10°E-40°E. The SLP anomaly fields are effectively gradient fields that drive circulation (Scheunemann et al. 2009). Over the Cape south coast, low-level circulation is important to facilitate moisture advection from the surrounding ocean (Rouault et al. 2002; Singleton and Reason 2006, 2007a) - hence the choice of the SOM domain. A full description on the development of the SLP anomaly SOM can be found in Engelbrecht et al. (2015). In this paper, the composite maps of the 850 hPa geopotential height fields based on the SLP anomaly SOM are employed to represent the archetypical atmospheric states. The decision to employ the 850 hPa geopotential height fields to present the synoptic types in this study is to allow for presenting the synoptic types over a domain extending further northwards. The 850 hPa pressure level takes the typical height of 1,500 m of the South African plateau into consideration. The presentation of the synoptic types over a domain that includes a larger part of the subcontinent can complement the description of the synoptic types as the circulation over South Africa and surrounding oceans normally consist of segments of several circulation types. It can be noted that the synoptic types identified by the SLP anomaly SOM and those represented by the 850 hPa geopotential height composite maps over the larger domain, are consistent as the 850 hPa composite maps are derived from the daily entries in each node of the SLP anomaly SOM.

NCEP reanalysis data (Kalnay et al. 1996) are utilized to identify and track COLs over the period 1979-2011. COLs have a typical length scale of 1,000 km (Singleton and Reason 2007b) and are therefore well resolved by the 2.5° resolution of the NCEP data. A COL is defined as a cold cored closed-low at 500 hPa that is displaced from the westerly wind regime (Favre et al. 2012). The daily-average geopotential height and temperature fields at 500 hPa are utilized for identifying and tracking COLs in the domain bounded by 40°S-20°S and 10°E-40°E. All the COLs that occurred for at least 24-h over this domain are considered in this study. Firstly, closed-lows are identified by locating geopotential minima in a procedure where the geopotential at each grid point is compared to the geopotential values of the square of eight surrounding grid points on the latitude longitude grid. After closed-lows have been identified in the time series of 500 hPa geopotential fields, tracks are constructed by identifying the geopotential minima at time step $t+1$ nearest to the geopotential minima at time step t. The distance between the closed-lows at time step t and time step $t+1$ needs to be <1,000 km in order to secure a sound mean daily speed of the potential COL. The mean daily speed of a COL in the South African region does not exceed 42 km/h (Favre et al. 2012). Any geopotential minima can only be used in a single track. From this closed-low track dataset, tests described in Favre et al. (2012) to ensure that tracks are of extra-tropical origin, are detached from the westerlies and possess a cold-core are employed.

Rainfall associated with cold-cored systems occurs mainly some hundreds of kilometres to the northeast, east and southeast of the centres of these systems. From the constructed COL dataset for the period 1979-2011, all the COLs that occurred west of 32.5°E, following Favre et al. (2013), were considered to be potentially responsible for rainfall over the region. Such COLs associated with rainfall over the region, at least at a single station, were defined as rainfall producing COLs.

3.2.3 Grouping of similar synoptic types into main circulation types

The synoptic types identified by the SOM consist of various configurations of the main circulation types. Each of the SOM nodes is classified into one of the main circulation types - following the grouping performed in Engelbrecht et al. (2015). These groups represent circulation types representative of troughs southwest of the subcontinent, troughs southeast of the subcontinent, ridging high pressure systems, ridges east/southeast of the subcontinent, tropical-temperate troughs and weak synoptic flow. The groups of synoptic types used here fall within the subdivisions of circulation types (anticyclones, cyclones, ridges, troughs and zonal flow) identified and described by Taljaard (1995). Troughs southwest or southeast of the subcontinent fall within the west wind trough circulation type (e.g. Taljaard 1995), with the distinguishing factor being the position of the westerly trough relative to the subcontinent. Cold fronts, occurring during winter and summer as well as leader fronts, a winter circulation type, typically fall within these two groups while ridging high pressure systems and ridges east/southeast of the subcontinent are variations of ridges as described by Taljaard (1995). Tropical-temperate troughs, although part of the trough family, are considered separately as these systems are captured explicitly in the SOM (e.g. Tozuka et al. 2014) and due to its importance with regard to rainfall contribution over South Africa (Harrison 1984; Washington and Todd 1999; Hart et al. 2013). COLs are part of the cyclone/low pressure family (Taljaard 1995) and co-occur with ridging high pressure systems (Katzfey and McInnes 1996; Favre et al. 2012; Engelbrecht et al. 2015) and tropical-temperate troughs (Hart et al. 2013; Engelbrecht et al. 2015). However, due to the infrequent occurrence of COLs (Engelbrecht et al. 2015), these systems are difficult to explicitly be captured in the SOM. COLs are therefore considered with ridging high pressure systems and tropical-temperate troughs in the analysis presented in this paper, unless where it is indicated that COLs are considered explicitly as identified by the objective COL identification and tracking algorithm (see section 2.2). The group of similar synoptic types termed weak synoptic flow is similar to the zonal flow circulation type identified by Taljaard (1995). However, a difference may be that the circulation type zonal flow described by Taljaard (1995) can be associated with weak or tight pressure gradients, whereas the circulation type weak synoptic flow in this study is defined to be characterized by weak pressure gradients over the Cape south coast region.

Classification of the synoptic types into groups is feasible by visual inspection of the 850 hPa geopotential height node composites (typically as would be performed by an experienced weather forecaster), but introduces the challenge of objectivity due to the circulation over the study domain not normally characterized by a single circulation type. Classification of the synoptic types into groups representative of troughs southwest of the subcontinent, troughs southeast of the subcontinent, ridging high pressure systems, ridges east/southeast of the subcontinent, tropical-temperate troughs and weak synoptic flow was therefore achieved by careful consideration of the SOM node anomaly fields (850 hPa geopotential height composites) relative to climatology (not shown) and a hierarchical clustering method, Ward's minimum variance method (Wilks 2011). Ward's method was applied to the SOM nodes based on the SLP anomaly fields to aid in grouping of the synoptic types into the main circulation types.

3.2.4 Large-scale climate modes

The Oceanic Niño Index (ONI) is obtained for DJF, MAM, JJA and SON for 1979 to 2011 (32 DJF seasons and 33 MAM, JJA and SON seasons each) from the Climate Prediction Center (CPC) (www.cpc.ncep/noaa.gov/products/analysis_monitoring/ensostuff/ensoyears.shtml). The ONI is a 3-month running mean of ERSST.v3b (Smith et al. 2008) sea-surface temperature (SST) anomalies in the Niño 3.4 region (5°N - 5°S, 120°W - 170°W), and has already been used as an ENSO indicator for southern African variability and predictability studies (Landman et al. 2009; Landman et al. 2012). Monthly SAM (Mo 2000) index values are also obtained from CPC (www.cpc.ncep.noaa.gov/products/precip/CWlink/daily_ao_index/monthly.aao.index.b79.current.ascii.table), and are used to derive the SAM index for DJF, MAM, JJA and SON for 1979 to 2011.

An objective of the paper is to further our current understanding (Weldon and Reason 2014) of the ENSO link and rainfall variability over the Cape south coast. As ENSO and SAM are related (Gong et al. 2010; Fogt et al. 2011), the teleconnection investigation performed here included an analysis that aims to address the potential link between SAM and the occurrence of synoptic regimes.

In order to determine whether the climate modes, ENSO and SAM, are separately correlated with the occurrence of synoptic regimes for each of the seasons DJF, MAM, JJA and SON, a synoptic regime index is derived. This index considers the frequency distribution of synoptic regimes within the SOM space and was derived for each of the seasons (DJF, MAM, JJA and SON) from the pattern correlation between the interannual frequency distribution within the SOM space and a reference frequency distribution. The reference frequency distribution is represented by the average frequency distribution of the wet years for the particular season. In this manner, a unique time series is developed for each of the seasons, which are then utilized in the correlation analysis with ENSO and SAM.

3.3 Results

3.3.1 Seasonal cycle of synoptic types

The 850 hPa geopotential height node-averaged fields are shown in Fig. 2 while the seasonal cycle of each node expressed as the percentage occurrence is shown in Fig. 3. Nodes with a strong winter occurrence are observed in the bottom row of the SOM (nodes 1 to 6), while nodes occurring most frequently in summer are found in the top row (nodes 29 to 35). The nodes in the top row of the SOM also show a high frequency of occurrence during the transitional seasons, autumn and spring. However, the highest frequency of occurrence during autumn is found over the left-central part of the SOM (node 15) representative of a surface trough over the far western part of the country linking up with a westerly trough to the southwest of the subcontinent (Fig. 2). During spring, nodes located over the right-central part of the SOM (in particular node 21), representative of ridging high pressure systems, exhibit the highest frequency of occurrence. The various configurations of winter frontal systems are represented by nodes 1 to 6. Frontal systems without a pronounced winter occurrence, e.g. represented by nodes 8 and 9, are characterized by a weaker pressure gradient than frontal systems with a strong winter occurrence, e.g. nodes 1 and 2 (Fig. 2). The frontal systems characterized by stronger pressure gradients are the synoptic types contributing least to annual rainfall over the Cape south coast (Engelbrecht et al. 2015), while these systems are the important rain-producing systems over the winter rainfall region (Lennard and Hegerl 2015). Ridging high pressure systems and tropical-temperate troughs, found in the top right part of the SOM (nodes 27, 28, 33, 34 and 35), are major contributors to annual rainfall over the Cape south coast (Engelbrecht et al. 2015). Noteworthy is that these systems sometimes co-occur with COLs (Engelbrecht et al. 2015). Nodes representative of synoptic types that occur throughout the year, but lacks evidence of a preferred season of occurrence, are found in the central part of the SOM (Fig. 3), and are in general insignificant with regard to annual rainfall contribution over the region (Engelbrecht et al. 2015). It is noteworthy that Ward's method provides results that are consistent with the grouping of synoptic types into a number of main synoptic types as described above. For example, nodes 28 and 35, indicative of ridging highs are grouped together by Ward's method. Similarly, nodes 33 and 34, indicative of tropical-temperate troughs, are grouped together.

Fig. 2 Node-averaged 850 hPa heights of the 35-node SOM developed from daily SLP anomaly fields for the period 1979-2011

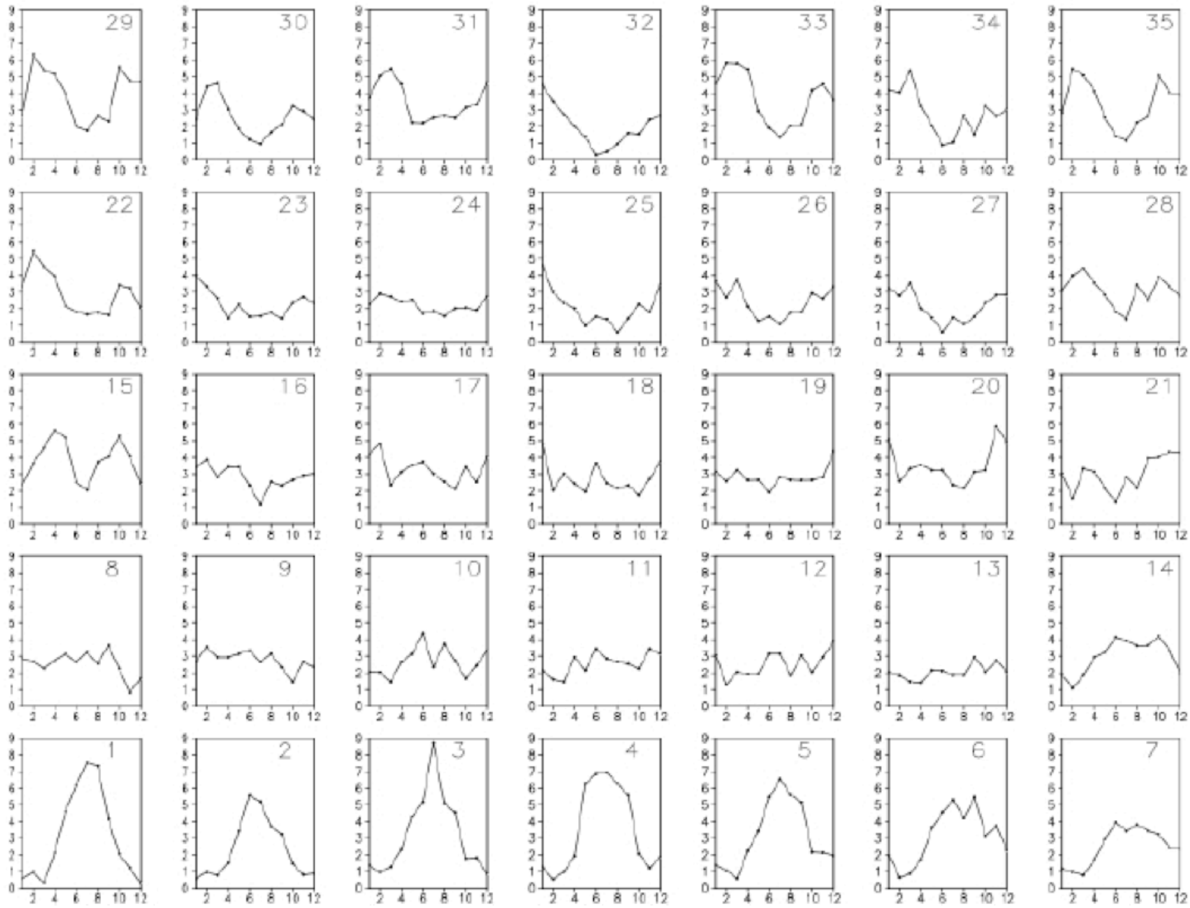

Fig. 3 Annual cycle (months indicated on the x-axis) of the percentage occurrence (y-axis) for the synoptic types identified by the SOM (node number indicated in the top-right of each panel)

3.3.2 Circulation anomalies during seasons of anomalous rainfall

Figure 4 shows the rainfall totals for 32 DJF (1979/80-2010/11), MAM (1980-2011), JJA (1980-2011) and SON (1980-2011) seasons. A similar analysis at annual time scales is not meaningful, because of a given year having the potential to be wet (or dry), for very different reasons. For example, a year with above-normal rainfall induced by a wet SON will exhibit different synoptic frequencies than a wet year associated with a wet JJA.

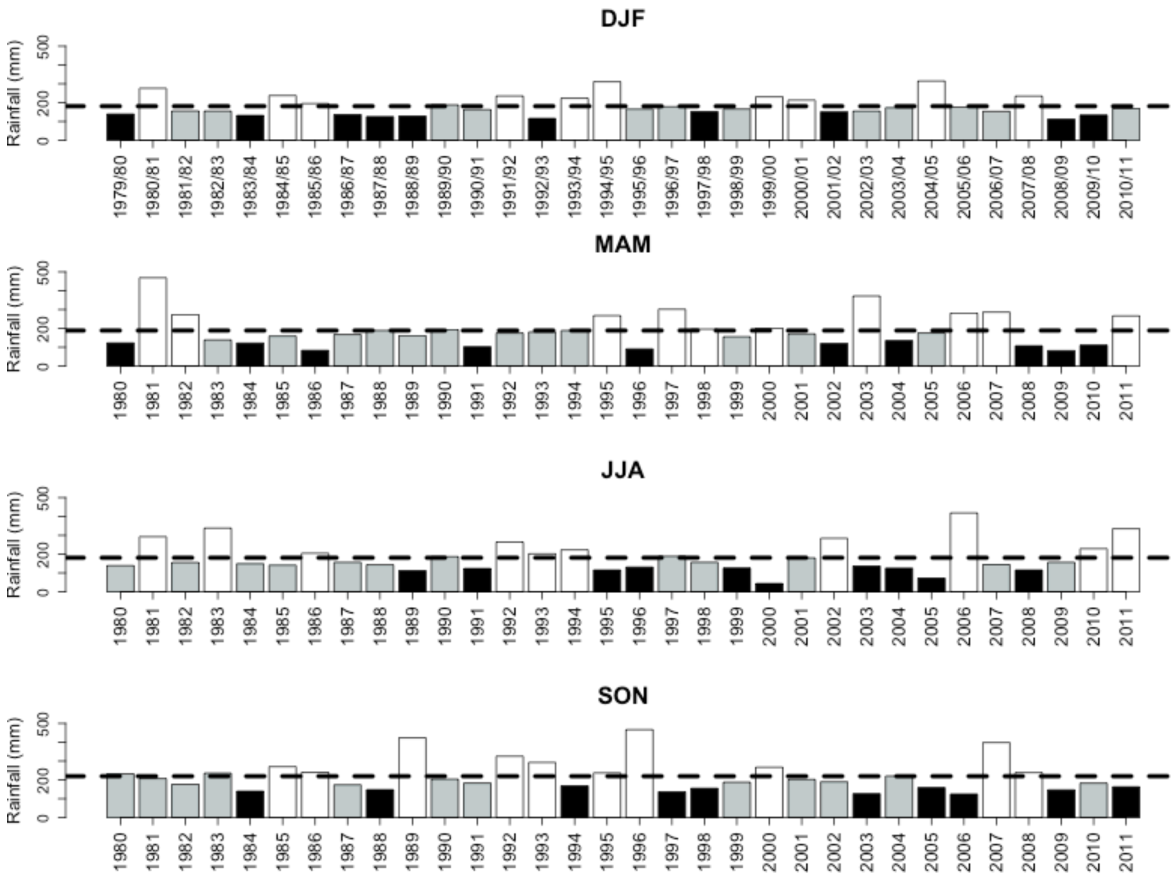

Fig. 4 The seasonal rainfall (mm) over the Cape south coast for 32 DJF, MAM, JJA and SON years over the period 1979 to 2011. The long-term mean rainfall for each seasons is indicated by a black dashed line. Seasons of above-normal, near-normal and below-normal rainfall are indicated by white, grey and black respectively

Circulation anomalies associated with wet and dry seasons are presented in terms of the frequency of synoptic archetypes occurring during the relevant wet and dry seasons. Circulation anomalies associated with the SOM-nodes for seasons of above-normal, near-normal and below-normal rainfall are calculated relative to the relevant long-term mean for each of the nodes and are expressed as a percentage change of the actual node value before the relevant individual seasons are averaged for the wet, normal and dry seasons (Fig. 5).

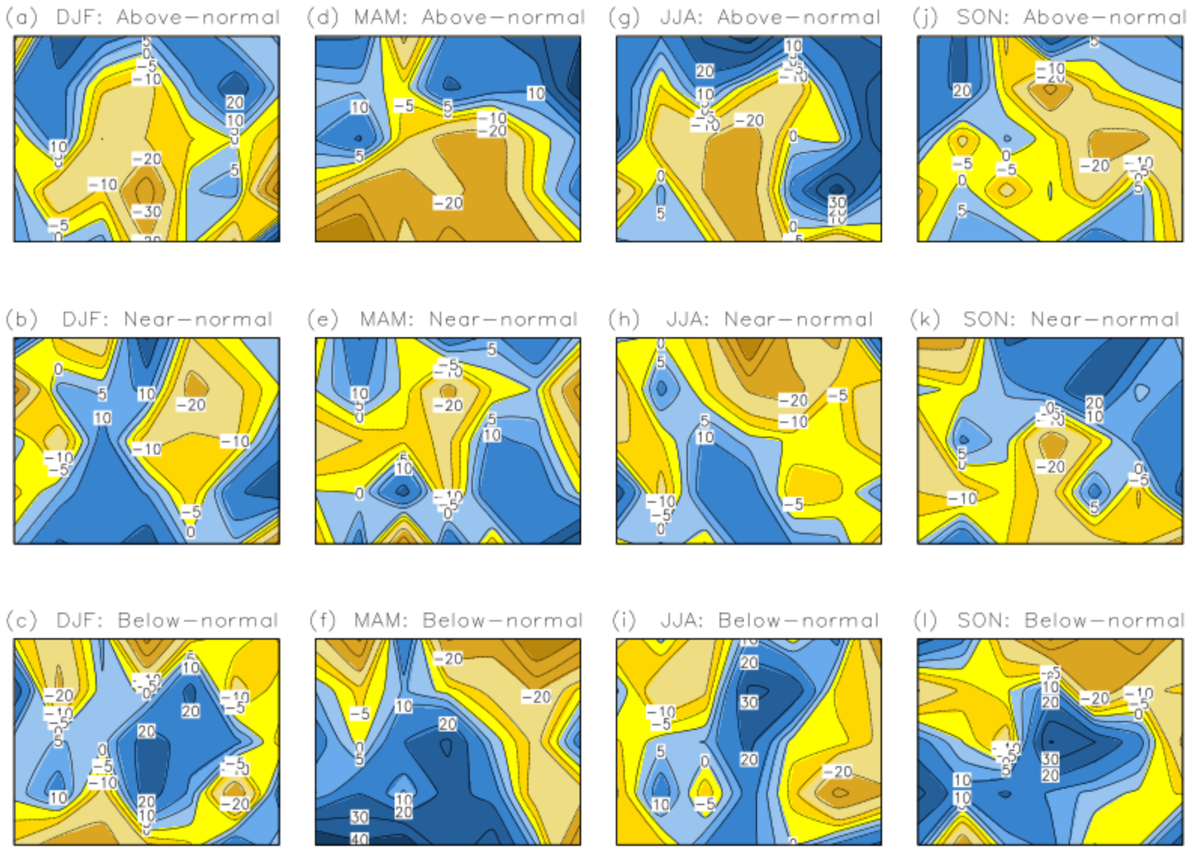

Fig. 5 Average circulation anomalies for seasons of above-normal (top row), near-normal (middle row) and below-normal (bottom row) rainfall as represented by the SOM-node frequency expressed as a percentage change for each of the nodes relative to the relevant long-term mean frequency of the relevant SOM-node. Positive (negative) anomalies are indicated by blue shaded (yellow shades)

Rainfall anomalies are presented by using two different anomaly metrics to aid in the interpretation of rainfall characteristics that occur during wet and dry seasons. Figure 6 shows the average rainfall anomalies (mm) relative to the climatological value of the actual node for the relevant wet, normal and dry seasons. Figure 7 shows the rainfall percentage associated with each SOM-node, averaged for seasons of above-normal, near-normal and below-normal rainfall. Evident from Fig. 5 is the contrasting frequency relative to the climatological frequency of synoptic archetypes that occur during seasons of above-normal (Fig. 5a, d, g and j) and below-normal (Fig. 5c, f, i and l) rainfall. Table 1 shows the Kendall's tau rank correlation between the 35 node frequencies associated with above-normal rainfall and the corresponding 35 frequencies associated with below-normal rainfall, for each of the four seasons. The contrasting frequency of occurrence of the synoptic archetypes during wet and dry DJF seasons is significant at the 95% level of confidence (Kendall's tau rank correlation) while differences in the synoptic archetype frequencies between wet and dry MAM and JJA seasons are significant at the 90% and 99% level of confidence (Kendall's tau rank correlation) respectively (Table 1). The Pearson product-moment correlation coefficients suggest for this relationship to be linear, in particular for JJA (not shown). Interesting to note is that such a reserved symmetry in terms of the frequency of synoptic archetypes does not exist for dry and wet SON seasons (Table 1), although synoptic archetype frequencies differ significantly between dry and normal SON seasons (not shown). The rainfall anomalies (Fig. 6) mirror the corresponding circulation anomalies (Fig. 5) with regard to the sign of the anomaly, illustrating the link between the total rainfall and the frequency of synoptic types, which suggests that the frequency of occurrence of these synoptic archetypes plays a role in determining whether seasons are dry/wet. The percentage rainfall associated with each node in the SOM during wet and dry seasons (Fig. 7) reveals further that the nodes associated with rainfall are very similar during above-normal (Fig. 7a, d, g and j), near-normal (Fig. 7b, e, h and k) and below-normal (Fig. 7c, f, i and l) rainfall seasons. Circulation anomalies during seasons of near-normal rainfall are characterized by a mixture of circulation anomalies that also occur during wet and dry seasons.

Table 1. Kendall's tau rank correlation between the frequency of synoptic archetypes during seasons of above-normal versus seasons of below-normal rainfall (see Fig. 5), where * = 90% level of confidence, ** = 95% level of confidence and *** = 99% level of confidence

DJF	**MAM**	**JJA**	**SON**
-0.26 **	-0.208 *	-0.415 ***	-0.0605

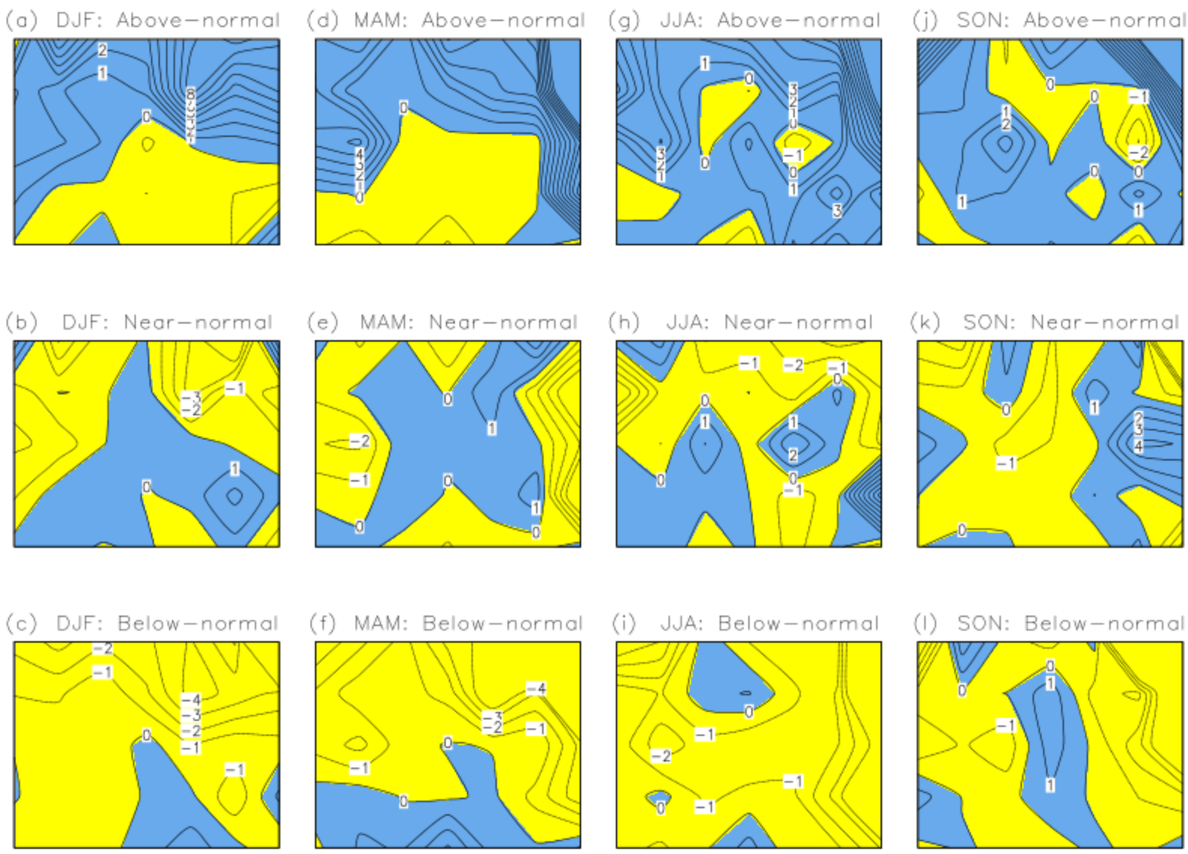

Fig. 6 Average rainfall anomalies (mm) for seasons of above-normal (top row), near-normal (middle row) and below-normal (bottom row) rainfall as represented by the rainfall associated with each of the nodes relative to the relevant long-term mean rainfall of the relevant SOM-node. Positive (negative) anomalies are indicted in blue (yellow)

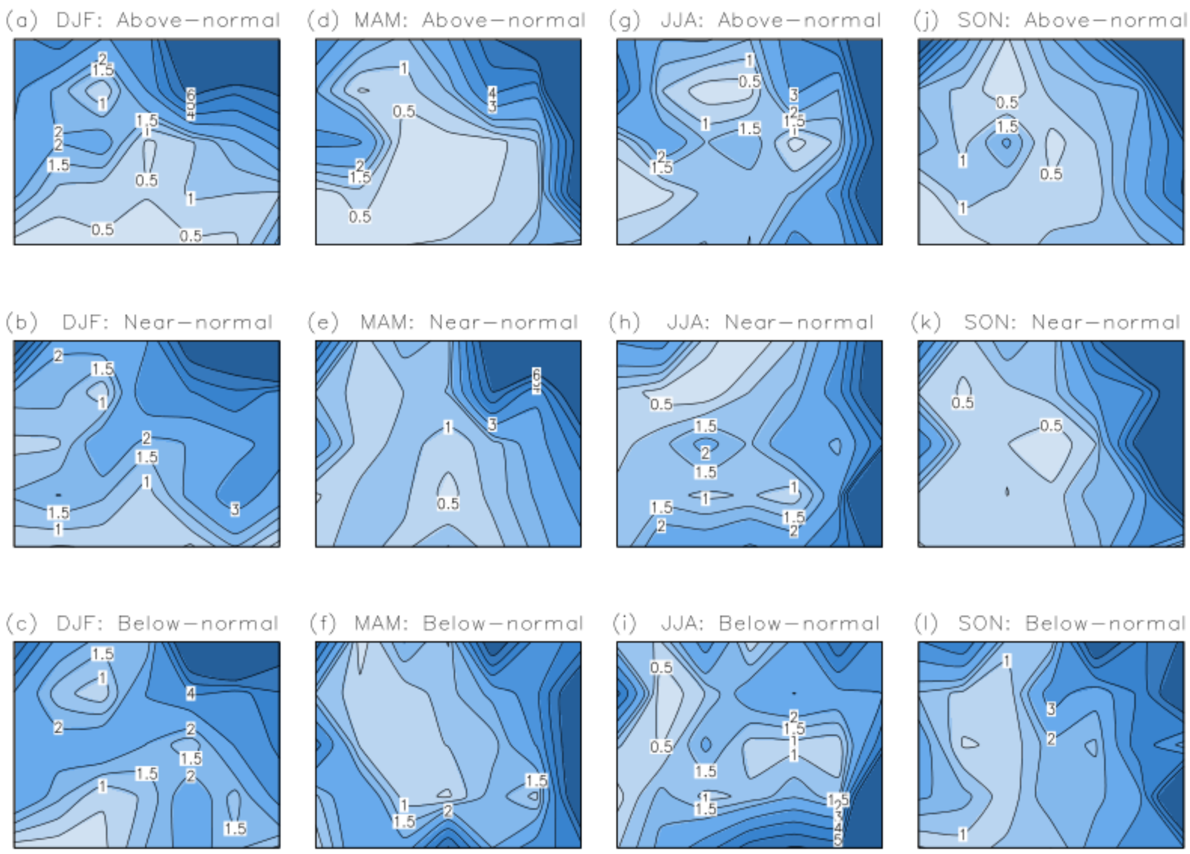

Fig. 7 Average percentage of rainfall for the SOM-nodes associated with seasons of above-normal (top row), near-normal (middle row) and below-normal (bottom row) rainfall

Figure 8 shows the node-averaged meridional vertically integrated moisture flux for the SOM. The main rainfall-producing synoptic types found in the far right part of the SOM (e.g. nodes 14, 21 and 28) are associated with a vertically integrated northward moisture flux with the largest moisture flux located to the south of the subcontinent (Fig. 8). Other main rainfall-producing nodes (e.g. nodes 22, 29, 30, 33, 34 and 35) are characterized by a vertically integrated southward moisture flux in a northwest-southeast orientated band over the interior extending over the ocean southeast of the subcontinent in some of these nodes, characteristic of cloud bands typical of summer (Todd et al. 2004; Hart et al. 2010, 2013; Tozuka et al. 2014).

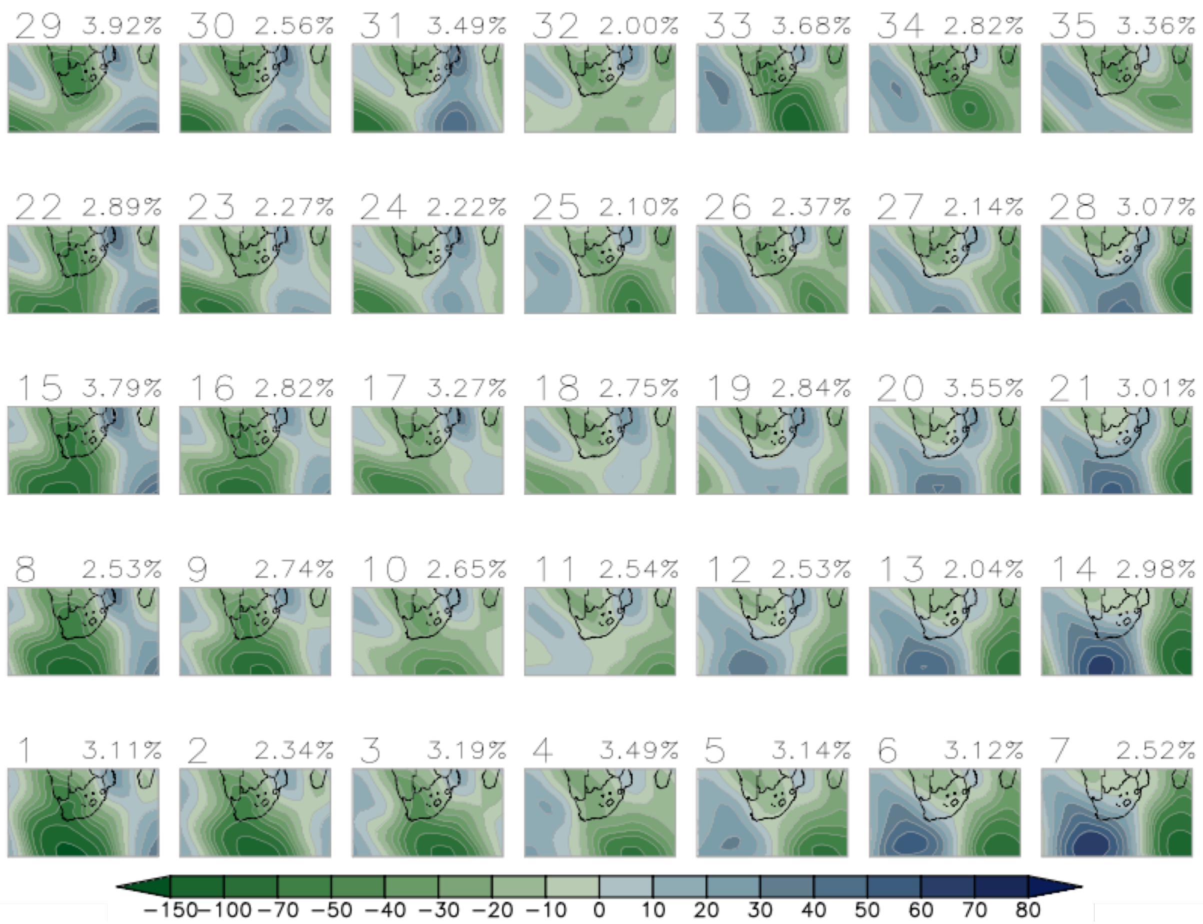

Fig. 8 Node-averaged meridional vertically integrated moisture flux (g $m^{-1}s^{-1}$)

Vertical profiles of the meridional moisture flux over the Cape south coast, represented by the location at 35° S and 25° E, for wet and dry DJF, MAM, JJA and SON seasons, are shown in Fig. 9. For the purpose of visibility, vertical profiles for selected main rainfall-producing nodes, representative of these main rainfall-producing synoptic types, are shown. In general, three different moisture profiles are observed - moisture profiles characterized by a northward moisture flux (e.g. 28), a southward moisture flux (e.g. node 29) and profiles with a northward flux in the low-levels and a southward flux in the mid-levels (e.g. nodes 33 and 35). Considerable variation occurs in the latter case. For example, node 35 is characterized by a prominent northward low-level moisture flux during most seasons (Fig. 9), as may be expected from low-level ridging along the Cape south coast. Node 35 exhibits a more pronounced low-level northward moisture flux compared to node 33, being stronger and notably deeper, extending up to 775 hPa. This relatively strong northward moisture flux, overlayed by a southward moisture flux, is characteristic of convective overturning (Taljaard 1996), also known as "undercutting" and can act as a trigger for convection. Node 33 represents a very different vertical moisture flux profile. Here a prominent southward flux is always present, especially in the mid-levels (700 hPa), as may be expected to occur in association with tropical-temperate troughs.

As expected, maximum moisture fluxes associated with each node occur mostly at the pressure level closest to sea level, 1000 hPa here, with the moisture being advected northwards. For example, during DJF, MAM and SON node 28 is associated with the maximum northward moisture flux while node 14, representative of a winter synoptic type (Fig. 3), is associated with the maximum northward moisture flux during JJA. The exception is synoptic types representative of node 29, characterized by a southward moisture flux with the maximum moisture flux occurring at pressure levels closest to the height of the plateau over the interior, being the strongest during MAM and SON (Fig. 9).

Moisture profiles during wet and dry seasons are quite similar, with wet seasons having a slightly stronger moisture flux, particularly evident for nodes 14 (JJA), 28 (MAM and SON) and 35 (SON). However, exceptions are observed for nodes 14 and 33 during DJF when moisture profiles of dry seasons have larger moisture fluxes than those of wet seasons. Node 14, representative of frontal systems, has a higher frequency of occurrence during dry seasons – explaining the larger moisture flux as confirmed in specific humidity profiles (data not shown). The larger moisture flux associated with node 33 during dry DJF seasons is due to stronger winds (not shown). Austral summer months during years of anomalous low rainfall over South Africa have been linked to the jet stream located anomalously equatorwards (Tennant and Reason 2005), implying stronger winds and cold fronts to have more equatorwards tracks.

Other contrasting circulation anomalies that are characteristic of below-normal and above-normal rainfall seasons occur over the central part of the SOM. These nodes are representative of weather systems associated with an equatorward pressure gradient (zonally orientated high pressure over the subcontinent and surrounding oceans with zonally orientated low pressure further southwards). An equatorward pressure gradient (e.g. node 18) is not favourable for moisture advection over the Cape south coast. During above-normal (below-normal) rainfall seasons, an anomalously low (high) occurrence of weather systems characterized by this weak synoptic flow occurs.

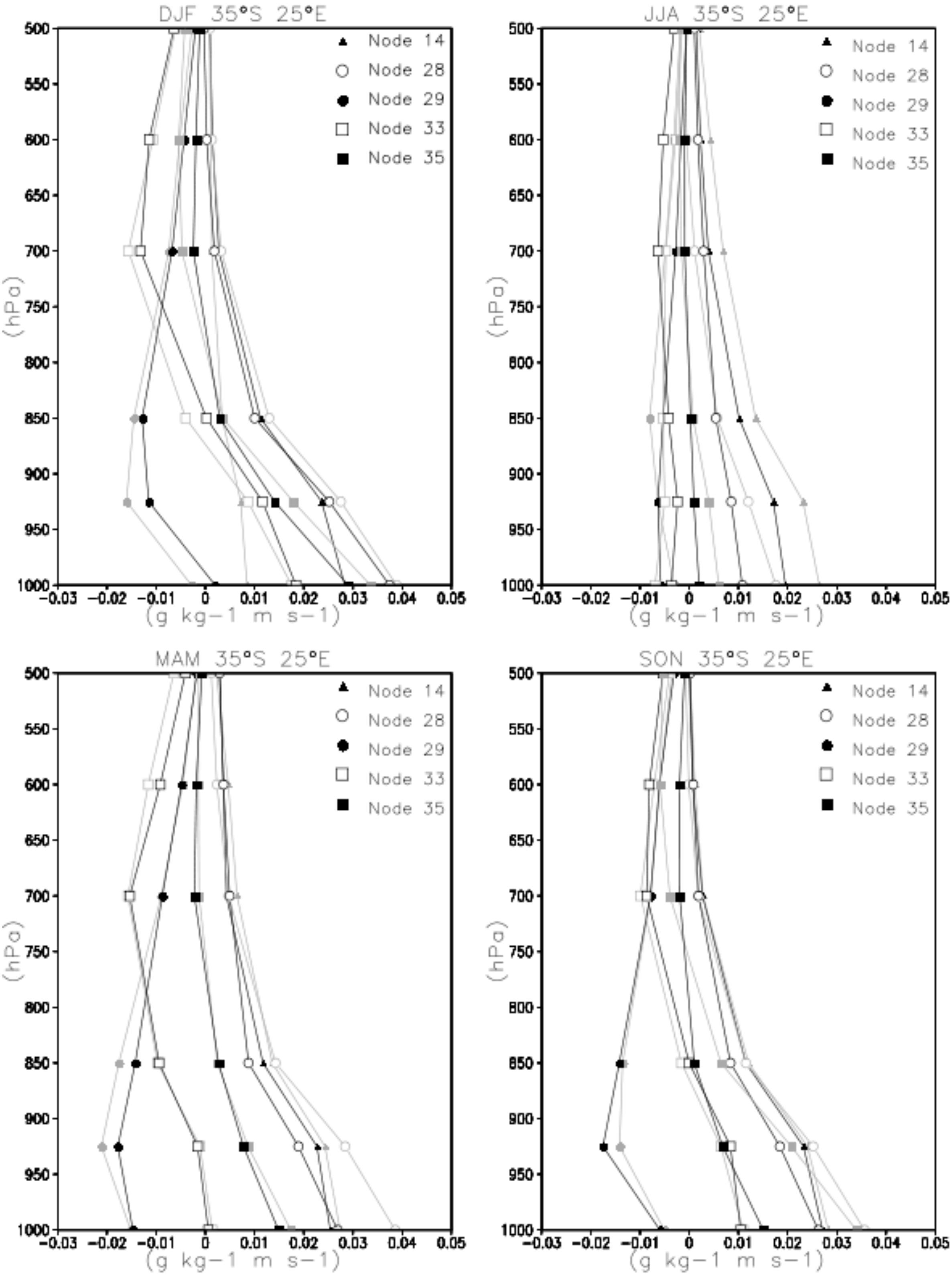

Fig. 9 Vertical profile of the meridional moisture flux (g kg^{-1} m s^{-1}) at 35° S and 25° E for wet (grey) and dry (black) DJF, MAM, JJA and SON seasons

3.3.3 Synoptic type rainfall and interannual variability of seasonal rainfall

Climatological seasonal rainfall totals over the Cape south coast are very similar (Table 2). Rainfall-producing synoptic types with an occurrence throughout the year includes ridging high pressure systems from the southwest and COLs while the contribution by tropical-temperate troughs and frontal systems peak during October to April and May to August respectively (Engelbrecht et al. 2015). In the case of ridging high pressure systems, seasonality is observed in the preferred configuration of this synoptic type that contributes to rainfall. For example, ridging high pressure systems from the southwest represented by nodes 7 and 14 are characteristic of winter, while nodes 20, 27 and 35 exhibit summer peaks in their occurrence (Fig. 3). An objective of this paper is to identify important synoptic types and/or configurations within a specific synoptic type that are linked to interannual variability of seasonal rainfall over the Cape south coast. A direct approach to address this question is to test whether a significant positive correlation exists between the rainfall associated with the synoptic types and the total seasonal rainfall. It is firstly tested whether rainfall associated with nodes representative of a similar synoptic type collectively correlate with seasonal rainfall totals.

Table 2. Climatological seasonal rainfall totals (mm)

DJF	MAM	JJA	SON
181	189	181	219

During DJF and MAM, rainfall associated with ridging high pressure systems from the southwest, ridges situated east of the subcontinent and tropical-temperate troughs (Table 3) exhibit a significant positive rank correlation with the respective seasonal rainfall totals, suggesting that these synoptic types are linked to interannual variability of DJF and MAM rainfall. During JJA and SON, rainfall associated with ridging high pressure systems from the southwest and ridges situated east of the subcontinent exhibit a significant positive rank correlation with JJA and SON rainfall totals respectively (Table 3). Ridging high pressure systems from the southwest seem to have the strongest link to interannual variability of seasonal rainfall - significant at the 99% level of confidence during DJF, MAM, JJA and

SON, followed by ridges situated east of the subcontinent (Table 3). For the latter, the link to interannual variability seems stronger during DJF and MAM compared to JJA and SON. Pearson product-moment correlation coefficients indicate that this relationship is linear (not shown). Ridging high pressure systems from the southwest show the strongest linear relationship with interannual variability of seasonal rainfall. It may be noted that the maximum COL occurrence co-occurs with nodes within the groups representing ridging high pressure systems from the southwest (Fig. 2, node 35) and ridges situated east of the subcontinent (Fig. 2, node 29) (Engelbrecht et al. 2015). This is likely to influence the positive correlation of these groups with seasonal rainfall totals as COLs are associated with heavy rainfall events (Rouault et al. 2002; Singleton and Reason 2006, 2007a).

Table 3. Kendall's tau rank correlation between circulation type seasonal rainfall (mm) and total seasonal rainfall (mm) over the period 1979 to 2011, where * = 90% level of confidence, ** = 95% level of confidence and *** = 99% level of confidence

Grouped synoptic types / main circulation types	**Trough southwest**	**Trough southeast**	**Ridging high pressure**	**Ridge east**	**Tropical temperate trough**	**Weak synoptic flow**
Nodes	1, 2, 3, 8, 9, 10	4, 5, 6, 11, 12	7, 13, 14, 20, 21, 27, 28, 35	17, 24, 29, 30, 31	15, 16, 22, 23, 25, 26, 32, 33, 34	18, 19
DJF	0.16	-0.19	0.42^{***}	0.33^{***}	0.26^{**}	-0.006
MAM	-0.2	-0.14	0.69^{***}	0.58^{***}	0.32^{**}	-0.06
JJA	0.16	0.07	0.58^{***}	0.28^{**}	0.19	-0.05
SON	-0.05	0.09	0.6^{***}	0.24^{*}	0.17	-0.09

The various configurations within the grouped synoptic types (represented by the individual nodes shown in Fig. 2), represent variations of attributes such as geographical and seasonal location, intensity and some structural features. In an attempt to highlight or isolate what specific configuration within a synoptic type is the preferred driver of interannual variability of seasonal rainfall, the seasonal rainfall associated with the individual nodes was also correlated with seasonal rainfall totals (Table 4). Noteworthy, is the presence of 2 specific configurations of ridging high pressure systems from the southwest, those with the most southward located axis (Fig. 2, nodes 28 and 35), that are correlated with rainfall totals for DJF, MAM, JJA and SON. Ridging high pressure systems from the southwest representative of nodes 28 and 35 are suggested to be a driver of interannual variability of SON rainfall in particular with correlations significant at the 99% level of confidence (Table 4). In the case of the tropical-temperate troughs, a significant correlation with DJF, MAM and SON rainfall totals exists. During DJF, rainfall associated with tropical-temperate troughs with the smallest node-averaged zonal wind component over and to the south of the country (nodes 32) are correlated to DJF rainfall totals, consistent with the jet stream that is located further poleward during years of above-normal rainfall over the summer rainfall region and hence weaker winds (Tennant and Reason 2005). During MAM and SON other configurations of tropical-temperate troughs are linked to interannual variability of seasonal rainfall, illustrating the seasonality that can occur within a specific group of synoptic types.

Table 4. Nodes for which the node-associated rainfall is significantly correlated with the seasonal rainfall totals over the period 1979 to 2011. Node numbers are indicated in **bold**. Kendall's tau rank correlation and the significance level is indicated in brackets where * = 90% level of confidence, ** = 95% level of confidence and *** = 99% level of confidence

Seasons	Nodes for which the node associated rainfall is significantly correlated with the seasonal rainfall totals
DJF	**27** (0.27**), **28** (0.23*), **32** (0.3**), **35** (0.22*)
MAM	**2** (-0.3**), **4** (-0.33***), **15** (0.25**), **16** (0.32**), **25** (0.24*), **27** (0.28**), **28** (0.22*), **30** (0.45***), **33** (0.26**), **34** (0.3**), **35** (0.32**)
JJA	**1** (0.25*), **2** (0.22*), **4** (-0.26**), **13** (0.3**), **21** (0.27**), **28** (0.44***), **29** (0.24*), **35** (0.25*)
SON	**8** (-0.29**), **16** (0.24*), **22** (0.22*), **28** (0.38***), **33** (0.24*), **35** (0.4***)

COLs contribute to 16% of annual rainfall totals, co-occurring with ridging high pressure systems and tropical-temperate troughs (Engelbrecht et al. 2015). The nature of COLs to cause high impact rainfall events that have the ability to produce 24-h rainfall totals that exceed the relevant climatological monthly rainfall (Singleton and Reason 2006, 2007a; Muller et al. 2008), warrants the consideration of a linkage between COL-induced rainfall and interannual variability in seasonal rainfall. Mean seasonal rainfall totals attributed to COLs are of comparable magnitude for MAM, JJA and SON with mean seasonal total rainfall during DJF only half or less of any of the other seasons (Table 5). Over South Africa COLs occur most frequently during MAM (31%), followed by JJA (29%), SON (22%) and DJF (18%) (Table 5), similar to COL seasonal frequencies from Singleton and Reason (2007b) and Favre et al. (2013). The relationship between the frequency of COLs and COL-induced rainfall is not linear. Although spring (SON) has a lower frequency of COLs than autumn (MAM) and winter (JJA), it is the season when the highest percentage of COLs is associated with rainfall over the Cape south coast. Spring, when defined as October-November-December (OND), is also the season when COL-induced rainfall over South Africa is on average widespread (Favre et al. 2013). During winter (JJA), the mean seasonal rainfall attributed to COLs over the Cape south coast is a maximum (38 mm) (Table 5). Favre et al. (2013) also identified winter (defined as July-August-September (JAS)) to be the season with the largest contribution to annual COL rainfall. South Africa on average, however, receives the largest contribution to annual COL rainfall during OND (Favre et al. 2013).

The influence of rainfall associated with COLs on seasonal rainfall totals is shown in Fig. 10. A weak and non-significant correlation exists for summer (DJF), the season with the lowest mean frequency of COLs and COL-associated rainfall. Autumn (MAM) and winter (JJA) have the highest and most significant (99% level of confidence) correlation between COL-associated seasonal rainfall totals and all seasonal rainfall totals. A weak but significant correlation exists for spring (SON) which may be attributed to ridging high pressure systems that contribute largely to October rainfall, the month observed with the highest area-averaged monthly rainfall totals along the Cape south coast (Engelbrecht et al. 2015). The Pearson product-moment correlation coefficients indicate that the relationship between COLs and interannual rainfall variability is linear, in particular for JJA and MAM (not shown). Even though the frequency of occurrence of COLs is low, as illustrated by the absence of a node dedicated only to COLs in the SOM, COLs can have a notable impact on seasonal rainfall totals (e.g. JJA 2006, Fig. 10) – an indication of the intensity of COLs.

Table 5. Climatological seasonal statistics for COL induced rainfall in mm (second column), percentage of COL occurrences over South Africa (third column) and percentage of COLs that produce rainfall over the Cape south coast (fourth column)

Attribute	**Long-term average seasonal COL rain (mm)**	**Long-term average seasonal COL distribution over South Africa (%)**	**Long-term average percentage of COLs over South Africa associated with rain over the Cape south coast**
DJF	15.3 mm	18%	56%
MAM	33.8 mm	31%	61%
JJA	38.4 mm	29%	63%
SON	30.6 mm	22%	68%

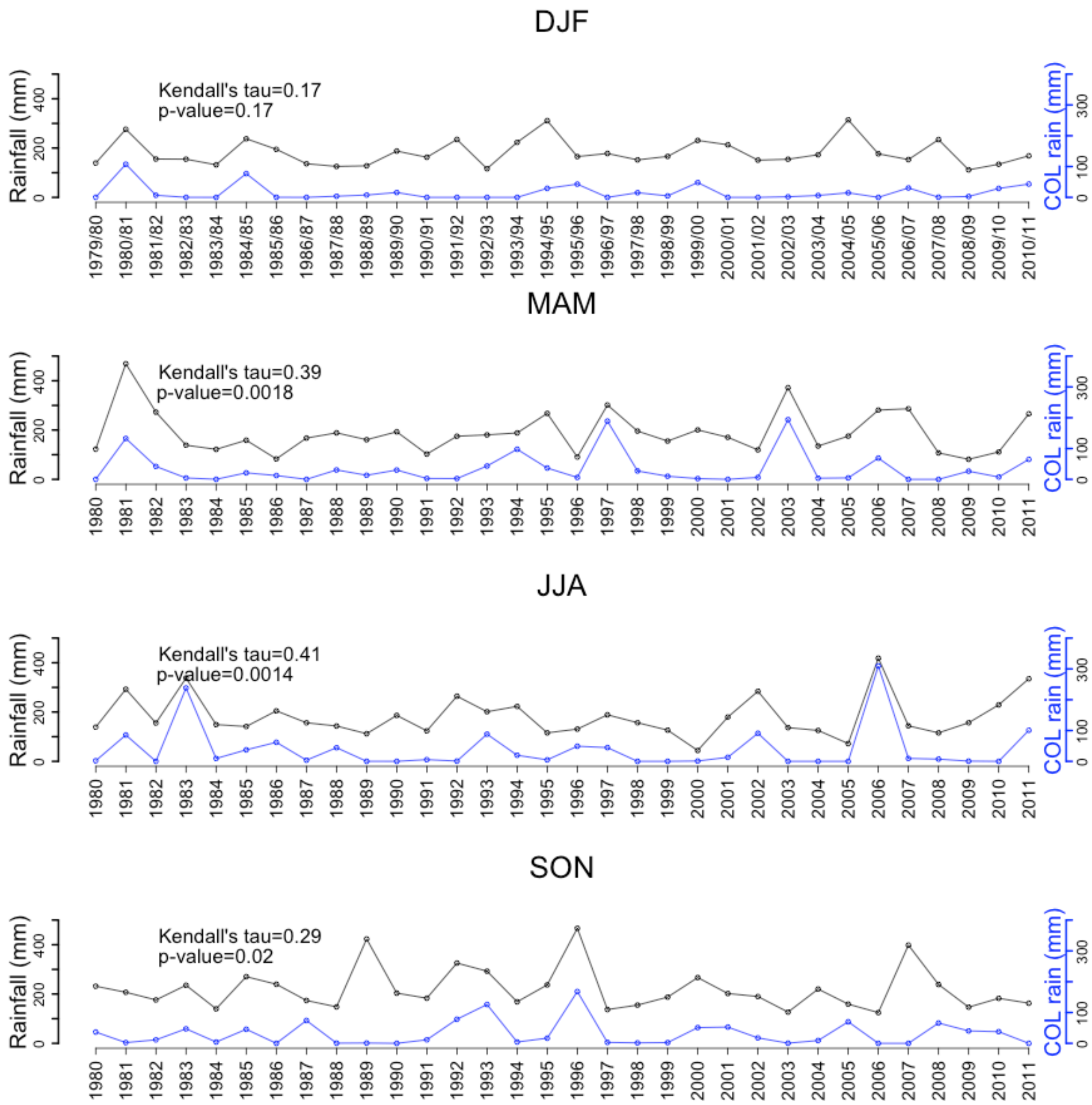

Fig. 10 Kendall's tau rank correlation between seasonal rainfall totals and the corresponding COL-induced totals

The geographical location of COLs during wet and dry seasons exhibits different regions of preferred occurrence (Fig. 11). The mean COL frequency anomaly for wet DJF seasons is characterized by COLs most frequently located over the western part of the Northern Cape and Southwestern Cape. During MAM, JJA and SON wet seasons are in general characterized by an increase in the frequency of COLs occurring countrywide. Noteworthy are areas of increased COL activity during wet seasons just off the Cape south coast and over the interior to the northwest of the Cape south coast, consistent with increased mid-latitude cyclone system density associated with wet years (Weldon and Reason 2014). During seasons of below-normal rainfall, the aforementioned areas are generally characterized by a negative mean COL frequency anomaly, consistent with a polewards shift of storm tracks (Weldon and Reason 2014).

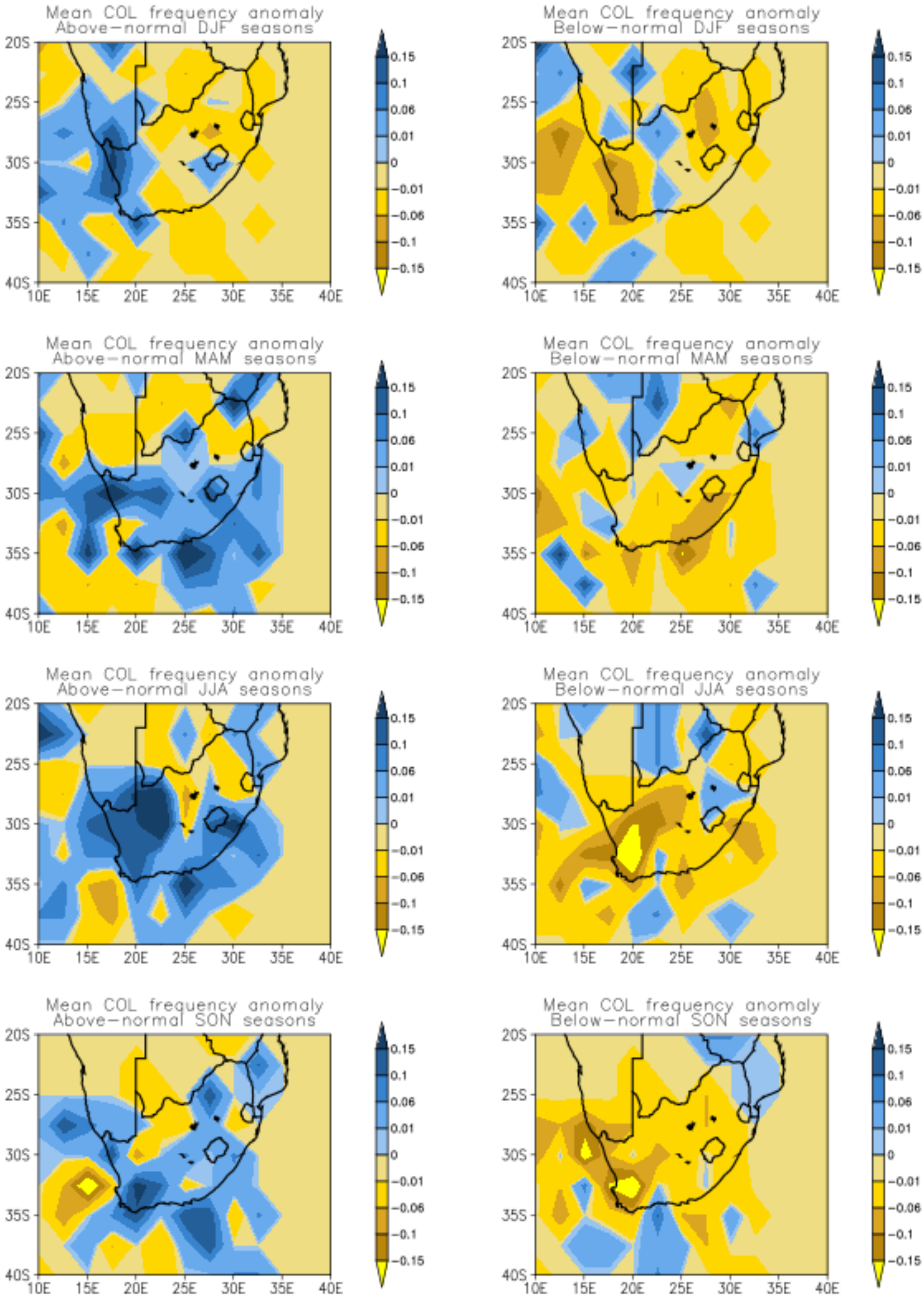

Fig. 11 Geographic location of COLs (COL centre frequency per grid point) for DJF, MAM, JJA and SON seasons of above-normal (top) and below-normal (bottom) rainfall relative to the climatological mean of COL centre frequency per grid point.

3.3.4 Large-scale climate modes

The SAM is significantly (99% level of confidence) linked to the frequency distribution of nodes within the SOM space for the DJF (Fig. 12a) and MAM (Fig. 12b) seasons, while the relationship with ENSO is somewhat weaker (95% level of confidence) and valid for DJF (Fig. 12c) and SON (Fig. 12d). This implies that for these seasons, given the predictability of ENSO (Barnston et al. 2011) and to a lesser extent SAM (Fogt et al. 2011; Gong et al. 2010), at the seasonal time scale, the skillful predictability of intraseasonal variability may be feasible (at the seasonal time scale). This relationship between the frequency distribution of nodes within the SOM space with SAM and ENSO respectively is linear according to Pearson product-moment correlation coefficients (not shown). Interesting to note is that the nature of the relationships between rainfall variability over the Cape south coast with ENSO and SAM respectively, are similar to that over the summer rainfall region where the positive (negative) phase of SAM (ENSO) is positively linked to rainfall. Over the winter rainfall region of South Africa, the relationships between rainfall with ENSO and SAM are reversed. Over the Cape south coast wet-day frequency during early winter (June) is positively (negatively) linked to the positive (negative) phase of ENSO (Weldon and Reason, 2014). Frontal systems representative of node 3 (Fig. 2) occur anomalously more frequent (the percentage change relative to climatology is 50%) during El Niño events in June while they occur anomalously less frequent (the percentage change relative to climatology is -57%) during La Nina events in June.

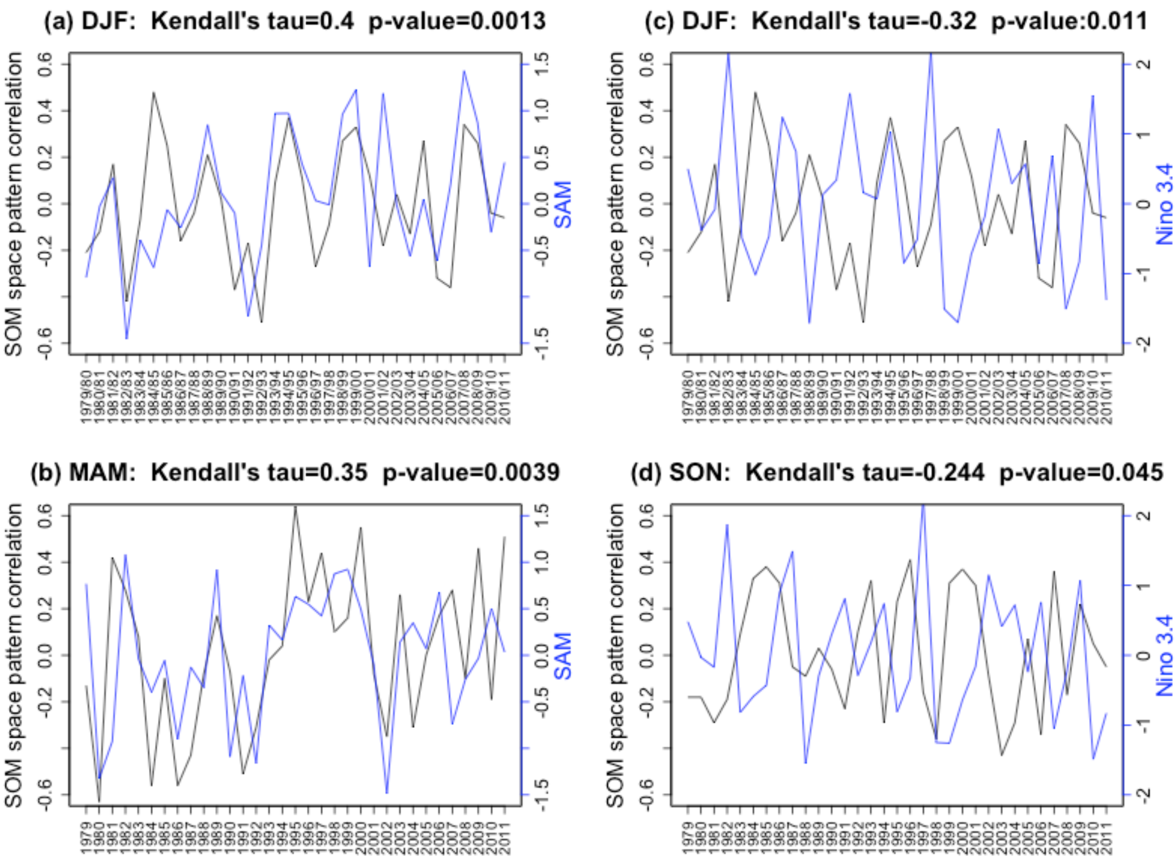

Fig. 12 Pattern correlation between the interannual frequency distribution of nodes within the SOM space and that of the average seasonal frequency distribution of nodes within the SOM space for the relevant wet season versus (a) the corresponding SAM index for DJF, (b) the corresponding SAM index for MAM, (c) the corresponding ONI for DJF and (d) the corresponding ONI for SON. The Kendall's tau values and level of significance are indicated in the respective title bars

3.4 Discussion and conclusions

The association between interannual variability of seasonal rainfall over the Cape south coast of South Africa and synoptic types was investigated. The method of SOMs was employed to relate daily low-level circulation fields obtained from NCEP with daily area-averaged rainfall for the period 1979 to 2011. The daily circulation statistics obtained from the SOM analysis were employed to determine seasonal anomaly fields for each SOM node for seasons of above-normal, near-normal and below-normal rainfall totals. Similarly, rainfall anomalies relative to the climatological mean as well as the average percentage of rainfall associated with each node for seasons of above-normal, near-normal and below-normal rainfall were determined. Analysis of synoptic type frequencies illustrated that, based on the frequency anomaly relative to the climatological frequency of the synoptic types, it is possible to distinguish anomalously wet DJF, MAM and JJA seasons from being anomalously dry. During SON, a discernable difference in the frequency of synoptic types is absent. During wet seasons, the main rainfall-producing synoptic types, representative of ridging high pressure systems and tropical-temperate troughs, occur more frequently. Noteworthy is that these synoptic types remain the main rain-producing synoptic types during dry seasons, but with an anomalously low frequency of occurrence. Being able to use synoptic type frequencies to discriminate between wet and dry seasons has potential implications for seasonal forecasting over the Cape south coast with regard to the confidence in discriminating between an above-normal or below-normal rainfall outlook. Skillful predictions of the differential synoptic type distributions for wet and dry seasons may be a requirement of skillful intra-seasonal rainfall prediction over the region.

Rainfall-producing westerly waves nearing the subcontinent are weakly linked to interannual variability of JJA rainfall, even though these systems are not regarded as the main rainfall-producing synoptic types over the Cape south coast. Indeed, during MAM and SON some configurations of westerly wave associated rain are negatively correlated with the respective seasonal rainfall totals. Rainfall associated with the main synoptic types representative of ridging high pressure systems and tropical-temperate troughs are linked to interannual variability of seasonal rainfall. A strong link is suggested for high pressure systems ridging from the southwest during DJF, MAM, JJA and SON while ridges east/southeast of the subcontinent and tropical-temperate troughs exhibit seasonality in its link to interannual variability of seasonal rainfall over the Cape south coast. Ridges east/southeast of the subcontinent exhibit a stronger link during DJF and MAM compared to JJA and SON while a link between tropical-temperate troughs is indicated to exist only during DJF and MAM. Specific configurations of ridging high pressure systems that are linked to interannual variability of seasonal rainfall, exhibit their ridging axis to be located further polewards (in particular nodes 28 and 35) than those not directly linked to interannual variability of seasonal rainfall. Both these nodes (28 and 35) are representative of weather systems with strong upper-air control. Node 35 is associated with the occurrence of COLs, while node 28 is associated with sharp upper-air troughs. The specific tropical-temperate trough configuration linked to interannual variability of DJF rainfall is suggestive of a slower moving tropical-temperate trough (node 32) with the zonal wind exhibiting similar characteristics to those of wet summers over the summer rainfall region of South Africa

(Tennant and Reason 2005). The zonal wind characteristics associated with node 32 are in contrast to the mean circulation associated with wet winters over the winter rainfall region when an anomalously strong jet is found just upstream of the subcontinent (Reason and Rouault 2005) that has also been linked to El Niño conditions (Philippon et al. 2012). In general, this node (node 32) occurs mostly in La Niña years. The DJF seasons corresponding with the 10 DJF seasons of the highest occurrence of this node (node 32), display a preference for La Niña years as it consists of 5 La Niña years, 2 El Niño years and 3 neutral years.

A strong link is suggested between COL-induced rainfall and rainfall variability over the Cape south coast for MAM, JJA and SON, with the strongest link found for JJA. Winter is also the season when the mean contribution by COLs to seasonal rainfall totals is the largest in the region (Favre et al. 2013; Engelbrecht et al. 2015). Regarding the geographical location of COLs, there seem to be distinct regions of preferred occurrence during wet and dry seasons, with anomalously more COLs located over the country during wet seasons, in particular over the southern and western parts.

Rainfall variability over the Cape south coast seems to be linked, as demonstrated by the frequency distribution of synoptic types within the SOM space, to the large-scale climate modes of ENSO and SAM. This link may be attributed to the association between ENSO and SAM (L'Heureux and Thompson 2006). The frequency distribution of nodes within the SOM space associated with wet seasons exhibits a statistically significantly positive correlation with the SAM during DJF and MAM, while this relationship associated with ENSO is negative (implying a positive relationship between rainfall and La Niña) and valid for DJF and SON. This result supports the state described by node 32, the slower moving tropical-temperate trough discussed above, contributing to rainfall variability and the potential role it has during La Niña events. Interesting to note though is that the seasons during which the ENSO association occurs over the region, coincide with spring to early autumn during which a positive association exists between COL occurrences and La Niña events (Favre et al. 2013). With rainfall variability over the Cape south coast linked to the large-scale climate drivers SAM and ENSO, as well as the occurrence of synoptic regimes during wet and dry seasons distinct with regard to their frequency and location within the SOM space, intraseasonal predictability applicable to the region seems feasible and needs to be explored further.

3.5 Acknowledgements

Constructive comments from three anonymous reviewers improved the manuscript. This research was funded by the Water Research Commission (Project K5/2257/1) and the Applied Centre for Climate and Earth System Studies (ACCESS). Rainfall data were supplied by the South African Weather Service. Support for this study by the Agricultural Research Council and editorial contributions by Dr Thomas Fyfield is greatly acknowledged. General discussions with Drs L. Dyson, J. Malherbe and F. Engelbrecht are appreciated.

3.6 References

Barclay JJ, Jury MR, Landman W (1993) Climatological and Structural Differences Between Wet and Dry Troughs over Southern Africa in the Early Summer. Meteor Amos Phys 51:41-54

Barnston AG, Tippett MK, L'Heureux ML, Li S, DeWitt DG (2011) Skill of real-time seasonal ENSO model predictions during 2002-2011: Is our capability increasing? Bull. Am Meteorol Soc 93:631-651.doi:10.1175/BAMS-D-11-00111.1

Cook C, Reason CJC, Hewitson BC (2004) Wet and dry spells within particular wet and dry summers in the South African summer rainfall region. Clim Res 26:17-31

Crétat J, Richard Y, Pohl B, Rouault M, Reason C, Fauchereau N (2012) Recurrent daily rainfall patterns over South Africa and associated dynamics during the core of the austral summer. Int J Climatol 32:261-273. doi:10.1002/joc.2266

Engelbrecht CJ, Landman WA, Engelbrecht FA, Malherbe J (2015) A synoptic decomposition of rainfall over the Cape south coast of South Africa. Clim Dyn 44:2589-2607. doi:10.1007/s00382-014-2230-5

Fauchereau N, Pohl B, Reason CJC, Rouault M, Richard Y (2009) Recurrent daily OLR patterns in the southern Africa/southwest Indian Ocean region, implications for South African rainfall and teleconnections. Clim Dyn 32:575-591

Favre A, Hewitson B, Tadross M, Lennard C, Cerezo-Mota R (2012) Relationships between cut-off lows and the semiannual and southern oscillations. Clim Dyn 38:1473-1487. doi:10.1007/s00382-011-1030-4

Favre A, Hewitson B, Lennard C, Cerezo-Mota R, Tadross M (2013) Cut-off lows in the South Africa region and their contribution to precipitation. Clim Dyn 41:2331-2351. doi:10.1007/s00382-012-1579-6

Fogt RL, Bromwich DH, Hines KM (2011) Understanding the SAM influence on the South Pacific ENSO teleconnection. Clim Dyn 36:1555-1576

Gong T, Feldstein SB, Luo D (2010) The impact of ENSO on wave breaking and southern annular mode events. J Atmos Sci 67:2854-2870

Harrison MSJ (1984) A generalized classification of South African rain-bearing synoptic systems. Int J Climatol 4:547-560

Hart NCG, Reason CJC, Fauchereau N (2010) Tropical-extratropical interactions over Southern Africa: three cases of heavy summer season rainfall. Mon Weather Rev 138:2608-2623

Hart NCG (2012) Synoptic-scale rainfall patterns over southern Africa: Scale-interactions with large-scale modes of variability. Unpublished PhD thesis. 99pp

Hart NCG, Reason CJC, Fauchereau N (2013) Cloud bands over southern Africa: seasonality, contribution to rainfall variability and modulation by the MJO. Clim Dyn 42:1199-1212. doi:10.1007/s00382-012-1589-4

Holloway A, Fortune G, Zweig P, Barrett L, Benjamin A, Chasi V, de Waal J (2012) Eden and Central Karoo Drought Disaster 2009 – 2011; “The Scramble for Water.” For the Provincial Disaster Management Centre, Western Cape by the Disaster Mitigation for Sustainable Livelihoods Programme, Department of Geography and Environmental Studies, Stellenbosch University. 158 pp.

Jury MR, Pathack BMR, Sohn BJ (1992) Spatial structure and interannual variability of summer convection over southern Africa and the SW Indian Ocean. S Afr J Sci 88:275-280

Jury MR, Levey K (1993) The climatology and characteristics of drought in the eastern Cape of South Africa. Int J Climatol 13: 629-641

Kalnay E, Kanamitsu M, Kistler R, Collins W, Deaven D, Gandin L, Iredell M, Saha S, White G, Woollen J, Zhu Y, Leetmaa A, Reynolds B, Chelliah M, Ebisuzaki W, Higgins W, Janowiak J, Mo KC, Ropelewski C, Wang J, Jenne R, Joseph D (1996) The NEP/NCAR 40-year reanalysis project. Bull Am Meteorol Soc 77:437-471

Katzfey JJ, McInnes KL (1996) GCM simulations of Eastern Australia cutoff lows. J Clim 9:2337-2355

Kohonen T (2001) Self-organizing maps. 3rd ed. Springer

Landman WA, Kgatuke MJ, Mbedzi M, Beraki A, Bartman A and du Piesanie A (2009) Performance comparison of some dynamical and empirical downscaling methods for South Africa from a seasonal climate modeling perspective. Int J Climatol 29:1535-1549 doi:10.1002/joc.1766

Landman WA, Beraki A (2012) Multi-model forecast skill for mid-summer rainfall over southern Africa. Int J Climatol 32:303-314. doi:10.1002/joc.2273

Landman WA, DeWitt D, Lee DE, Beraki A, Lötter D (2012) Seasonal Rainfall Prediction Skill over South Africa: One- versus Two-Tiered Forecasting Systems. Weather and Forecasting 27: 489-501

Lennard C, Hegerl G (2015) Relating changes in synoptic circulation to the surface rainfall response using self-organizing maps. Clim Dyn 44:861-879 doi:10.1007/s00382-014-2169-6

L'Heureux ML, Thompson DWJ (2006) Observed relationships between the El Niño-Southern Oscillation and the extratropical zonal-mean circulation. J Climate 19:276-287

Malherbe J, Landman WA, Engelbrecht FA (2014a) The bi-decadal rainfall cycle, Southern Annular Mode and tropical cyclones over the Limpopo River Basin, southern Africa. Clim Dyn 42:3121-3138. doi 10.1007/s00382-013-2027-y

Malherbe J, Landman WA, Olivier C, Sakuma H, Luo J- J (2014b) Seasonal forecasts of the SINTEX-F coupled model applied to maize yield and streamflow estimates over north-eastern South Africa. Meteorol Appl 21:733-742. doi:10.1002/met.1402

Mason SJ, Jury MR (1997) Climatic variability and change over southern Africa: a reflection on underlying processes. Prog Phys Geog 21:23-50

Mo KC (2000) Relationships between Low-Frequency Variability in the Southern Hemisphere and Sea Surface Temperature Anomalies. J Climate 13:3599-3610

Muller A, Reason CJC, Fauchereau N (2008) Extreme rainfall in the Namib Desert during summer 2006 and influences of regional ocean variability. Int J Climatol 28:1061-1070. doi:10.1002/joc.1603

Philippon N, Rouault M, Richard Y, Favre A (2012) The influence of ENSO on winter rainfall in South Africa. Int J Climatol 32:2333-2347. doi:10.1002/joc.3403

Pohl B, Fauchereau N, Reason CJC, Rouault M (2010) Relationships between the Antarctic Oscillation, the Madden-Julian Oscillation, and ENSO, and consequences for rainfall analysis. J Clim 23:238-254

Pohl B, Rouault M, Sen Roy S (2014) Similation of the annual and diurnal cycles of rainfall over South Africa by a regional climate model. Clim Dyn 43:2207-2226. doi: 10.1007/s00382-013-2046-8

Reason CJC, Allan RJ, Lindesay JA, Ansell TJ (2000) ENSO and climatic signals across the Indian Ocean basin in the global context: Part I, interannual composite patterns. Int J Climatol 20:1285-1327

Reason CJC, Rouault M, Melice JL, Jagadheesha D (2002) Interannual winter rainfall variability in SW South Africa and large scale ocean-atmosphere interactions. Meteorol Atmos Phys 80:19-29

Reason CJC, Rouault M (2005) Links between the Antarctic Oscillation and winter rainfall over western South Africa. Geophys Res Lett 32: L07705. 10.1029/2005GL022419

Rouault M, White SA, Reason CJC, Lutjeharms JRE, Jobard I (2002) Ocean-atmosphere interaction in the Agulhas current region and a South African extreme weather event. Weather Forecast 17:655-669

Schuenemann KC, Cassano JJ, Finnis J (2009) Synoptic forcing of precipitation over Greenland: climatology for 1961-99. J Hydrometeorol 10:60-78

Singleton AT, Reason CJ (2006) Numerical simulations of a severe rainfall event over the Eastern Cape coast of South Africa: sensitivity to sea surface temperature and topography. Tellus 58:355-367

Singleton AT, Reason CJ (2007a) A numerical model study of an intense cutoff low pressure system over South Africa. Mon Weather Rev 135:1128-1150

Singleton AT, Reason CJ (2007b) Variability in the characteristics of cut-off low pressure systems over subtropical southern Africa. Int J Climatol 27:295-310

Smith TM, Reynolds RW, Peterson TC, Lawrimore J (2008) Improvements to NOAA's Historical Merged Land-Ocean Surface Temperature Analysis (1880-2006). J Climate 21:2283-2296

Taljaard JJ (1985) Cut-off lows in the South African region. South African Weather Bureau, Technical paper 14

Taljaard JJ (1995) Atmospheric circulation systems, synoptic climatology and weather phenomena of South Africa. Part 2: Atmospheric circulation systems in the South African region. South African Weather Bureau, Technical paper 28

Taljaard JJ (1996) Atmospheric circulation systems, synptic climatology and weather phenomena of South Africa. Part 6: Rainfall in South Africa. South African Weather Bureau, Technical paper 32

Tennant WJ, Hewitson BC (2002) Intra-seasonal rainfall characteristics and their importance to the seasonal prediction problem. Int J Climatol 22:1033-1048

Tennant WJ, Reason CJC (2005) Associations between the Global Energy Cycle and Regional Rainfall in South Africa and Southwest Australia. J Climate 18:3032-3047

Todd M, Washington R, Palmer PI (2004) Water vapour transport associated with tropical-temperate trough systems over southern Africa and the southwest Indian Ocean. Int J Climatol 24:555-568

Tozuka T, Abiodun BJ, Engelbrecht FA (2014) Impacts of convection schemes on simulating tropical-temperate troughs over southern Africa. Clim Dyn 42:433-451

Van Heerden J, Terblance DE, Schulze GC (1988) The Southern Oscillation and South African summer rainfall. J Climate 8:577-597

Washington R, Preston A (2006) Extreme wet years over southern Africa: Role of Indian Ocean sea surface temperatures. J Geophys Res 111: D15104, doi:10.1029/2005JD006724

Washington R, Todd M (1999) Tropical-temperate links in the Southern African and southwest Indian Ocean satellite-derived daily rainfall. Int J Climatol 19:1601-1616

Weldon D, Reason CJC (2014) Variability of rainfall characteristics over the South Coast region of South Africa. Theor Appl Climatol 115:177-185. doi:10.1007/s00704-013-0882-4

Wilks DS (2011) Statistical methods in the atmospheric sciences, 3rd edn. Academic Press, Amsterdam

Synopsis

A link between interannual rainfall variability of seasonal rainfall over the Cape south coast of South Africa and associated variations in the frequencies of occurrence of different synoptic types has now been demonstrated. In addition, it is also shown that the distribution of synoptic types is linked to the SAM and ENSO. This discovery has been achieved through the formulation of a new type of climate index, which relates the distribution of synoptic type frequencies in the SOM space to the large-scale modes of variability. The third and fourth objectives of the study have therefore been addressed. The results related to objective four indicate the potential for the interannual variability in the intraseasonal synoptic type variability over the region to be predictable. In the following chapter, the predictability of the intraseasonal variability of synoptic types over the Cape south coast of South Africa at the seasonal time scale is investigated by making use of archived forecasts of the Met Office Seasonal Forecast System 5 (GloSea5).

Chapter 4: Seasonal predictability of intraseasonal synoptic type variability over the Cape south coast of South Africa by making use of the Met Office Global Seasonal Forecast System 5

Preface

This chapter consists of one research paper that has been submitted for peer-review as follows:

Engelbrecht CJ, Landman WA, Graham RJ and McLean P. 2015. Seasonal predictability of intraseasonal synoptic type variability over the Cape south coast of South Africa by making use of the Met Office Global Seasonal Forecast System 5. Submitted to International Journal of Climatology.

In this paper, the predictability of intraseasonal characteristics of synoptic type occurrences on the seasonal time scale over the all-year rainfall region of South Africa is assessed by utilizing an ensemble of model simulations. The archived GloSea5 forecasts considered here consist of 12 ensemble members at a lead-time of 1-month and are subsequently analysed during the austral spring and summer seasons. In the previous chapter it has been shown that during both SON and DJF a link exists between the Nino 3.4 SST anomalies and the frequency distribution of synoptic types associated with wet SON and DJF seasons, therefore implying potential predictability of the intraseasonal variability of synoptic types during these seasons (given the predictability of ENSO). In this chapter, this hypothesis is tested, thereby addressing objective 5 of the study.

My co-authors are WA Landman, RJ Graham and P McLean. I conceptualized the paper, performed the analysis and interpreted the results.

Seasonal predictability of intraseasonal synoptic type variability over the Cape south coast of South Africa by making use of the Met Office Global Seasonal Forecast System 5

C.J. Engelbrecht[1,2] , W.A. Landman[2,3], Richard J Graham[4] and Peter McLean[4]

1. Institute for Soil, Climate and Water, Agricultural Research Council, Pretoria, South Africa

2. Department of Geography, Geoinformatics and Meteorology, University of Pretoria, Pretoria, South Africa

3. Climate Studies, Modelling and Environmental Health, CSIR Natural Resources and Environment, Pretoria, South Africa

4. Met Office Hadley Center, FitzRoy Road, Exeter EX1 3PB, UK

Abstract

The predictability of intraseasonal characteristics of synoptic type occurrences on the seasonal time scale over the all-year rainfall region of South Africa (35°S-33°S and 21°E-27°E) is assessed by utilizing an ensemble of simulations performed by the atmosphere-ocean coupled model administered by the Met Office, UK. Hindcasts of daily sea-level pressure fields of 14 austral spring (September-October-November (SON)) and summer (December-January-February (DJF)) seasons initialized in August and November respectively, are used in this study. Through the use of self-organizing maps, intraseasonal predictability is assessed by the objective evaluation of the frequency of synoptic types that occurred over the region as simulated by the model against a baseline synoptic type occurrence. Deterministic and probabilistic assessment of synoptic type frequency forecasts indicate that intraseasonal circulation variability over the Cape south coast region is marginally predictable at interannual time scales, more so during SON than DJF.

4.1 Introduction

The Cape south coast (Figure 1), geographically located within the domain bounded by 35°S-33°S and 21°E-27°E (Taljaard, 1996; Mason, 1998; Landman et al., 2001a; Rouault and

Richard, 2003; Weldon and Reason, 2014), lacks the strong rainfall seasonality (Weldon and Reason, 2014; Engelbrecht et al., 2015) found over the remainder of South Africa. The country otherwise receives mostly summer rainfall (e.g. Fauchereau et al., 2009), with winter rainfall limited to the far southwestern part of the country (e.g. Philippon et al., 2011). The Cape south coast, known for receiving all-year rainfall, is also host to agricultural activities (Weldon and Reason, 2014) of importance similar to the winter and summer rainfall regions of the country. Along the coastal areas of this region, some of South Africa's prime milk and deciduous fruit production farms are found. As the larger part of South Africa's economy is dependent on agriculture, the need for seasonal forecasts exists as the 1991/1992 drought over the summer rainfall region illustrated (Mason, 1998). Given that potential predictability is the highest in a tropical atmosphere (Mason et al., 1996; Mason, 1998), the development of seasonal forecast systems for the South African region have mostly focused on the December-January-February (DJF) rainfall season (e.g. Bartman et al., 2003; Landman and Goddard, 2005) when the regional circulation exhibits tropical attributes (Rautenbach and Smith, 2001). Also, a well-documented El-Niño Southern Oscillation (ENSO) signal exists for the summer rainfall region in southern Africa (Lindesay et al., 1986). El Niño events are often associated with below-normal summer rainfall over southern Africa, and may in fact lead to severe drought (Mason, 1998). La Niña events, on the other hand, are typically associated with above-normal summer rainfall, and in some cases with devastating floods. Furthermore, DJF is an important season regarding agricultural activities over the summer rainfall region (Bartman et al., 2003). Most of the main maize production areas of South Africa are found over the summer rainfall region (Moeletsi et al., 2011; Malherbe et al., 2014). Seasonal forecasts can benefit farming communities (Klopper et al., 2006), as has been illustrated for the summer rainfall region during DJF (Klopper, 1999). It has indeed been found that seasonal forecasts of rainfall totals have their highest skill over the northeastern interior of the summer rainfall region during DJF, in particular during ENSO seasons (Landman and Beraki, 2012). Landman et al. (2001b) and Landman and Goddard (2002) have found that the skillful prediction of seasonal rainfall totals over the summer rainfall region of southern Africa is based on statistical downscaled forecasts, where the best known predictor is seasonal mean low-level circulation. Since modelled low-level circulation is such a strong candidate for statistical downscaling on the seasonal time scale, such circulation should also be a good estimator of potential predictability at the intraseasonal (frequency of the different types of circulation patterns within the season) time scale, although in-depth investigation is required to test this notion.

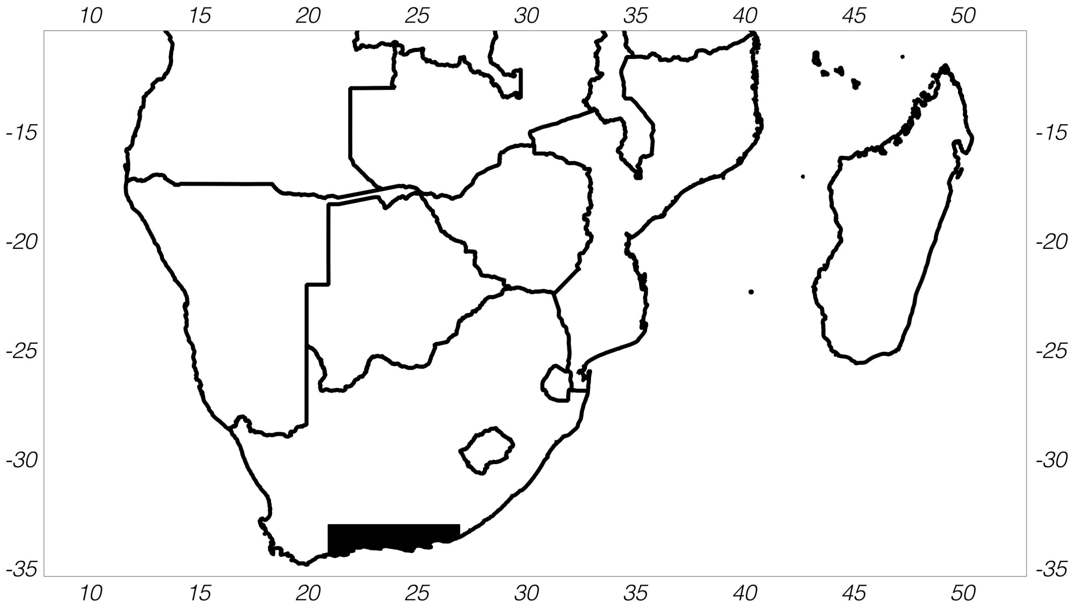

Figure 1. Geographical location of the Cape south coast (indicated by the solid black rectangle bounded by the ocean to the south).

It has recently been illustrated that seasons of anomalous rainfall over the southwestern Cape and the Cape south coast regions of South Africa are correlated with two of the large-scale climate modes of global variability, namely ENSO and the Southern Annular Mode (SAM) (Philippon et al., 2011; Engelbrecht and Landman, 2015). It has been demonstrated that interannual variability of the intraseasonal circulation variability in the Cape south coast region is correlated with SAM and ENSO (Engelbrecht and Landman, 2015). Due to the predictability of these large-scale climate modes at seasonal time scales, the potential to predict intraseasonal circulation regimes relevant to the Cape south coast is implied. It may be noted that seasons with similar rainfall totals can have very different rainfall characteristics within the season, particular for regions located in the sub-tropics (Tennant and Hewitson, 2002). A need exists for the inclusion of within-seasonal characteristics in seasonal forecasts to inform agricultural decision making (Vogel and O'Brien, 2006). This need is based on the notion that it is not necessarily the mean seasonal circulation or rainfall totals that determine the quality of crop yield or to secure pasture, but rather the distribution of rainfall through the season as related to the frequency of occurrence of certain circulation regimes.

The aim of this paper is to investigate predictability of intraseasonal circulation variability over the Cape south coast region of South Africa. The forecast system applied in the research is the Met Office Global Seasonal Forecast System 5 (GloSea5). The forecast system, experimental design of the hindcasts performed and statistical verification methodology are discussed in Section 2. The forecasts of intraseasonal circulation variability are verified in Section 3, using both deterministic and probabilistic forecasts. The focus is on the predictability of the DJF and September-October-November (SON) seasons due to the well documented ENSO signal that exists over southern Africa for the former season and because the month of peak rainfall over the Cape south coast is found within the latter season (Engelbrecht et al., 2015). Conclusions are drawn in Section 4.

4.2 Data and methodology

4.2.1 Reanalysis and forecast data

Hindcasts of the fully coupled model GloSea5 are used in this study. The horizontal resolution of the atmosphere in GloSea5 is 0.83° longitude × 0.56° latitude and 0.25° in the global ocean (MacLachlan et al., 2014; Camp et al., 2015). In this study, daily sea-level pressure (SLP) fields for 14 SON (1996-2009) and DJF (1996/1997-2009/2010) seasons are used to study synoptic circulation type frequencies. For each of the 14 SON and DJF seasons, 12 ensemble members are available. The hindcasts are initialized from four start dates and with three ensemble members per start date. A stochastic physics scheme is employed to achieve spread between members initialized on the same date (MacLachlan et al., 2014). A full description of GloSea5 can be found in MacLachlan et al. 2014.

National Centers for Environmental Prediction (NCEP) reanalysis data (Kalnay et al., 1996) is used as observational data from which the baseline synoptic type frequencies are calculated. NCEP synoptic type frequencies are calculated for the same 14 SON and DJF seasons for which GloSea5 data are available. NCEP reanalysis data has a horizontal resolution of 2.5°. Due to the difference in horizontal resolution of the GloSea5 and NCEP data, the model output was converted to the coarser horizontal resolution of NCEP by applying a bicubic interpolation function on the model data. The clustering method used in this study for classification of synoptic types, the self-organizing map (SOM), requires for both the model and NCEP data to have a common horizontal resolution.

4.2.2 Identification of synoptic types

Application of the SOM to identify synoptic types is a very popular practice in the atmospheric sciences in South Africa (e.g. Hewitson and Crane, 2002; Tennant and Hewitson, 2002; Tennant, 2003; Malherbe et al., 2012, 2013; Van Schalkwyk and Dyson, 2013; Lennard and Hegerl et al., 2014; Dyson, 2015; Engelbrecht et al., 2015). A detailed discussion on SOMs and the application to synoptic climatology can be found in Hewitson and Crane (2002) who pioneered the application of SOMs in the climatological research. The SOM algorithm was first described by Kohonen (1984) and the software, referred to as SOM_PAK, can be downloaded from http://www.cis.hut.fi/research/som-research. SOMs identify a number of nodes within a data space (Tennant, 2003) without assumptions made about the distribution of the observed data (Hewitson and Crane, 2002). The nodes are identified spanning the entire multi-dimensional data space (Tennant, 2003; Lennard and Hegerl, 2014), making it possible to associate individual data elements with a node (Tennant, 2003). It is this attribute that makes SOMs the ideal clustering method to calculate frequencies associated with each node during the post-processing phase.

The SOMs are trained on the SLP fields of NCEP reanalysis data for the SON seasons from 1996 to 2009 and for the DJF seasons from 1996/97 to 2009/10. Separate SOMs are developed for SON and DJF. The size of a SOM is chosen subjectively and the degree of generalization needed is typically considered in the choice of the number of nodes (Tennant, 2003; Lennard and Hegerl, 2014). Similarly to Tennant (2003), the number of SOM nodes in this study is chosen to represent the daily circulation during SON and DJF in approximately a tenth of the original degrees of freedom. SON seasons consist of 91 days/season and DJF seasons of 90 days/season (91 days/season during leap years), hence the selection of the SOM size (number of nodes) to be 3×3 for both the SON and DJF SOMs. A 3×3 SOM is also developed for austral summer in a study by Morioka et al. (2010) where climate variability in the southern Indian Ocean is investigated. To account for model bias, which can be problematic when a direct intercomparison is made between observations and model data, the respective long-term mean is subtracted from all the datasets before subjected to development of the SOMs, similar to the procedure described in Tennant (2003). Following the procedure described in Tennant (2003), the daily SLP model forecasts of all 12 ensemble members from which the long-term mean is subtracted are then subjected to the SOM trained on daily NCEP

SLP fields in order to determine the frequency of association between the model forecasts and the SOM nodes. The NCEP synoptic types as identified by the SOM are therefore used to assess the full set of GloSea5 fields.

Observed COL days identified on 500 hPa in daily geopotential height fields for all the SON and DJF seasons are mapped to the SOM nodes of the respective seasons. A detailed description on the development of the COL database used in this study is described in Engelbrecht et al. (2015).

4.2.3 Verification methodology

Seasonal forecasting is inherently probabilistic (Wilks, 2011), however, deterministic assessments of the forecast skill may complement probabilistic assessments (e.g. Landman and Beraki, 2012; Diro, 2015). This study employs a range of deterministic and probabilistic assessments of skill towards evaluating the GloSea5 system's ability to forecast the interannual variability of the intraseasonal attributes of circulation.

As a first step towards assessing the predictability of the intraseasonal frequencies of synoptic types, the model's ability to portray the climatological frequencies of synoptic types is investigated. The ensemble mean of the model forecasts of synoptic type occurrences for SON and DJF are deterministically compared to the relevant baseline synoptic type occurrences and presented as node frequency errors, similar to Tennant (2003). Differences in node frequency are divided by the observed frequencies to present the errors as percentage errors. Model weaknesses and strengths with regard to the simulation of the frequency of synoptic types within a climatological context are shown by the node frequency errors (Tennant, 2003).

A seasonal forecast system must capture interannual variability (Tennant, 2003; Diro, 2015). In this study, intraseasonal characteristics of synoptic types as represented by the frequency distribution within the SOM space are evaluated on an interannual basis over the 14 SON (1996-2009) and DJF (1996/1997-2009/2010) seasons. For example, the forecast frequency distribution of synoptic types (based on the ensemble mean) for SON 1996 is compared to the observed SON 1996 frequency distribution of synoptic types by calculation of the anomaly correlation. The forecast (observed) frequency distribution of synoptic types can be regarded as a field forecast (observation) where the nodes within the SOM space represent grid points of the field. The anomaly correlation is a special case of a pattern correlation. Similarities in the patterns of departure are detected and the anomaly correlation is not sensitive to biases (conditional and unconditional) in the forecasts (Wilks, 2011), making it very suitable for comparison of the frequency distribution of nodes within the SOM space between model forecasts and observations. The uncentered anomaly correlation is used in this study: Anomalies for forecasts and observations are calculated by subtraction of the corresponding climatological values for each SOM node (e.g. Murphy and Epstein, 1989). The anomaly correlation ranges between -1 and 1, with 1 being a perfect score (Wilks, 2011). The anomaly correlation does not measure actual skill, as it is not expressed against a reference forecast. Even so, a high correlation still implies skill. The anomaly correlation is often used to evaluate deterministic forecasts against persistence (e.g. Wilks, 2011). However, if persistence also exhibits high skill, a high anomaly correlation is not of any use. The anomaly correlation is used here to evaluate the GloSea5 node frequency distribution forecasts to persistence. For GloSea5 to outperform the persistence node frequency distribution forecasts, higher anomaly correlation values are needed compared to anomaly correlation values associated with persistence.

For the purpose of probabilistic forecasts, synoptic type occurrences are evaluated by introducing three equiprobable categories namely below-normal, near-normal and above-normal, defined by the 33^{rd} and 67^{th} percentile values of the ensemble mean climatological record. The ability of the forecast system to discriminate between an event and a non-event (Hudson et al., 2011), also known as resolution, is addressed by calculation of the relative operating characteristic (ROC) (Mason and Graham, 2002; Wilks, 2011). A ROC curve is constructed by plotting the observed hit rates against the false alarm rates (Wilks, 2011), using a set of increasing probability thresholds. In this study, the thresholds 0, 0.2, 0.4, 0.6, 0.8 and 1 are used. For a forecast that discriminates perfectly between the occurrence of events and their non-occurrence, the area underneath the ROC curve (referred to as the ROC score) is 1 while a forecast system with a ROC score ≤ 0.5 is considered unable to discriminate between events and non-events (Hudson et al., 2011). The diagonal line passing through (0,0) and (1,1) represents the no-skill line on the ROC curve – here, the hit rates equal the false alarm rates (Hudson et al., 2011).

In addition to the ROC score we also employ the reliability diagram in our assessments (Hamill, 1997; Warner, 2011; Wilks, 2011). The reliability diagram and ROC are typically used together when assessing forecast systems (e.g. Landman and Beraki, 2012; Lazenby et al., 2014; Malherbe et al., 2014). The reliability diagram shows the observed relative frequency for each of the forecast probability thresholds. As with the ROC, probability thresholds in intervals of 20% are used in this study. For a perfectly reliable forecast, the forecast probability equals the observed frequency, and is found on the diagonal line through (0,0) and (1,1) (Warner, 2011).

A new measure of the forecast system's ability to distinguish between the below-normal, normal and above-normal occurrence of synoptic type frequencies is introduced next. For each node and for each season (e.g. SON) occurring during the 14-year period, a forecast probability is assigned, for its frequency of occurrence to be in a particular tercile category (e.g. a probability for the frequency of occurrence to be in the above-normal category). This probability value is paired with the actual outcome (e.g. a value of 1 is assigned if the frequency of occurrence of the node is in fact above normal, a value of 0 is assigned otherwise). A straight line is subsequently fitted to all paired numbers obtained in this way for a specific season (across all nodes and across the period under consideration). A perfect probabilistic forecast would yield a straight line connecting the points (0,0) and (1,1) in the x-y plane. A reference forecast based on the climatological probabilities (e.g. always forecasting 0.333 as the probability of a node to exhibit an above-normal frequency) yields a line with 0 slope, implying that forecasts yielding positive slopes have skill over this reference forecast. A forecast yielding a negative slope is less skillful than this reference measure, and may be regarded as being unable to skillfully distinguish between the occurrence and non-occurrence of events in a particular tercile category. Because the forecast line is fitted to the accumulated number of observed-forecast pairs it may be regarded as a measure of the average performance of the forecast to predict the frequency of occurrence across the SOM space. Lines fitted to forecasts based on persistence are also calculated as an additional reference forecast to measure model performance against. Persistence is defined by the outcome of the relevant metric precisely one year earlier.

4.3 Results

4.3.1 Assessment of the GloSea5 synoptic type climatology

Nodes within the SOM space are essentially composites of input maps with similar spatial distributions (Grotjahn et al., 2015). The SOMs have been constructed on SLP anomaly fields rather than the full NCEP fields. The corresponding anomaly fields of the model data are mapped onto these SOMs, thereby effectively eliminating problems that may arise due to model biases in SLP. Nevertheless, the synoptic type climatologies that are shown for SON (Figure 2a) and DJF (Figure 2b) are expressed in terms of the composite full SLP fields that corresponds to the SLP anomaly fields. Similar synoptic types occur during SON and DJF, but with a notable difference of high pressure systems being stronger and situated slightly more towards the equator during SON. High pressure systems ridging from the southwest have been shown to be the main contributor to the October rainfall peak along the Cape south coast (Engelbrecht et al., 2015) and the realistic simulation of their frequencies is therefore important. The various configurations of high pressure systems during SON are found over the central to right-hand side of the SOM (e.g. nodes 2, 3, 5, 6, 8 and 9), illustrating an inherent characteristic of a SOM to group similar nodes together (Lennard and Hegerl, 2014). Nodes 3 and 6 are representative of high pressure systems ridging from the southwest onto the Cape south coast and are the nodes associated with the highest area-averaged rainfall per node occurrence over the 14 SON seasons (1996 to 2009). The area-averaged rainfall is derived from the daily rainfall of 12 weather stations over the Cape south coast described in Engelbrecht et al. (2015). The nodes on the left side of the SOM (nodes 1, 4 and 7) are characterized by various trough systems. Nodes 1, 4, 7 and 8 are representative of synoptic types associated with the smallest amount of area-averaged rain per node occurrence. It can therefore be suggested that an association between rainfall characteristics and the synoptic type distribution within the SOM space exists. Moreover, out of a total of 49 cut-off low (COL) days recorded over the 14-year period during SON, 33 COL days (67%) occurred within nodes 3, 6 and 9, illustrating a notable clustering in the distribution of COL days within the SOM space (Figure 3). Since COLs are weather systems that are associated with high-impact rainfall events over the Cape south coast (e.g. Taljaard, 1996; Singleton and Reason, 2006, 2007) it is suggested that the nature of rainfall within the season might be predictable at interannual time scales, provided that the intraseasonal characteristics of the circulation are predictable. For DJF, nodes 4, 7, 8 and 9 are associated with the highest amount of rainfall per node occurrence. However, the amount of rainfall per node occurrence for the nodes associated with the highest rainfall per node is consistently smaller during DJF compared to SON. For example, the two nodes with the highest amount of rainfall (per node occurrence) for SON are 5.4 and 4.31 mm versus 2.9 and 2.6 mm for DJF. With regard to the frequency distribution of COL days within the SOM space during DJF, the highest number of COL days occurred within nodes 8 and 9 (7 COL days each out of a possible 41 COL days), however, the variation of COL days is significantly less across the SOM compared to the case for SON.

Following the approach of Tennant (2003), Figure 4 shows the mean synoptic type frequency errors of the GloSea5 climatology (as constructed from the 14 years of hindcasts that were mapped onto the NCEP SOM) expressed as a percentage of NCEP-observed mean frequencies for SON and DJF. In the worst case of model performance, the simulated synoptic types for all days would map to a single observed node. The SOM methodology implies that each node is constructed from approximately the same number of daily synoptic fields, that is the climatological frequencies of occurrence of nodes are approximately the same. During a 90-day season, each node may therefore be expected to be mapped by approximately 10 synoptic patterns (10 days) (interannual variability will of course cause some variability). This implies a maximum node percentage error in the order of 800 %. The strengths and weaknesses of the model with regard to representing the frequencies of occurrence of specific synoptic types can be determined by considering the frequency errors (Tennant, 2003). During both SON and DJF, the frequency errors (%) are generally small, implying that the 14-year climatological model frequencies of the synoptic types agree very well with the observed frequencies for the corresponding period. With regard to spatial variance as well as the meridional and zonal gradient characteristics of the different nodes, node frequency errors do not seem to correspond strongly to specific characteristics of these attributes. It may be noted though, that the nodes where the largest errors are found are mostly nodes with lower spatial variance. For example, during SON and DJF nodes 5 and 4 exhibit this characteristic, respectively. Still, the node frequency errors are relatively small (taking into account that these errors may be as large as 800 %).

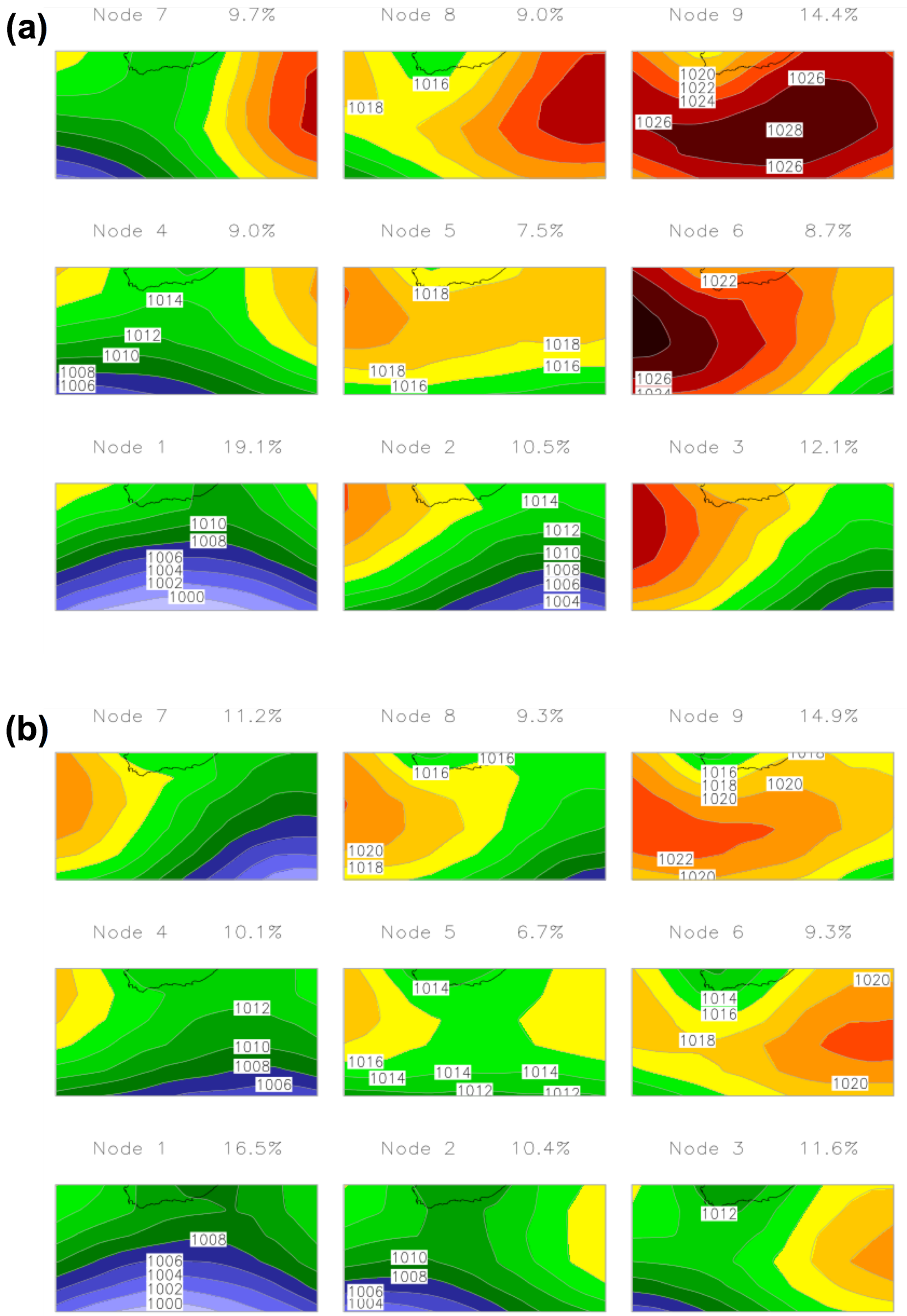

Figure 2. SLP composites of the 9 nodes identified by the SOM for SON (a) and DJF (b) that is developed on SLP data from which the long-term mean is removed to account for model bias.

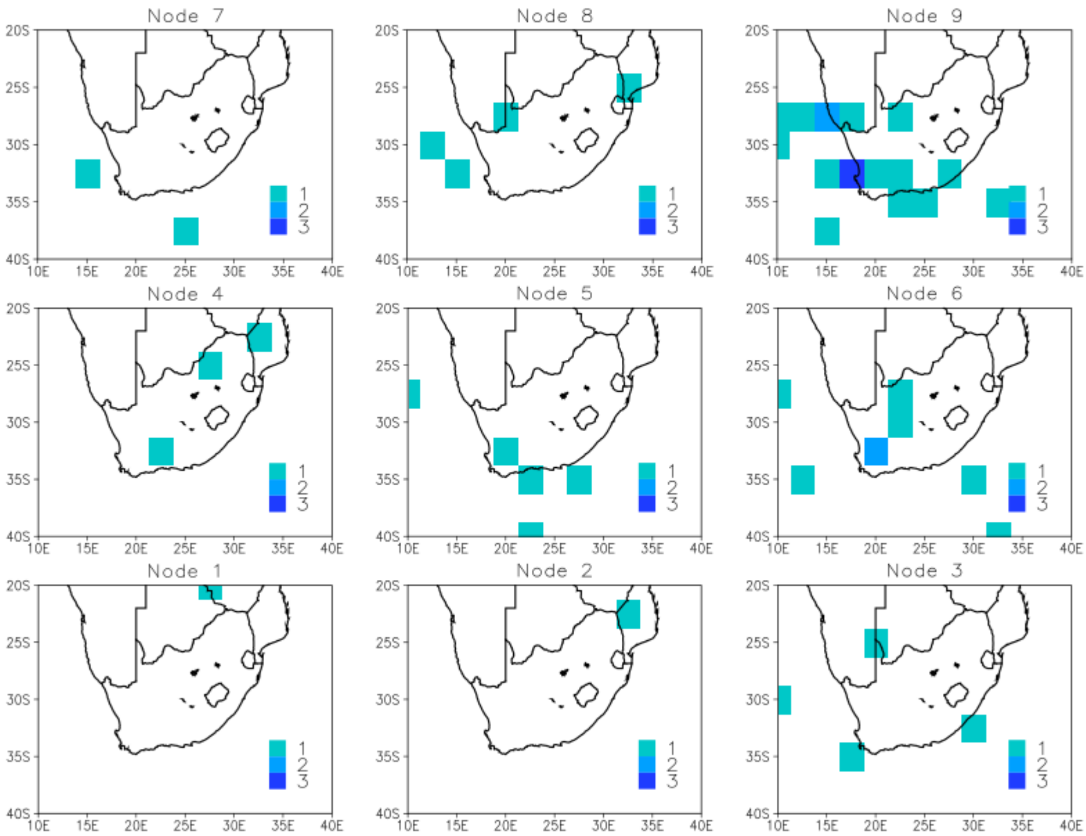

Figure 3. Geographical location of COLs in each of the nodes for the 14 SON seasons. The frequency legend is indicated in the bottom right corner of each panel.

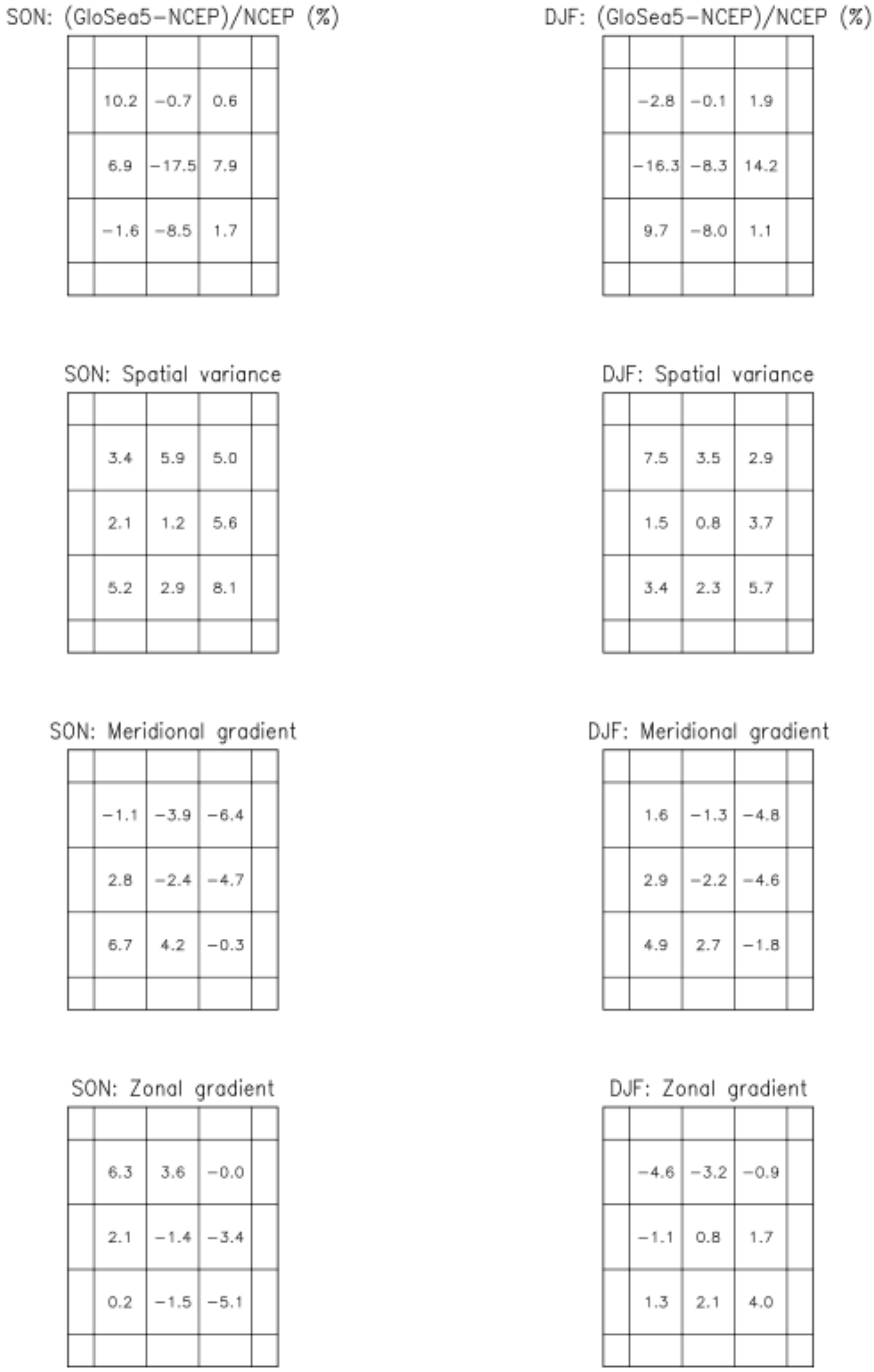

Figure 4. SOM node frequency errors of the GloSea5 ensemble mean expressed as a percentage of NCEP frequencies for SON and DJF (top row). Node spatial variance (second row), meridional gradient (third row) and zonal gradient (bottom row) for SON and DJF.

4.3.2 Deterministic assessment of forecast skill

Figure 5 shows the anomaly correlation of the GloSea5 node frequency distribution forecasts for SON (Figure 5a, solid line) and DJF (Figure 5b, solid line) as well as the corresponding persistence forecasts (dotted lines). The forecasts are obtained from the ensemble average of the 12 contributing forecast members, and may therefore be regarded as deterministic (Section 2). The forecast anomalies are calculated relative to the GloSea5 climatological frequencies constructed for the 14-year period. The anomaly correlations are subsequently calculated for each SON and DJF season in the 14-year time series, relative to the node frequencies present in NCEP reanalysis data. The NCEP anomalies are calculated relative to the 14-year NCEP climatology. Positive anomaly correlation coefficients are indicative of correspondence between the forecast anomalies and observed anomalies across the SOM, whilst a negative anomaly correlation yields a mismatch in the distribution of positive and negative anomalies between the forecast and observations. It is insightful in this respect that 9 (10) of the 14 anomaly correlation coefficients are positive for SON (DJF). Moreover, using persistence as reference forecast, anomaly correlation values are often negative and generally smaller than the anomaly correlation values based on the GloSea5 forecasts. More specifically, during SON (DJF), 11 (7) out of the 14 seasons exhibit skillful deterministic forecasts of the synoptic type frequency distribution within the SOM space relative to persistence forecasts. The three SON seasons that had no forecast skill relative to persistence were all below-normal rainfall seasons (1998, 2006 and 2009).

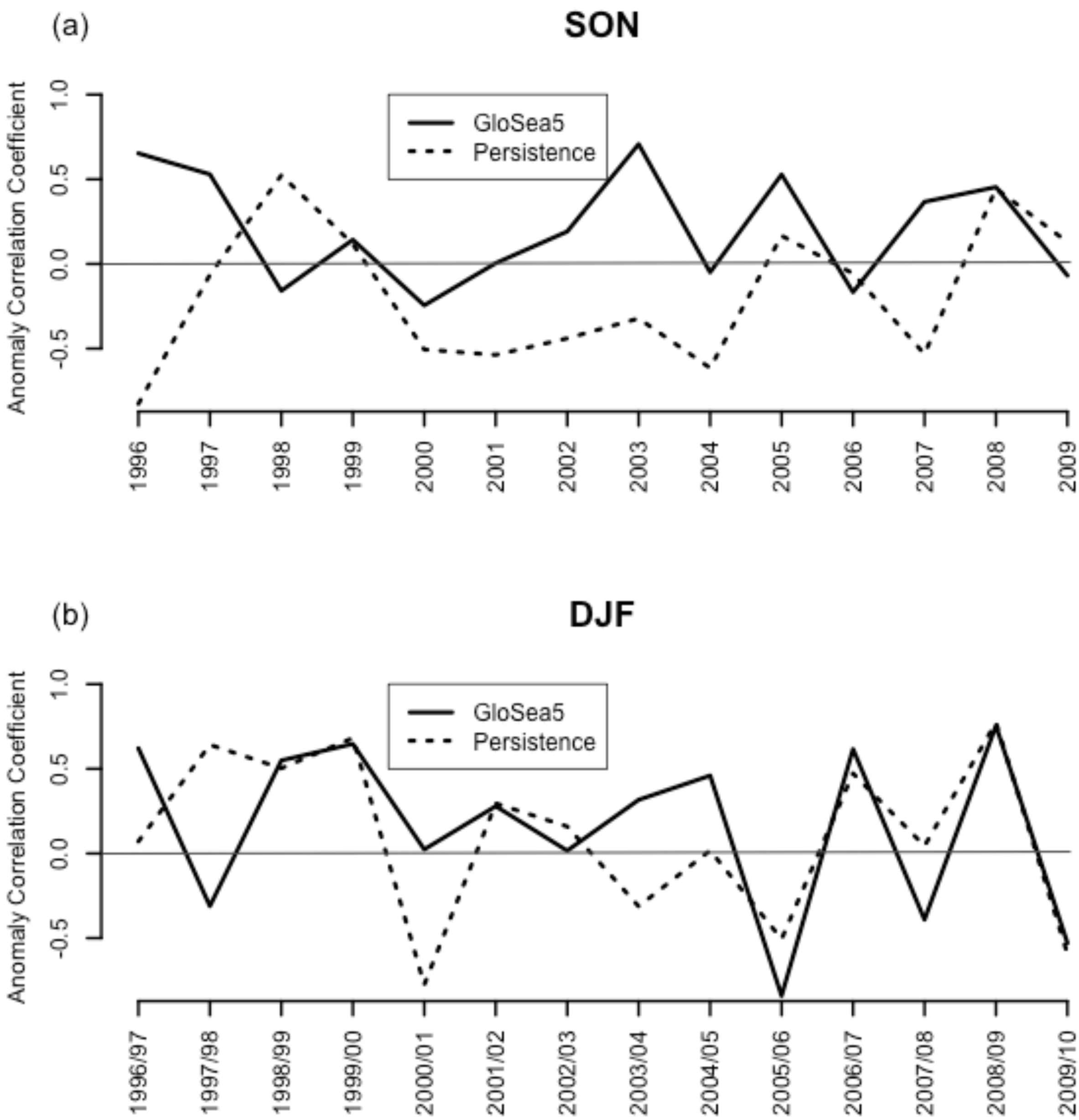

Figure 5. Anomaly correlation coefficient for GloSea5 (solid lines) and persistence (dotted lines) forecasts for (a) SON and (b) DJF.

A direct comparison between NCEP and GloSea5 node frequencies for selected seasons is shown in Figure 6. The 1996 SON season was an exceptionally wet season while the 1997/1998 and 2009/2010 DJF seasons are chosen based on the presence of relatively strong El Niño events during these two seasons. The direct comparison between observed and forecast node frequencies for the relevant shouldering season is also shown. During SON 1996, the frequency of the nodes typically associated with the largest contribution to rainfall in the mean, is simulated fairly well (nodes 3, 6 and 9). Even so, the general pattern with regard to the simulation of the node frequency during SON 1996 seems to be that synoptic systems representative of high pressure systems situated east/southeast of the country are simulated more frequently than observed (e.g. nodes 7, 8 and 9), while high pressure systems advancing from the west (e.g. nodes 3 and 6) are simulated slightly less frequently than observed. The largest difference between observed and simulated node frequency occurred at node 5 – this node is characterized be relatively small spatial variance compared to the other nodes. The frequency of occurrence of synoptic types of the DJF season that followed (1996/1997) was simulated very well. During SON 1997, synoptic systems representative of frontal systems were over simulated at the expense of almost all the other synoptic types. This characteristic continued in DJF 1997/1998. The 2009 SON season was characterized by an under simulation of advancing high pressure systems (nodes 3, 6 and 9) while frontal systems and tropical temperate troughs were over simulated. During DJF 2009/2010 a clear preference of the over or under simulation of a family of synoptic types is absent.

The direct comparison between observed and forecast node frequencies for the selected seasons seems to indicate that during seasons associated with normal or above normal rainfall (SON 1996 and DJF 1996/1997) synoptic type frequencies are simulated better compared to that of dry seasons (SON 1997, DJF 1997/1998, SON 2009 and DJF 2009/2010). However, the anomaly correlation (Figure 5) provides evidence of the GloSea5 ensemble-average forecasts to be superior over persistence and is indicative of deterministic skill in forecasting the intraseasonal distribution of the frequency of occurrence of synoptic types at interannual time scales. The next section explores the skill of the forecast system for the case of probabilistic measures of the intraseasonal distribution of synoptic types.

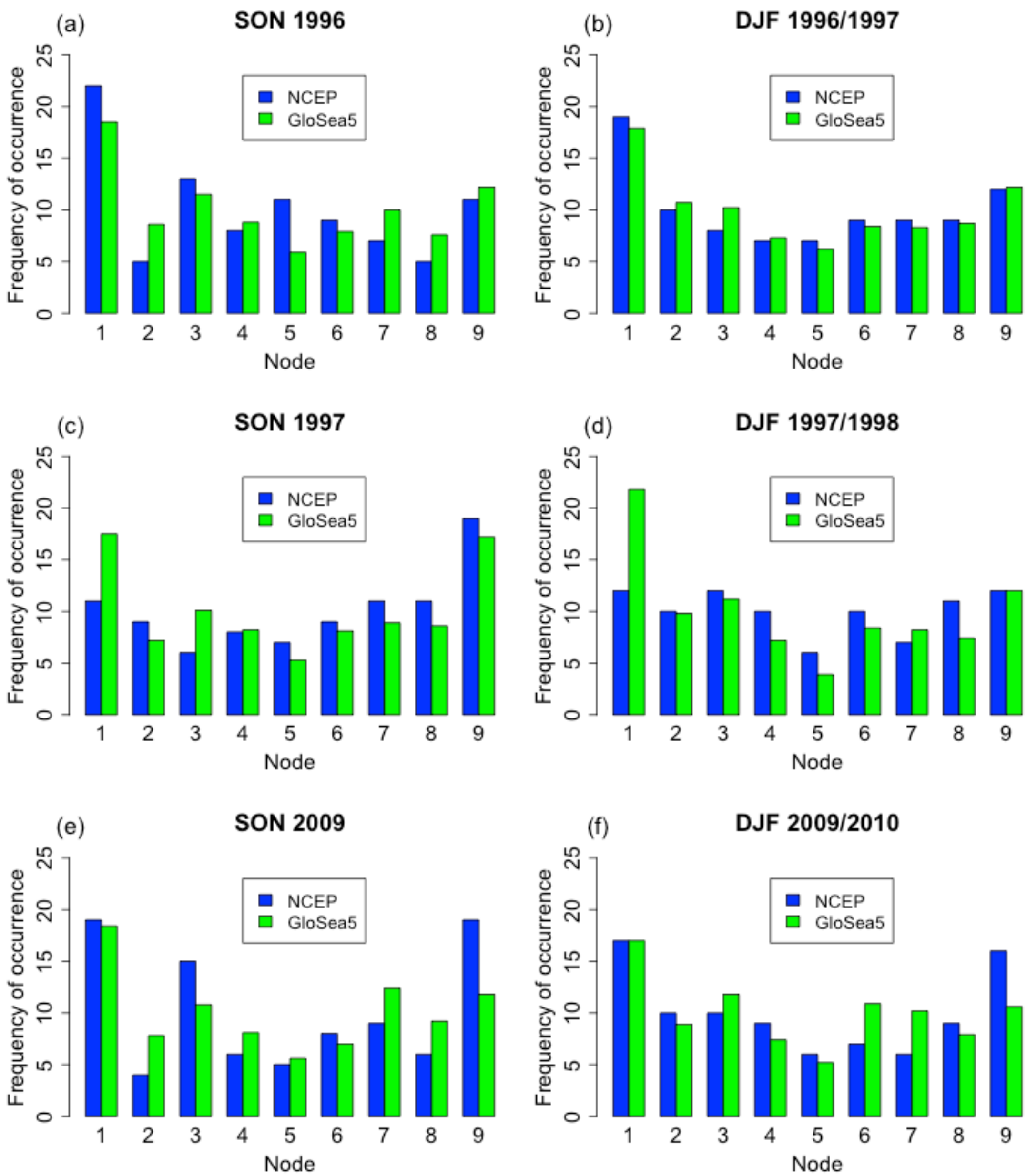

Figure 6. Node frequencies for (a) SON 1996, (b) DJF 1996/1997, (c) SON 1997, (d) DJF 1997/1998, (e) SON 2009 and (f) DJF 2009/2010. NCEP (GloSea5) node frequencies are indicated in blue (green).

4.3.3 Probabilistic assessment of the GloSea5 synoptic type forecasts

ROC curves are used to determine whether the GloSea5 forecasts can discriminate between the occurrence of above-normal seasonal frequencies of nodes, and the non-occurrence of above-normal frequencies. Similarly, the ability to discriminate between the occurrence of below-normal frequencies and the non-occurrence of such frequencies is investigated. Figure

7 shows the ROC curves for below-normal (Figure 7a and c) and above-normal (Figure 7b and d) SON (Figure 7a and b) and DJF (Figure 7c and d) node frequencies. Each ROC curve was calculated from 126 forecasts, obtained for the 9 nodes across 14 seasons. The ROC scores for both categories and both seasons are above 0.5, which means that the GloSea5 system has more than a 50% chance to discriminate above (below) normal frequencies of occurrence of nodes from normal and below (above) normal frequencies. This discrimination is of similar skill for the below-normal and above-normal categories, and for both the SON and DJF seasons.

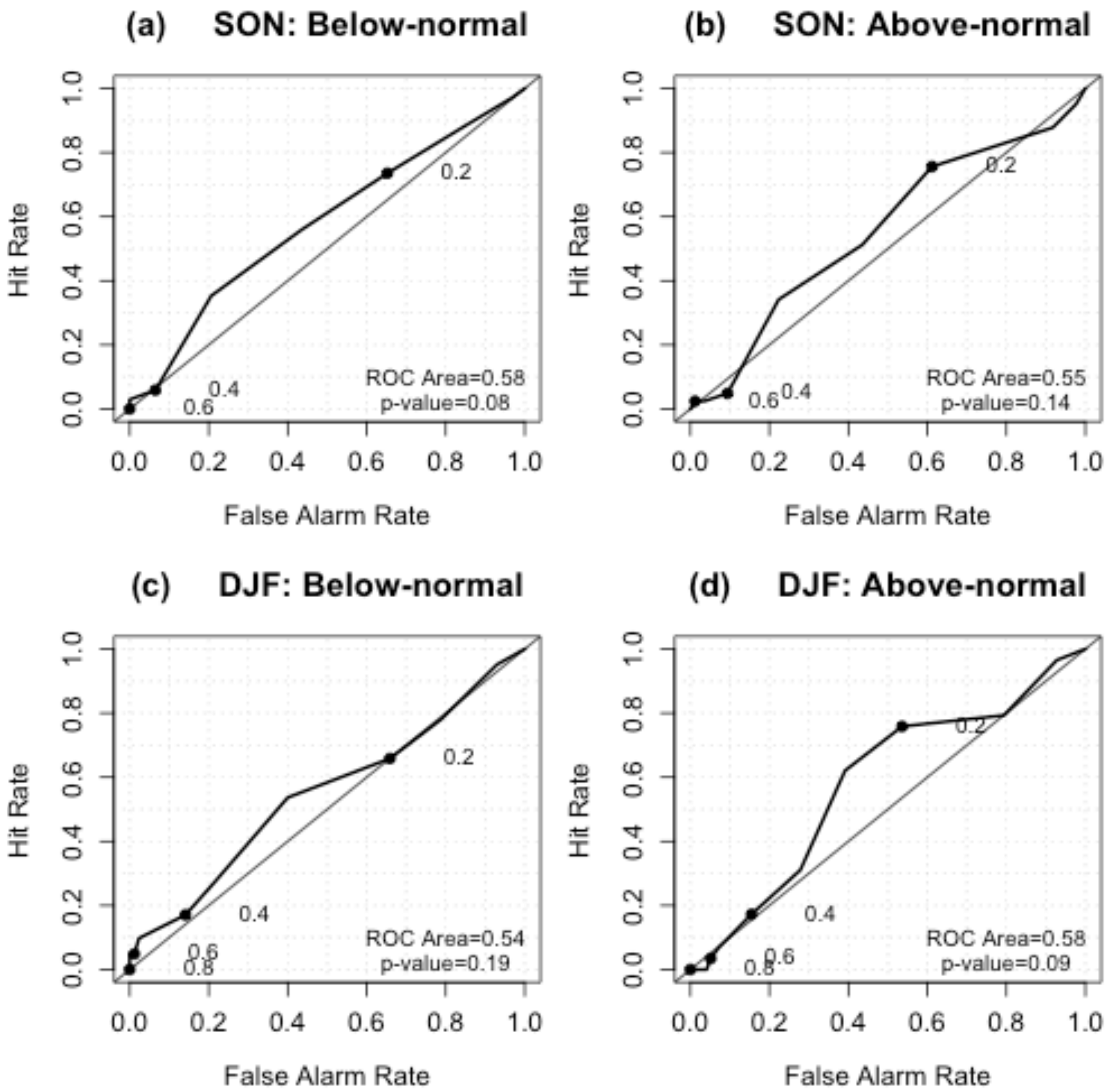

Figure 7. ROC curves, averaged over the 9 different nodes and 14 years, for (a) SON below-normal, (b) SON above-normal, (c) DJF below-normal and (d) DJF above-normal node frequency categories.

Figure 8 shows the reliability diagrams for the below-normal (Figure 8a and c) and above-normal (Figure 8b and d) categories, and for SON (Figure 8a and b) and DJF (Figure 8c and d). A perfectly reliable forecast would yield a reliability curve coinciding with the diagonal. The relative frequencies of each of the forecast thresholds 0.2, 0.4, 0.6, 0.8 and 1 are also shown in the form of a histogram. For forecasts associated with a probability threshold larger than 0.4, the reliability curves for both seasons and both categories fall below the diagonal, implying that the forecasts are overconfident when predicting these relatively high probabilities. Forecasts between the probability thresholds 0.2 and 0.4 are more reliable. The forecasts indicating probabilities less than 0.2 are generally underconfident. The frequency histograms for the lower and upper tercile forecasts for SON indicate a peak in forecast probability similar to the corresponding climatological probability – indicative thus that the forecasts lack sharpness. This lack is also true for the lower tercile forecasts for DJF. The forecasts for the upper tercile for DJF are an exception. Here the forecast probability frequency peak occurs in a probability bin that does not contain the climatological probability, indicating a degree of sharpness.

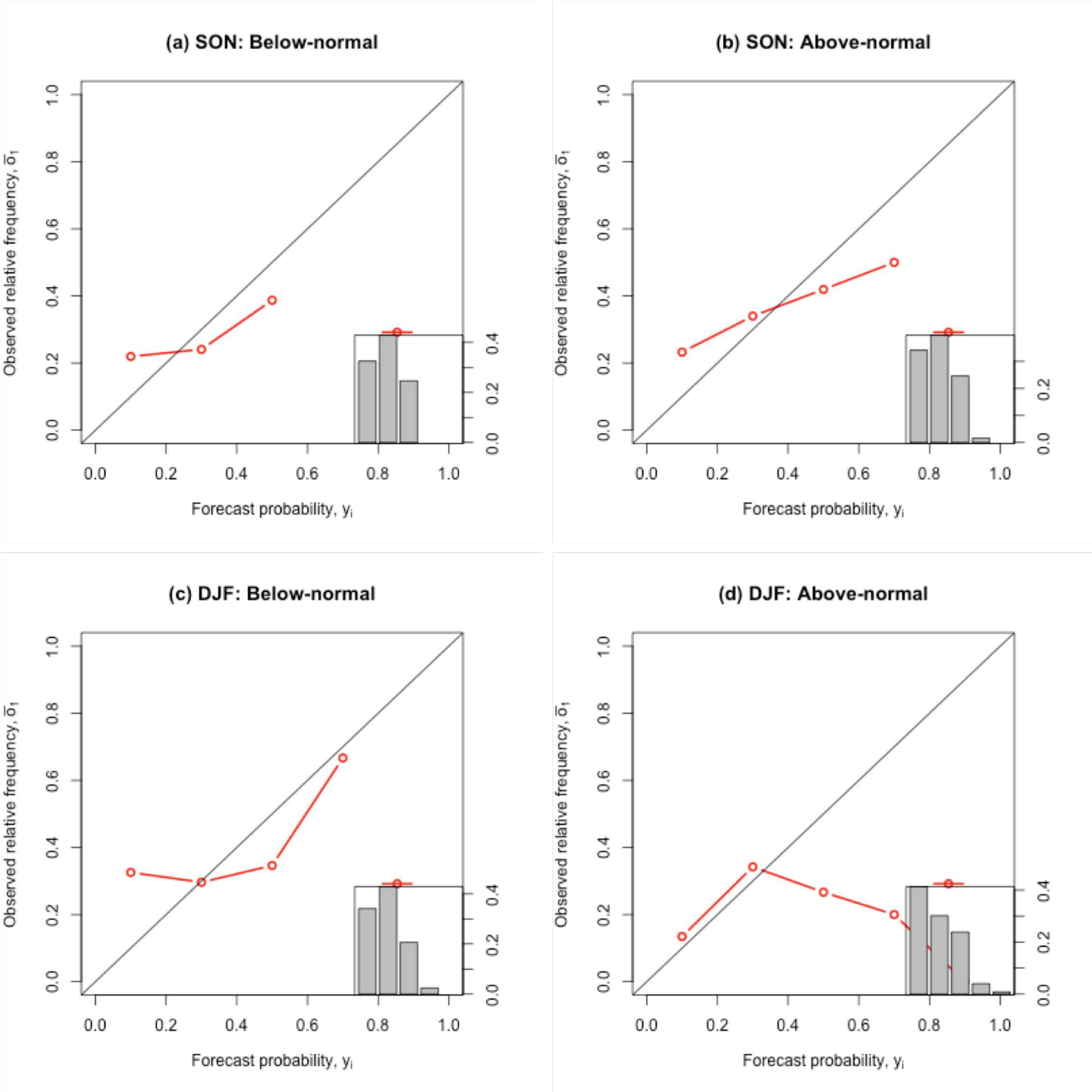

Figure 8. Reliability plots for (a) SON below-normal, (b) SON above-normal, (c) DJF below-normal and (d) DJF above-normal node frequency categories.

Figure 9 measures the ability of the forecast system to distinguish between the occurrences of synoptic type frequencies to be in a specific tercile category. The occurrence or non-occurrence of each synoptic type is depicted by an X-coordinate of either 0 or 1, across the SOM and over the full 14-year period. The associated forecast probabilities for the synoptic types determine the Y-coordinates of the points plotted. A straight line is subsequently fitted to all paired numbers obtained in this way. Always forecasting the climatological probability of 0.333 for a specific category yields a line of zero slope, and this determines a benchmark measure of skill. In the case of the SON forecasts, positive slopes are obtained for all the tercile categories, with the steepest slope (highest skill) obtained for the below-normal category. Regression lines are also shown for persistence forecasts, these all have negative slopes indicating that forecasting the synoptic type frequencies using persistence is not skillful. For DJF, the GloSea5 forecasts are once again skillful for climatology, across all three categories, with forecasts for the below-normal category the most skillful. The persistence forecasts in this case show marginal skill over climatology, suggesting some degree of auto-correlation in DJF synoptic type frequencies from one year to the next.

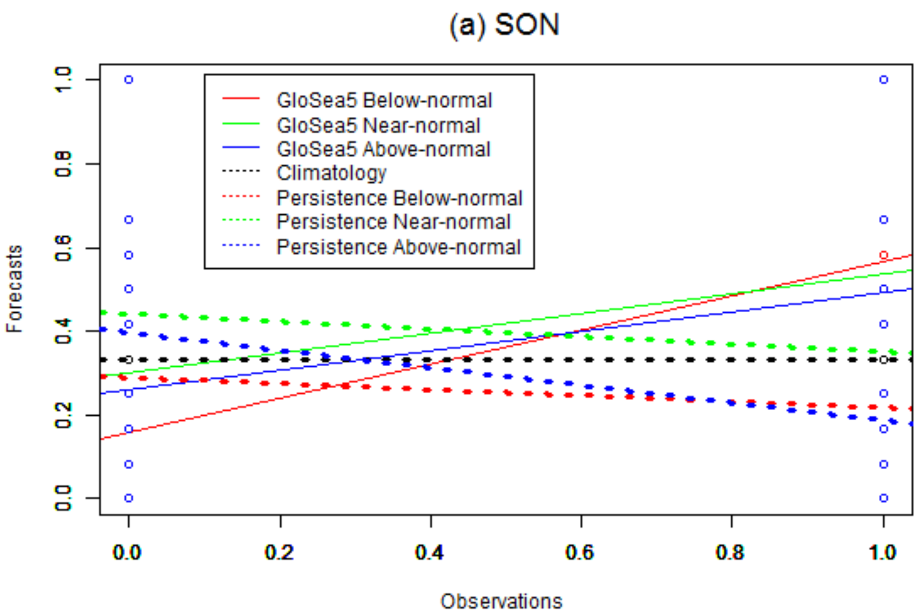

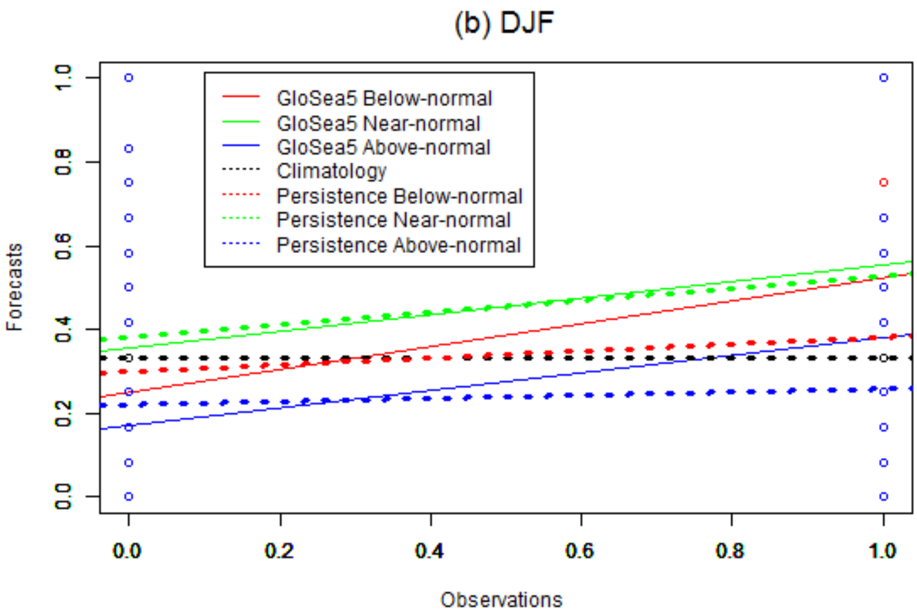

Figure 9. Skill of the synoptic type frequency distribution tercile category forecasts for (a) SON and (b) DJF. Solid lines indicate GloSea5 forecasts and dotted lines reference forecasts. Note that the 0.2, 0.4, 0.6 and 0.8 ticks on the x-axis are superfluous.

4.4 Conclusions

Studies of seasonal forecast skill over southern Africa have to date focused on the summer rainfall region, where a strong association between rainfall and ENSO is known to exist. Moreover, the majority of these verification studies focused primarily on the prediction of seasonal total rainfall or seasonal mean temperatures, thus not focusing on the verification of intraseasonal predictions. However, the recent study of Engelbrecht and Landman (2015) has revealed a link between the interannual variability of intraseasonal circulation over the Cape south coast region of South Africa and two large-scale modes of variability: ENSO and SAM. The predictability that exists for ENSO and SAM at interannual time scales therefore implies potential skill in the seasonal forecasting of intraseasonal circulation attributes over the Cape south coast region. This hypothesis was investigated in the paper, using the GloSea5 forecast system of the UKMO.

A SOM approach was applied to divide the regional circulation patterns occurring over the Cape south coast region into 9 synoptic types. The climatological frequencies of these synoptic types as represented by the ensemble mean of the GloSea5 forecasts were found to compare very satisfactorily with observed synoptic type frequencies. Deterministic verification of the ensemble mean forecasts of synoptic type frequencies on an interannual time scale was performed. The deterministic node frequency distribution forecasts fare somewhat better for SON than DJF, according to the anomaly correlation. The forecast system exhibits modest but significant skill over persistence.

Next, the skill of probabilistic forecasts of the frequency of occurrence of synoptic types was explored. ROC scores, calculated across the SOM and across 14 years of data, indicate that the forecast system is marginally skillful in distinguishing synoptic type frequencies occurring in the upper/lower tercile categories from the remaining categories. Reliability diagrams were also constructed, and these indicate a tendency for the forecast system to be overconfident, specifically for the case of higher probability forecasts. Finally, a new verification graphic was introduced that aims to determine whether the forecast system can distinguish between the occurrence and non-occurrence of synoptic types for the tercile categories across the SOM. It was found that the forecasts have skill over persistence and climatology in forecasting the intraseasonal variation of synoptic types over the Cape south coast region. This result might have potential implications for SON forecasts with regard to the nature of rainfall as the occurrence of COLs during SON seems to cluster to certain nodes within the SOM space. Probabilistic forecasts of high-impact rainfall events associated with COLs might have some potential during SON.

The overall message of the paper therefore is that intraseasonal circulation variability over the Cape south coast region is marginally predictable at interannual time scales. This result opens the door for prediction of Cape south coast seasons characterized by high frequencies of rainfall-producing systems such as COLs and ridging highs, or alternatively, seasons characterized by a lack of such systems.

4.5 Acknowledgments

This research was funded by the Applied Centre for Climate and Earth System Studies (ACCESS) in South Africa.

4.6 References

Bartman AG, Landman WA and Rautenbach CJ DE W. 2003. Recalibration of general circulation model output to austral summer rainfall over southern Africa. *International Journal of Climatology* **23**: 1407-1419. doi: 10.1002/joc.954.

Camp J, Roberts M, MacLachlan C, Wallace E, Hermanson L, Brookshaw A, Arribas A and Scaife AA. 2015. Seasonal forecasting of tropical storms using the Met Office GloSea5 seasonal forecast system. *Quarterly Journal of the Royal Meteorological Society*. doi: 10.1002/qj.2516.

Diro GT. 2015. Skill and economic benefits of dynamical downscaling of ECMWF ENSEMBLE seasonal forecast over southern Africa with RegCM4. *International Journal of Climatology*. doi: 10.1002/joc.4375.

Dyson L. 2015. A heavy rainfall sounding climatology over Gauteng, South Africa, using self-organising maps. *Climate Dynamics*. doi: 10.1007/s00382-015-2523-3.

Engelbrecht CJ, Landman WA, Engelbrecht FA and Malherbe J. 2015. A synoptic decomposition of rainfall over the Cape south coast of South Africa. *Climate Dynamics* **44**: 2589-2607. doi: 10.1007/s00382-014-2230-5.

Engelbrecht CJ and Landman WA. 2015. Interannual variability of seasonal rainfall over the Cape south coast of South Africa and synoptic type association. *Climate Dynamics*. doi: 10.1007/s00382-015-2836-2.

Fauchereau N, Pohl N, Reason CJC, Rouault M and Richard Y. 2009. Recurrent daily OLR patterns in the Southern Africa/South-west Indian Ocean region, implications for South African rainfall and teleconnections. *Climate Dynamics* **32**: 575-591. doi: 10.1007/s00382-008-0426-2.

Grotjahn R, Black R, Leung R, Wehner MF, Barlow M, Bosilovich M, Gershunov A, Gutowski WJ Jr, Gyakum JR, Katz RW, Lee YY, Lim YK and Prabhat. 2015. North American extreme temperature events and related large scale meteorological patterns: a review of statistical methods, dynamics, modeling, and trends. *Climate Dynamics*. doi: 10.1007/s00382-015-2638-6.

Hamill TM. 1997. Reliability diagram for multicategory probabilistic forecasts. *Weather and Forecasting* **12**: 736-741.

Hewitson BC and Crane RG. 2002. Self-organizing maps: applications to synoptic climatology. *Climate Research* **22**: 13-26. doi: 10.3354/cr022013.

Hudson H, Alves O, Hendon HH and Marshall AG. 2011. Bridging the gap between weather and seasonal forecasting: intraseasonal forecasting for Australia. *Quarterly Journal of the Royal Meteorological Society* **137**: 673-689.

Kalnay E, Kanamitsu M, Kistler R, Collins W, Deaven D, Gandin L, Iredell M, Saha S, White G, Woollen J, Zhu Y, Leetmaa A, Reynolds B, Chelliah M, Ebisuzaki W, Higgins W, Janowiak J, Mo KC, Ropelewski C, Wang J, Jenne R and Joseph D. 1996. The NEP/NCAR 40-year reanalysis project. *Bulletin of the American Meteorological Society* **77**: 437-471.

Klopper E. 1999. The use of seasonal forecasts in South Africa during the 1997/98 rainfall season. *Water Sci. Adv*. **25**: 311-316.

Klopper E, Vogel CH and Landman WA. 2006. Seasonal climate forecasts – potential agricultural-risk management tools? *Climatic Change* **76**: 73-90. doi: 10.1007/s10584-005-9019-9.

Kohonen T. 1984. Self organization and associative memory, 2nd edn. Springer, Berlin Heidelberg New York, 312 pp.

Landman WA, Mason SJ, Tyson PD and Tennant WJ. 2001a. Retro-active skill of multi-tiered forecasts of summer rainfall over southern Africa. *International Journal of Climatology* **21**: 1-19.

Landman WA, Mason SJ, Tyson PD and Tennant WJ. 2001b. Statistical downscaling of GCM simulations to stream flow. *Journal of Hydrology* **252**: 221-236.

Landman WA and Goddard L. 2002. Statistical Recalibration of GCM Forecasts over Southern Africa Using Model Output Statistics. *Journal of Climate* **15**: 2038-2055.

Landman WA and Goddard L. 2005. Predicting southern African summer rainfall using a combination of MOS and perfect prognosis. *Geophysical Research Letters* **32**: L15809, doi: 10.1029/2005GL022910.

Landman WA and Beraki A. 2012. Multi-model forecast skill for mid-summer rainfall over southern Africa. 2012. *International Journal of Climatology* **32**: 303-314.

Landman WA, De Witt D, Lee DE, Beraki A and Lotter D. 2012. Seasonal Rainfall Prediction Skill over South Africa: One- versus Two-Tiered Forecasting Systems. *Weather and Forecasting* **27**: 489-501.

Lazenby MJ, Landman WA, Garland RM and De Witt DG. 2014. Seasonal temperature prediction skill over Southern Africa and human health. *Meteorological Applications* **21**: 963-974.

Lennard C and Hegerl G. 2014. Relating changes in synoptic circulation to the surface rainfall response using self-organising maps. *Climate Dynamics*. doi: 10.1007/s00382-014-2169-6.

Lindesay JA, Harrison MSJ and Haffner MP. 1986. The southern oscillation and South African rainfall. *South African Journal of Science* **82**: 196-198.

MacLachlan C, Arribas A, Peterson KA, Maidens A, Fereday D, Scaife AA, Gordon M, Vellinga M, Williams A, Comer RE, Camp J, Xavier P and Madec G. 2014. Global Seasonal forecast system version 5 (GloSea5): a high-resolution seasonal forecast system. *Quarterly Journal of the Royal Meteorological Society*. doi: 10.1002/qj.2396.

Malherbe J, Engelbrecht FA, Landman WA and Engelbrecht CJ. 2012. Tropical systems from the southwest Indian Ocean making landfall over the Limpopo River Basin, southern Africa: a historical perspective. *International Journal of Climatology* **32**: 1018-1032. doi:10.1002/joc.2320.

Malherbe J, Landman WA and Engelbrecht FA. 2013. The bi-decadal rainfall cycle, southern annular mode and tropical cyclones over the Limpopo River Basin, southern Africa. *Climate Dynamics* **42**: 3121-3138. doi: 10.1007/s00382-013-2027-y.

Malherbe J, Landman WA, Olivier C, Sakuma H, Luo J- J (2014b) Seasonal forecasts of the SINTEX-F coupled model applied to maize yield and streamflow estimates over north-eastern South Africa. *Meteorological Applications* **21**: 733-742. doi:10.1002/met.1402.

Mason SJ. 1998. Seasonal forecasting of South African rainfall using a non-linear discriminant analysis model. *International Journal of Climatology* **18**: 147-164.

Mason SJ and Graham NE. 2002. Areas beneath the relative operating characteristics (ROC) and levels (ROL) curves: statistical significance and interpretation. *Quarterly Journal of the Royal Meteorological Society* **128**: 2145-2166.

Mason SJ, Joubert AM, Cosijn C and Crimp SJ. 1996. Review of seasonal forecasting techniques and their applicability to southern Africa. *Water SA* **22**: 203-209.

Moeletsi ME, Walker S and Landman WA. 2011. ENSO and implication on rainfall characteristics with reference to maize production in the Free State Province of South Africa. *Physics and Chemistry of the Earth* (A/B/C) **36**: 715-726. doi: 10.1016/j.pce.2011.07.043.

Morioka Y, Tozuka T and Yamagata T. 2010. Climate variability in the southern Indian Ocean as revealed by self-organizing maps. *Climate Dynamics* **35**: 1075-1088. doi: 10.1007/s00382-010-0843-x.

Murphy AH and Epstein ES. 1989. Skill Scores and Correlation Coefficients in Model Verification. *Monthly Weather Review* **117**: 572-581.

Philippon N, Rouault M, Richard Y and Favre A. 2011. The influence of ENSO on winter rainfall in South Africa. *International Journal of Climatology* **32**: 2333-2347. doi: 10.1002/joc.3403.

Rautenbach CJdeW and Smith IN. 2001. Teleconnections between global sea-surface temperatures and the interannual variability of observed and model simulated rainfall over southern Africa. *Journal of Hydrology* **254**: 1-15.

Rouault M and Richard Y. 2003. Intensity and spatial extension of drought in South Africa at different time scales. *Water SA* **29**: 489-500.

Singleton AT and Reason CJ. 2006. Numerical simulations of a severe rainfall event over the Eastern Cape coast of South Africa: sensitivity to sea surface temperature and topography. *Tellus* **58**: 355-367.

Singleton AT and Reason CJ. 2007. A numerical model study of an intense cutoff low pressure system over South Africa. *Monthly Weather Review* **135**: 1128-1150.

Taljaard JJ. 1996. Atmospheric circulation systems, synoptic climatology and weather phenomena of South Africa. Part 6: Rainfall in South Africa. South African Weather Bureau, Technical paper 32.

Tennant W and Hewitson BC. 2002. Intra-seasonal rainfall characteristics and their importance to the seasonal prediction problem. *International Journal of Climatology* **22**:1033-1048. doi: 10.1002/joc.778.

Tennant W. 2003. An assessment of intraseasonal variability from 13-Yr GCM Simulations. *Monthly Weather Review* **131**: 1975-1991.

Van Schalkwyl L and Dyson LL. 2013. Climatological characteristics of fog at Cape Town International airport. *Weather and Forecasting* **28**: 631-646. doi: 10.1175/WAF-D-12-00028.1.

Vogel C and O'Brien K. 2006. Who can eat information? Examining the effectiveness of seasonal climate forecasts and regional climate-risk management strategies. *Climate Research* **33**: 111-122.

Warner TT. 2011. Numerical Weather and Climate Prediction. Cambridge University Press, 550 pp.

Weldon D and Reason CJC. 2014. Variability of rainfall characteristics over the South Coast region of South Africa. *Theoretical and Applied Climatology* **115**: 177-185. doi: 10.1007/s00704-013-0882-4.

Wilks DS. 2011. Statistical Methods in the Atmospheric Sciences. 3rd ed. Academic Press, Amsterdam.

Synopsis

In this final chapter, it has been demonstrated that some predictability of the intraseasonal variability of synoptic types influencing the all-year rainfall region on the interannual time scale exists. Between the two seasons tested, higher skill has been found for SON as opposed to DJF. This result differs from what has been found over the summer rainfall regions of South Africa that has a DJF skill maximum when mostly tropical influences dominate the atmospheric circulation. Notwithstanding, the demonstrated predictability of SON synoptic characteristics offers the potential to make SON predictions for uptake by the users community. Objective 5 of the study has thereby been addressed.

Chapter 5: Summary and Conclusions

The study started by performing a daily synoptic decomposition of rainfall over the all-year rainfall region over the 33-year period from 1979 to 2011. This part of the work entailed the development of a synoptic type climatology based on daily sea-level pressure circulation prior to relating rainfall on a daily time scale to each of the identified synoptic types. This approach of utilizing each day in the 33-year time series made it possible to quantify the contribution of the different identified synoptic types to mean annual rainfall over the region. Previous studies addressed the contribution of COLs and tropical-temperate troughs to rainfall over the country at weather station scale and therefore over the all-year rainfall region, while the contribution by other synoptic types to rainfall over the all-year rainfall region have not been quantified prior to this study (e.g. ridging high pressure systems from the southwest, frontal systems, ridging high pressure systems from the east/southeast). New insights have been gained regarding the important rain-producing synoptic types of the all-year rainfall region in South Africa. The general perception of the COL being a major rainfall producing system over the Cape south coast has been objectively quantified. A surprising result however, is the importance of ridging high pressure systems and associated low-level flow as the main rainfall producing system over the region. This result is of key importance to dynamic seasonal forecasting and climate simulation over the Cape south coast. The well-known bi-modal rainfall distribution with peaks during autumn and spring has been reassessed and an additional rainfall peak during August has been identified, implying that this region seems to instead have a multi-modal rainfall distribution. Since the publication of the paper (Chapter 2) in which the multi-modal rainfall distribution has been described, the result has been referred to in a paper on CORDEX simulations, thereby demonstrating the value of the research to model verification. The synoptic forcing responsible for the uniqueness of the seasonal rainfall cycle over the all-year rainfall region has also been quantified.

From this foundation the study proceeded to explore the interannual variability of the synoptic types that bring rainfall to the Cape south coast region. It has been found that synoptic types that contribute to significant portions of rain during a specific season (i.e., summer, autumn, winter, spring) occur more frequently during wet seasons than during dry seasons. Using this insight, a new type of atmospheric circulation index was formulated. This formulation is based on the pattern correlation between the average synoptic type frequencies associated with wet seasons and the frequencies associated with a particular season. Correlating this value with the main modes of southern hemisphere variability, namely ENSO and SAM, revealed that the new index for spring and summer is negatively correlated to Nino 3.4 SST anomalies, whilst the summer and autumn index values are positively correlated with SAM. Since there is evidence that ENSO and SAM are predictable at seasonal time scales, these findings indicate the potential for skilful prediction of the intraseasonal variability of synoptic types over the Cape south coast region at the seasonal time scale. This result is important towards obtaining reliable early warnings of seasons with anomalously high frequencies of high-impact weather events occurring over the region.

The study concluded with an investigation of the predictability of the intraseasonal variability of synoptic type frequencies at the seasonal time scale over the Cape south coast. The GloSea5 system consisting of 12 ensemble members was applied for this purpose at a 1-month lead time, with a focus on the spring and summer seasons. Deterministic measures of skill of the ensemble average forecast of synoptic type frequencies reveal that the forecasts are skilful over persistence, particularly for spring. Moreover, the forecast frequencies are positively correlated to the observed frequencies over time, with the correlations being statistically significant for more than half of the period considered. Probabilistic estimates of the forecast skill reveal that the system can skilfully predict the occurrence of below-normal and above-normal node frequencies, for both the spring and summer seasons. The system has skill over persistence and climatological anomalies in identifying below-normal, normal and above-normal node frequencies across the SOM space. Although all the measures of skill indicate skill levels somewhat lower than those recorded for the prediction of summer rainfall totals over South Africa's summer rainfall region with its strong ENSO signal, the results still indicate that the forecast system is capable of producing skilful forecasts of intraseasonal variability in circulation. This finding is a newly established result that deserves further investigation for the larger southern African region, towards providing a variety of users with information of the intraseasonal occurrence of high impact weather events at the seasonal time scale.

Major results of this study are summarized as follows:

- Regarding the synoptic decomposition of rainfall over the all-year rainfall region:

- High pressure systems ridging from the southwest contribute to 46% of the annual rainfall while these systems have a frequency of occurrence of 23%
- The subset of ridging high pressure systems from the southwest occurring in conjunction with COLs contribute to 7% of the annual rainfall
- Tropical-temperate troughs contribute to 28% of the annual rainfall
- The contribution of ridging high pressure systems from the southwest to rainfall increases from south to north, while the contribution of tropical-temperate troughs decreases from south to north. Here "south" is considered to be the all-year rainfall region and "north" the northward neighbouring regions
- COLs (with and without ridging high pressure systems from the southwest) contribute to 16% of the annual rainfall
- Regional variation occurs in the contribution of COLs to annual rainfall, ranging between 13% and 22% at the weather stations used in this study
- The relative contribution to rainfall by COLs is remarkable, considering that COL-induced rainfall days over this region occurs only on 4.2% of the time
- The contribution of COLs to extreme rainfall over the region is noteworthy, with the largest contribution to extreme rainfall found at the weather stations on or adjacent to the coast
- Quantification of rainfall associated with the subtle but systematic differences within a synoptic type now formally confirms the relative importance of the location of the system regarding its rainfall contribution, e.g. ridging high pressure systems where the ridge is located further southwards are more conducive to rainfall along the Cape south coast region than ridges located more equatorwards, even if the pressure distribution is otherwise similar.
- Seasonality is observed in the preferred configuration (e.g. node 14 and 28 that is more a winter and summer rain-bearing ridging high respectively) of ridging high pressure systems from the southwest that contributes to rainfall.

- Regarding the seasonal rainfall cycle over the all-year rainfall region:
  - Rainfall-producing synoptic types with an occurrence throughout the year includes ridging high pressure systems from the southwest and COLs, while the contribution by tropical-temperate troughs and frontal systems peak during October to April and May to August, respectively.

   - A multi-modal rather than a bi-modal rainfall distribution has been identified. The first peak occurs in autumn and is attributable to a combination of ridging high pressure systems, tropical-temperate troughs and COLs during March while COLs drive the April peak (co-occurring with ridging highs and tropical-temperate troughs); ridging high pressure systems from the southwest, troughs and COLs are responsible for the second peak in August; a third peak occurs in spring (October) and is largely the result of ridging high pressure systems from the southwest.

- Regarding interannual rainfall and synoptic type variability over the all-year rainfall region:
   - The anomalous frequency of occurrence of the different synoptic types for wet and for dry DJF, MAM and JJA seasons differ significantly within the SOM space, with the strongest and most significant differences during JJA, followed by DJF and MAM. During SON, the anomalous frequency of occurrence of the different synoptic types for wet and dry seasons is small and not statistically significant.
   - The main rain-producing synoptic types have a notably larger contribution to seasonal rainfall totals during wet seasons than during dry seasons. This result is consistent with a higher frequency of occurrence of the main rainfall-producing synoptic types during wet seasons compared to dry seasons.
   - The main rainfall-producing synoptic types are to a large extent consistent for wet and dry seasons.
   - Dry seasons are characterized by a smaller contribution to seasonal rainfall totals by all the different synoptic types, but with the largest negative rainfall anomalies associated with low frequencies of the main rain-producing synoptic types. Weather systems that disrupt the normal rainfall patterns seem to occur more frequently during dry seasons compared to normal and wet seasons.
   - The frequencies of occurrence of specific configurations of ridging high pressure systems, COLs and tropical-temperate troughs associated with rainfall are positively linked to interannual variability of seasonal rainfall.
   - Moisture profiles during wet and dry seasons are quite similar, but with wet seasons having a slightly stronger moisture flux.

- Ridging high pressure systems from the southwest seems to have the strongest link to interannual variability of all season rainfall. It is in particular rainfall from configurations of these systems where the ridging is taking place from far south that are linked to rainfall variability for all four seasons.
- Tropical-temperate troughs are also important systems regarding rainfall variability. During DJF, rainfall associated with tropical-temperate troughs with the smallest node-averaged zonal wind component over and to the south of the country are linked to interannual rainfall variability, exhibiting characteristics similar to that of atmospheric circulation associated with wet conditions over the summer rainfall region.
- Frontal-trough rainfall are weakly linked to interannual rainfall variability during JJA.
- A strong link has been demonstrated between COL-induced rainfall and rainfall variability for MAM, JJA and SON, with the strongest link found for JJA.
- Rainfall variability also seems to be linked to ENSO and SAM.

- Regarding the predictability of the intraseasonal variability of synoptic types over the all-year rainfall region at the seasonal time scale by making use of the GloSea5 forecast system of the UKMO:
    - Climatological frequencies of synoptic types as represented by the ensemble mean of the GloSea5 forecasts compared well with observed synoptic type frequencies.
    - The forecast system exhibits modest but clear skill over persistence for deterministic synoptic type frequency distribution forecasts of the ensemble mean.
    - For probabilistic forecasts of the above-normal or below-normal occurrence of synoptic type frequencies, the forecast system has marginal skill in discriminating between the occurrence of the synoptic type frequencies to be in the upper/lower tercile categories from the remaining categories.
    - The forecast system tends to be overconfident, specifically for the case of higher probability forecasts while lower probability forecasts are generally underconfident.
    - The lower tercile and upper tercile SON forecasts lack sharpness

- The lower tercile DJF forecasts lack sharpness, while some sharpness is indicated for the upper tercile DJF forecasts.
- Overall, it was found by both deterministic and probabilistic measures, that intraseasonal circulation variability is predictable at interannual time scales, more so during SON than during DJF, and that the skill is mostly modest.

This thesis has presented an in-depth study of the variability and predictability of a largely unexplored region over the Cape south coast. The analysis technique discovered characteristics of the region not previously documented and proved that some of these characteristics can be predicted in an operational forecast environment. Similar analysis and prediction studies can be applied over areas such as the summer rainfall region in order to obtain an improved and updated understanding of the climate dynamics at play over the subcontinent. The thesis has thusly not only contributed to an improved understanding of South coast climate, but has laid a foundation for future research that will help to enhance our current understanding of the Earth system we operate in.

Recommendation for future research:

Future research that includes the role of local SSTs in moisture flux attributes during dry and wet seasons along the Cape south coast is recommended. It has been shown in this study that dry and wet seasons are characterized by moisture flux profiles that do not differ significantly, suggesting that synoptic weather types dominate the rainfall variability. Identification of the dominant rainfall variability driver (SSTs versus synoptic weather types) is recommended for future research to contribute to our understanding of the Cape south coast climate.